

AUTONOMOUS UNIVERSITY OF BAJA CALIFORNIA
Faculty of Engineering, Architecture and Design
Master and Doctorate in Sciences and Engineering



Control of mechanisms through electroencephalographic signals

Thesis

for obtaining the degree of

Doctor in Sciences

that presents:

Francisco Javier Ramírez Arias

Director of thesis

Dr. Everardo Inzunza González

Ensenada, Baja California, Mexico, December, 2022.

AUTONOMOUS UNIVERSITY OF BAJA CALIFORNIA

Faculty of Engineering, Architecture and Design

Master and Doctorate in Sciences and Engineering

Control of mechanisms through electroencephalographic signals

Thesis

for obtaining the degree of

Doctor in Sciences

that presents:

FRANCISCO JAVIER RAMÍREZ ARIAS

and approved by the committee:

Dr. Everardo Inzunza Gonzalez
Director of thesis

Dr. Enrique Efrén García Guerrero
Co-director of thesis

Dr. Oscar Roberto López Bonilla
Committee member

Dr. Gilberto Manuel Galindo Aldana
Committee member

Dr. Juan Miguel Colores Vargas
Committee member

Ensenada, Baja California, Mexico, December 2022.

RESUMEN de la tesis de **Francisco Javier Ramírez Arias**, presentada como requisito para obtener el grado de **DOCTOR en CIENCIAS**, del programa de Maestría y Doctorado en Ciencias e Ingeniería de la Universidad Autónoma de Baja California. Ensenada, Baja California México, Diciembre 2022.

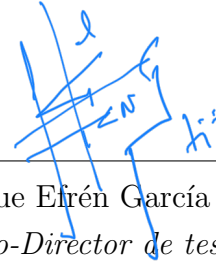
Control de mecanismos por medio de señales electroencefalograficas

Resumen aprobado por:



Dr. Everardo Inzunza González

Director de tesis



Dr. Enrique Eirén García Guerrero

Co-Director de tesis

En las interfaces cerebro-computadora (ICC), es crucial el análisis y el procesamiento de las señales electroencefalograficas (EEG) para mejorar la precisión de su clasificación, con proposito de lograr su aplicación en movimientos motores. Los algoritmos de aprendizaje máquina entre los que destacan ANN, CNN, SVM, entre otros, han realizado un progreso significativo dentro de este ámbito. Los objetivos de este trabajo es presentar el análisis y el procesamiento de las señales EEG utilizando diferentes técnicas de extracción de características para entrenar diversos algoritmos de clasificación con proposito de clasificar señales relacionadas a los movimientos motores. Los movimientos motores considerados provienen de la mano izquierda, mano derecha, ambos puños, pies y relajación, haciendo este un problema multiclase. En este trabajo, nueve algoritmos de aprendizaje maquina fueron entrenados mediante un conjunto de datos creado a partir de la extracción de características de señales EEG. Las señales EEG de 30 sujetos de la base de datos PhysioNet fueron utilizados para crear el conjunto de datos relacionado a los diferentes movimientos. Se han utilizado los electrodos C3, C1, CZ, C2, y C4 de acuerdo al estándar 10-10. Posteriormente se realizó la extracción de segmentos de señales EEG en donde fueron aplicadas una serie de mediciones relacionadas a parametros de tiempo y frecuencia, para obtener un conjunto de quince características. Se desarrolló una aplicación hecha a la medida en la versión de LabVIEW 2015™ para la lectura de las señales EEG, la selección de canales, filtrado del ruido, selección de banda, las operaciones de extracción de características, así como para la generación del archivo del conjunto de datos. El entorno de desarrollo de Matlab 2021™ fue utilizado para el entrenamiento, prueba y evaluación de las métricas de desempeño de los algoritmos de aprendizaje máquina. Dentro de este trabajo el modelo que presento las mejores métricas de desempeño fue la red neuronal artificial media con un área bajo la curva promedio de 0.9998, un coeficiente Cohen Kappa de 0.9552, un coeficiente de correlación de Matthews de 0.9819 y una perdida de 0.0147. Estas métricas sugieren la aplicabilidad de nuestro enfoque en diferentes escenarios, como la implementación en prótesis robóticas, donde el uso de características superficiales es una opción aceptable debido a que los recursos son limitados, como en un sistema embebido y dispositivos de cómputo limitados.

Palabras clave: BCI; extracción de características; inteligencia artificial; aprendizaje máquina; aprendizaje profundo; redes neuronales artificiales; comandos mentales; clasificación de señales; reconocimiento de patrones.

Thesis **ABSTRACT** of **Francisco Javier Ramírez Arias**, presented as requirement to obtain the degree of **DOCTOR in SCIENCES**, from the program of Master and Doctorate in Sciences and Engineering of Autonomous University of Baja California. Ensenada, Baja California México, December 2022.

Control of mechanisms through electroencephalographic signals

Abstract approved by:



Dr. Everardo Inzunza Gonzalez
Director of thesis



Dr. Enrique Efrén García Guerrero
Co-director of thesis

In Brain–Computer Interfaces (BCIs), it is crucial to process brain signals to improve the accuracy of the classification of motor movements. Machine learning (ML) algorithms such as artificial neural networks (ANNs), linear discriminant analysis (LDA), decision tree (D.T.), K-nearest neighbor (KNN), naive Bayes (N.B.), and support vector machine (SVM) have made significant progress in classification issues. This paper aims to present a signal processing analysis of electroencephalographic (EEG) signals among different feature extraction techniques to train selected classification algorithms to classify signals related to motor movements. The motor movements considered are related to the left hand, right hand, both fists, feet, and relaxation, making this a multiclass problem. In this study, nine ML algorithms were trained with a dataset created by the feature extraction of EEG signals. The EEG signals of 30 Physionet subjects were used to create a dataset related to movement. We used electrodes C3, C1, CZ, C2, and C4 according to the standard 10-10 placement. Then, we extracted the epochs of the EEG signals and applied tone, amplitude levels, and statistical techniques to obtain the set of fifteen features. LabVIEW™2015 version custom applications were used for reading the EEG signals; for channel selection, noise filtering, band selection, and feature extraction operations; and for creating the dataset. MATLAB 2021™ was used for training, testing, and evaluating the performance metrics of the ML algorithms. In this study, the model of Medium-ANN achieved the best performance, with an AUC average of 0.9998, Cohen’s Kappa coefficient of 0.9552, a Matthews correlation coefficient of 0.9819, and a loss of 0.0147. These findings suggest the applicability of our approach to different scenarios, such as implementing robotic prostheses, where the use of superficial features is an acceptable option when resources are limited, as in embedded systems or edge computing devices.

Keywords: EEG; BCI; feature extraction; artificial intelligence; machine learning; deep learning; artificial neural network; mental commands; signal classification; pattern recognition.

Dedicatoria y agradecimientos

Este trabajo de tesis es dedicado a las personas que han contribuido de alguna forma en mi formación personal, profesional y académica. Está dedicado a las personas que siempre han estado a mi lado en las buenas, y sobre todo en las no tan buenas. A las personas que forman parte de mi vida, de mi entorno y círculo social. A toda aquella persona que de alguna u otra manera me ha apoyado y me ha dedicado parte de su tiempo. Agradezco con especial cariño, respeto y admiración a todos mis maestros, profesores y directores de los diferentes trabajos académicos desarrollados, gracias por su tiempo, esfuerzo, recomendaciones y sugerencias.

Agradezco a mi madre, Maria Guadalupe Arias de los Palos su gran amor y cariño brindado en durante todo este tiempo y hasta la fecha. A mis hermanos Gabriela Guadalupe Ramírez Arias y Daniel Ramírez Arias, por estar siempre presentes, se les quiere mucho. A Nelly Zulay Varela Bravo, gracias por su incondicional apoyo y cariño, en general a la familia Varela Bravo, gracias. A todos mis tíos y tías de parte de la familia de mi madre y de mi padre. Con especial cariño se le agradecé a mi tío Norberto Arias de los Palos durante el apoyo brindado desde que tengo uso de razón.

Agradezco al comité de tesis, que se encuentra integrado por el Dr. Everardo Inzunza González, el Dr. Enrique Efrén García Guerrero, director y codirector de tesis respectivamente, al Dr. Oscar Roberto López Bonilla, Dr. Gilberto Manuel Galindo Aldana y Dr. Juan Miguel Colores Vargas, miembros del comité, gracias por su tiempo, participación, apoyo, comentarios, sugerencias, que ayudaron a nutrir este trabajo, y sin las cuales no habría sido posible su realización.

Agradezco también a mis compañeros de trabajo, por el apoyo y ánimo brindado durante todo este tiempo en la Facultad, son excelentes personas, y esperemos seguir consolidando amistades y proyectos en colaboración para beneficio de todos.

Agradezco a los directivos, y personal administrativo de la Facultad de Ciencias de la Ingeniería y Tecnología (FCITEC) por las facilidades en infraestructura, equipo, espacios y tiempo para el desarrollo de este proyecto de tesis.

Agradezco al Sindicato de Profesores Superación Universitaria de la Universidad Autónoma de Baja California el apoyo brindado para el pago de las cuotas del programa de doctorado. En especial al Mtro. Héctor Mejorado de la Torre, Coordinador Delegacional Tijuana, y al Mtro. José Silverio Rodríguez Arroyo. Esperando que este tipo de apoyos y otros se continúen otorgando a los profesores que formamos parte de la máxima casa de estudios. Por la realización plena del ser.

Por último, pero no menos importante me agradezco y me felicito, por haber encontrado el tiempo, las formas, y el espacio para decidirme y dedicarme a la realización de mis estudios de posgrado, los cuales son una necesidad si deseo continuar desarrollándome como profesor-investigador en esta casa de estudios. Gracias a todos, lo mejor para todos. Y con esto se cumple una promesa de años, mi abuela dijo que sería Doctor, pero no específico que tipo.

Table of Contents

Abstract	iii
Introduction	1
Background	3
Problem statement	7
Proposed solution	7
Research objectives	8
Specific research objectives	8
1. The brain	10
1.1. Brain signals	11
1.2. Neuroimaging methods	13
1.2.1. Magnetoencephalography (MEG)	14
1.2.2. Electrocorticography (ECoG)	15
1.2.3. Magnetic Resonance Imaging (MRI)	16
1.2.4. Functional Magnetic Resonance Imaging (fMRI)	17
1.2.5. Functional near-infrared spectroscopy (fNIRS)	17
1.2.6. Positron emission tomography (PET)	18
1.2.7. Single Photon Emission Computed Tomography (SPECT)	19
1.2.8. Electroencephalography EEG	19
1.3. Brain Computer Interface	21
1.3.1. Stages BCI	22
1.3.2. Signal acquisition	22
1.3.3. Signal processing	22
1.4. BCI Scenarios	23
1.5. State of the Art of BCI Applications	24
2. Classification Methods	26
2.1. Machine Learning Algorithms	28
2.1.1. Linear discriminant analysis	28
2.1.2. Decision trees	30
2.1.3. K-Nearest Neighbor (KNN)	31
2.1.4. Naive Bayes	32
2.1.5. Support vector machines	34
2.2. Artificial neural network	36
2.2.1. Activation function	38
2.2.2. Network topology	39
2.3. Classification methods used in robotics	40

3. Metodology	42
3.1. Hardware and Software	42
3.2. Input data	43
3.3. Proposed Method for EEG Signal Processing	44
3.3.1. EEG Signal Acquisition and Channel Selection	45
3.3.2. Pre-processing	45
3.3.3. EEG Band Separation	46
3.3.4. Feature Extraction	47
3.3.5. Signal Analysis	47
3.3.6. Dataset Preparation	48
3.3.7. Machine Learning Algorithm Training	50
4. Experimental results	51
4.1. Results obtained by the classification algorithms	51
4.1.1. Matrix of confusion	51
4.2. Scoring metrics	54
4.3. Performance Metrics	56
4.4. Comparative analysis of ML and ANN with ConfusionVis	60
4.5. Training time metrics	61
4.6. Discussion	62
4.7. Proposed Usage Scenario	63
5. Conclusions	65
5.1. Future Work	66
A. Fragment of the dataset created for this study	68
B. Front panel (App) for EEG signal analysis	69
C. Matlab Code for LDA Algorithm	70
D. Matlab Code for Tree Model	72
E. Matlab Code for KNN Model	74
F. Matlab Code for NB Model	76
G. Matlab Code for SVM Model	78
H. Matlab Code for Narrow-ANN Algorithm	80
I. Matlab Code for Medium-ANN Allgorithm	83
J. Matlab Code for Wide Model	85
K. Matlab Code for Bilyed Model	87

List of Figures

1.	Anatomy and areas of the brain. Modified from source: Sulek (2019)	10
2.	Brain wave sample of different band of frequencies. Modified from source Abhang et al. (2016)	13
3.	MEG device used for captures brain signals. From source: Proudfoot et al. (2014)	15
4.	Grid of sensor used in the neuroimage method of ECoG. Modified from source: Greiner et al. (2016)	16
5.	Magnetic resonance imaging scanner. Taken from source: Cohen Medical Cen- ters (2022)	16
6.	Function magnetic resonance imaging scanner. Taken from source: Romanows- ki et al. (2019)	17
7.	Function near-infrared spectroscopy system. Modified from source: Saikia et al. (2021)	18
8.	PET scanner. Taken from source: Cannon Medical Systems (2022)	18
9.	SPECT scanner. Taken from source: Siemens Healthineers (2022)	19
10.	The EEG method for measuring brain. Taken and modified from source: Worldshapers Health (2022)	19
11.	10-20 system for EEG electrode placement. Taken and modified from source: Chai et al. (2019)	20
12.	Components of BCI system. Modified from source: Aggarwal and Chugh (2019)	22
13.	Brain computer interface possible application scenarios. Modified from source: Brunner et al. (2015)	24
14.	Construction process of a classification model. Modified from source: Pramanik et al. (2021)	26
15.	Categories of most common algorithms for classification task.	27
16.	Steps of the LDA technique. Taken from source:Tharwat et al. (2017)	28
17.	General example of a Decision Tree. Modified from source: Datacamp (2022)	30
18.	Steps of the KNN algorithm. Modified from source: Chakure (2021)	31
19.	Classification by support vector machine. Modified from source: Ippolito (2021)	34
20.	Biological neural network.	36
21.	Artificial Neural Network.	37
22.	Artificial neural network, generic model.	38
23.	Examples of activation function used inside the artificial neural network.	39
24.	General topology of artificial neural network.	40
25.	Proposed method for classifying EEG signals.	42
26.	Proposed method for EEG signal classification.	44
27.	Selected electrodes for EEG signal classification. (a) Biomedical toolkit and (b) electrodes selected.	45
28.	EEG signals acquired from electrodes C3, C1, CZ, C2, and C4. (a) Original EEG signal and (b) filtered EEG signal.	46
29.	Block diagram for training, testing, and evaluating the ML algorithms.	50
30.	Scheme of the confusion matrix for binary classification.	51
31.	The confusion matrix (CM) of the four ANN algorithms trained for EEG signals classification, related to the movements of hands and feet: (a) CM of the Narrow-ANN algorithm, (b) CM of the Medium-ANN algorithm, (c) CM of the Wide-ANN algorithm, and (d) CM of the Bilayered-ANN algorithm.	52

32.	The confusion matrix (CM) of the five ML algorithms trained for EEG signals classification, related to the movements of hands and feet: (a) CM of the LDA algorithm, (b) CM of the D.T. algorithm, (c) CM of the KNN algorithm, and (d) CM of the N.B. algorithm, CM of the SVM algorithm.	53
33.	The receiver operating characteristic (ROC) curves of the four ANN algorithms trained for EEG signals classification, related to the movements of hands and feet: (a) ROC curves of the Narrow-ANN algorithm, (b) ROC curves of the Medium-ANN algorithm, (c) ROC curves of the Wide-ANN algorithm, and (d) ROC curves of the Bilayered-ANN algorithm.	57
34.	The receiver operating characteristic (ROC) curves of the top four ML algorithms trained for EEG signals classification, related to the movements of hands and feet: (a) ROC curves of the LDA algorithm, (b) ROC curves of the SVM algorithm, (c) ROC curves of the D.T. algorithm, and (d) ROC curves of the N.B. algorithm.	58
35.	ConfusionVis Theissler et al. (2022): Comparative evaluation of the multiclass classifiers based on confusion matrices. (a) Averaged Accuracy per model, (b) Confusion Matrix Similarity, (c) Error by class, and (d) Error by Model. . .	60
36.	Training time of the nine ML models.	61
37.	Suggested usage scenario for an application of mechatronic control system. .	64
38.	Fragment of the dataset created for this study.	68
39.	Front panel of software (App) developed for EEG signal analysis.	69

List of Tables

1.	Lobes of the brain and functions associated.	11
2.	Bands of frequency related to brain activity and associated cognitive task. .	12
3.	Neuroimaging methods advantages and disadvantages.	14
4.	Neuroimaging methods differences.	14
5.	BCI robotics and control applications.	25
6.	Classifier used in robotics and control applications.	41
7.	Tasks presented in the dataset to train the ML algorithms for EEG signal classification.	44
8.	Cut-off frequencies of bandpass filters for band extraction of EEG signals. . .	46
9.	Features of the EEG signal used to train the ML algorithms.	49
10.	List of algorithm used for EEG classification.	51
11.	The average score parameters of the EEG classification algorithms.	56
12.	Performance metrics of the nine ML algorithms trained for EEG signal classification.	59

Introduction

For more than 80 years, the brain's electrical activity can be recorded through electrodes placed on the surface of the skull Niedermeyer and da Silva (2005). This non-invasive neuroimaging technique, called electroencephalography (EEG), has made it possible to monitor brain activity. In 1973, the concept of brain-computer interface (BCI) was introduced Vidal (1977), a technology that uses EEG. Both technologies have been used in different fields of application. In the field of medicine they are used for the prediction and diagnosis of various clinical conditions such as; prediction of sleep disorders Kupfer et al. (1978); Kazemi et al. (2022); Tiwari and Arora (2022), attention deficit Ghaderyan et al. (2022), hyperactivity disorders Mahmoud et al. (2021), seizure disorders Affes et al. (2022); Mormann et al. (2000), peripheral neuropathies Bismuth et al. (2020) and musculoskeletal diseases Wei et al. (2010), prediction of epileptic seizures Shen et al. (2022); Tuncer and Bolat (2022); Ruijter et al. (2018), diagnosis of disorder of consciousness Bai et al. (2021); Lei et al. (2022), detection of tumors and concussions Abdulkader et al. (2015b); Selvam and Shenbagadevi (2011). These have also been used for the early determination of neurodegenerative disorders such as Alzheimer's Jeong (2004), Parkinson's Solís-Vivanco et al. (2018), and different types of dementia Stylianou et al. (2018).

One of the areas of research and application of computational sciences uses brain-computer interfaces (BCI), which translate brain signals into control commands that allow the user to communicate with the machine without the participation of muscles and peripheral nerves. BCI, in its simplest structure, can be considered an EEG device. The BCIs allow capturing different signals from the brain's surface, just like the EEG, with the main difference being that these signals are analyzed and processed in real-time. These electrical signals are capable of providing us with information about both the hemispheres and the different areas that the human brain has. The information provided by these electrodes can not only be used for the diagnosis and detection of tumors, brain injuries, sleep disorders, mental illnesses, and the diagnosis of psychological disorders. These also allow us to obtain information about the motor movements of the human body, such as hands, arms, legs, and feet, which can be used in applications of a biomedical, robotics, and assistance robotics.

In order to measure and record the brain's activities, different neuroimaging techniques are used, including magnetoencephalography (MEG) Gross (2019), electrocorticography (ECoG) Ince et al. (2009), intracortical neuronal recording, functional magnetic resonance (fMRI) Son et al. (2020), near-infrared spectroscopy (NIRS) Coyle et al. (2004), and electroencephalography (EEG), the latter being the neurophysiological technique Ramadan and Vasilakos (2017) most widely accepted by the scientific community and the private sector in the development of research in fields such as neuroscience, robotics, home automation, the Internet of Things, education, etc. Fontanillo Lopez et al. (2020).

EEG can be carried out using multiple electrodes placed under different international systems. The electrodes are considered an essential component in these systems because they must have good conductivity and contact with the surface, which improves the quality of the signal to be measured. These standards must be adhered to when attempting to conduct a clinical diagnosis. However, there is no standard definition for applications related to the control of robotic prostheses and mobile robots. Different research works focus on improving the electrodes because digital filtering functions can be embedded in them.

The data obtained through the different neuroimaging techniques can provide us with qualitative and quantitative information on the different brain regions, establish correlations and generate mathematical models, predictive models, and models that allow the classification of these data with a high percentage of reliability. Currently, it is possible to obtain information from specific parts or regions of the brain using a certain number of electrodes. It provides an alternative of cost, safety, portability, and reliability. These allow for establishing an effective neuroimaging method that covers many applications. However, some of the details that electroencephalography presents are that it has a low spatial resolution but good temporal resolution, and the signal-to-noise ratio is sometimes low because the electrodes are not at the origin of the signal. Different types of artifacts are present in EEG signals, caused by AC line noise, eye movements, and eye movements, among others.

Background

Electroencephalography (EEG) is a non-invasive procedure for measuring the electrical activity generated within the brain as a result of different mental processes Esqueda-Elizondo et al. (2022). The electrical signals are acquired through electrodes placed on the scalp's surface; thus, waves with different amplitudes and frequencies that refer to a person's mental state are obtained Teplan (2002). The frequency ranges span from 0 Hz to 100 Hz. Based on these ranges, the signals are classified as follows: delta, which ranges from 1 Hz to 4 Hz; theta, which contains signals from 4 Hz to 8 Hz; alpha, where the information range is between 8 Hz and 12 Hz; beta, where the range is between 12 Hz and 30 Hz; and gamma, with a range that covers from 30 Hz to 100 Hz Tiwari et al. (2018); Luján et al. (2021). Different ranges of signals are essential for identifying different clinical problems, such as schizophrenia Shoeibi et al. (2021), Alzheimer's, insomnia, epileptic disorders, brain tumors, and different injuries and infections related to the central nervous system. Furthermore, classification of motor impairment in neural disorders by means of EEG signals processing, has been a successful method for identifying central nervous system's roots of motor disabilities Vrbancic and Podgorelec (2018). Compared with other methods, this neuroimaging technique offers advantages such as portability, temporal resolution, safety, cost, small time constants, simple equipment, and effectiveness Abdulkader et al. (2015a).

The EEG neuroimaging method is the preferred method for developing Brain-Computer Interfaces (BCIs), both in the academic community and the private sector. Historically, BCI has been clinically applied for understanding motor impairment, both in verbal communication Neuper et al. (2003), limb movement Bartur et al. (2019), as well as cognitive impairment Sergeev et al. (2021), and offer a great advantage over electromyography pattern recognition Samuel et al. (2017b) due to the lack of neuromuscular signals under amputation conditions. BCIs are direct communication and control channels between users' brain and computers where muscle activity is not involved Wang et al. (2015); Zander and Kothe (2011). They are currently considered a powerful communication technology as they do not involve muscular routes to complete tasks such as communication, commands, and actions. The basis of these systems is the computer, whose central role is the analysis of EEG signals Aggarwal and Chugh (2019); Mudgal et al. (2020). BCIs are classified as exogenous and endogenous. Exogenous BCIs require external conditions or stimuli so that the brain can generate a

particular response based on the stimulus. Endogenous BCIs do not require external stimulation; however, they require some training on the user's part so that they can regulate brain rhythms Mudgal et al. (2020). Despite the differences mentioned, most BCI models contain the following elements: signal acquisition, information preprocessing, feature extraction, and classification Brunner et al. (2015); Abdulkader et al. (2015a). The acquisition of signals is carried out employing electrodes placed on the scalp's surface Jurcak et al. (2007), through which analog signals are obtained and then digitized by means of analog–digital converters. The next step is the preprocessing of the signals, whereby the following are removed: noise induced by the electrical line; the background noise of the brain; various artifacts that the EEG signals present as a result of some muscular activity such as eye movement, facial muscle activity, etc. Peng et al. (2011). Feature extraction is one of the crucial steps due to its impact on the performance of classification algorithms Khalid et al. (2014). Some of the obtained features are in the domains of time and frequency Khalid et al. (2014), i.e., mean, median, variance, maximum, and minimum, among others Saeidi et al. (2021); Stancin et al. (2021). The feature extraction process produces a vector containing the most relevant features of the EEG signals, used as input for classification algorithms. The next step is classification, which is carried out by different algorithms, including LDA, SVM Subasi and Ismail Gursoy (2010), KNN Yazdani et al. (2009), D.T. Edla et al. (2018), N.B., and ANN Saragih et al. (2020).

Currently, there are different fields of science, engineering, and research that evaluate and make use of BCIs to develop applications that present solutions to complex problems Han et al. (2018) Casey et al. (2021). These have been possible due to advances in high-density electronics, data acquisition systems that allow high-quality EEG signals to be acquired, intelligent systems that use machine and deep learning algorithms, and neural networks that allow pattern recognition and signal classification to be performed with high precision. In Brunner et al. (2015), the authors explain that BCIs can be used in the following six application scenarios: replace, restore, augment, enhance, supplement, and research tools. The authors of van Erp et al. (2012) commented that current and future BCI application areas are: device control, user status monitoring, assessment, training and education, gaming and entertainment, cognitive enhancement, safety, and security. Intelligent systems commonly incorporate machine learning (ML) approaches Navarro-Espinoza et al. (2022); Cerrada et al.

(2022); Enríquez Zárata et al. (2022). ML refers to a system able to learn from training data from certain activities so that the analytical model generation process is automated, and associated tasks can be completed or supplemented Janiesch et al. (2021b); Fong-Mata et al. (2020). Deep learning (DL) is a paradigm within ML based on the use of artificial neural networks (ANNs) Janiesch et al. (2021a). Commonly, ML algorithms focus on classifying EEG signals related to the motor and imaginary movements of hands and feet to carry out control actions, as presented in Cho et al. (2018); Roy et al. (2021); You et al. (2020); Faiz and Al-Hamadani (2019). DL is useful in areas with vast and high-dimensional data, therefore deep neural networks outperform ML algorithms for most text, images, video, voice, and audio processing techniques LeCun et al. (2015). Nevertheless, for low-dimensional data input, especially with insufficient training data, ML algorithms may still achieve superior results Zhang and Ling (2018), which are even better interpretable than deep neural network results Rudin (2019). The authors of Alomari et al. (2013) used power, mean, and energy as features to classify EEG signals related to the right and left hands through artificial neural networks (ANNs) and support vector machine (SVM). In Pinheiro et al. (2018), the authors used SVM to control the direction of a wheelchair by extracting the mean, energy, maximum value, minimum value, and dominant frequency characteristics of the EEG signals. In Bousseta et al. (2018), the authors used the Fast Fourier Transform and Principal Component Analysis as characteristics of the EEG signals to feed the SVM classifier to control a robotic arm. The authors of Tang et al. (2016) reported the use of EEG signals to control an exoskeleton and the use of SVM, LDA, and NN for their respective classification. Studies such as the one presented in Kant et al. (2020) have used pre-trained neural network models to classify EEG signals through time–frequency characteristics. Recent studies have focused on the proper selection of EEG signal characteristics and its effect on the accuracy of ML and DL algorithms, as presented in Stancin et al. (2021). ML and DL techniques are widely accepted and help to develop specific tasks within different applications Kaur et al. (2023); Theissler et al. (2022); Sabharwal and Miah (2022); Haque et al. (2022); Contreras-Luján et al. (2022); Aboneh et al. (2022); Bi et al. (2013). Moreover, they are increasingly used to obtain EEG data for pattern analysis, classification of group membership, and BCIs Saeidi et al. (2021); Abbasi and Goldenholz (2019); Majidov and Whangbo (2019); Craik et al. (2019); Padfield et al. (2019); Lawhern et al. (2018); Lotte et al. (2018). However, there are

still open research problems, such as the real-time processing of EEG signal classification and the optimization of ML algorithms for implementation on embedded systems or edge computing devices. Hence, research on and development of reliable, efficient, and robust systems for EEG signal classification, among others, should be pursued Abdulkader et al. (2015a); Mridha et al. (2021). The complexity of human movements for the manipulation of tools is very high and diverse, for an adult human brain that has automated different movements, it does not represent a major effort, however, for ML it requires the management of precise information inputs that allow programming and execution of free movement. Previous studies, offer multiple classes of motor imagery limb movements based on EEG spectral and time domain descriptors Samuel et al. (2017a), in this sense, there continues to be a need in machine learning to increase the reliability and accuracy of EEG signals used for programming human-like movements.

For the reasons stated above, the aim of this paper is to evaluate nine ML algorithms for the classification of EEG signals. The purpose is to find which ML model presents the best performance metrics for the identification of movement patterns in EEG signals for the control of a mechatronic system, in this case, a robotic hand prosthesis. The selected dataset consists of more than 1500 EEG recordings of 1–2 min in length from 109 subjects and is publicly available in Goldberger et al. (2000). In this study, we randomly selected 30 subjects to train, validate, and test the proposed method. The ultimate aim is to facilitate the development of robotic limb prosthetics, which is possible because ML algorithms can recognize patterns in EEG signals with complex dynamics. The hypothesis is that ML algorithms perform better in tasks of signal classification than standard methods. The novelty of this study is to provide a methodology for the classification of EEG signals by training several ML algorithms and employing processing, analysis, and feature extraction techniques in the time domain of various lapses of EEG signals related to motor tasks, which can be translated into commands for the control of mechanisms or mechatronic systems such as wheelchairs, robotic prostheses, and mobile robots.

Therefore, in this Ph.D thesis, a methodology is provided for extracting features from EEG signals and training five ML models and four ANN. Both the extraction of characteristics and the generated models of machine learning and artificial neural networks can be implemented in portable, low-cost, and consumption systems that control mechanisms through EEG sig-

nals. The novelty of this Ph.D thesis is developing a high-level graphic language application that allows the generation of different personalized data sets. The extracted data represents the EEG signals' most significant or relevant characteristics in the time domain. Specifically, the novelty lies in how the characteristics extracted from the EEG signals are positioned in the data set. These data sets allow the training, verification, and testing of machine learning algorithms and artificial neural networks. The experiments show that the proposed methodology provides good results for classifying EEG signals related to motor movements of the left hand, right hand, hands, feet, and relaxation. The development of machine learning models and artificial neural networks with classification percentages above 90 percent will allow the use of these models in robotic applications such as the control of biomedical prostheses.

Problem statement

The recording of EEG signals is more than 80 years old, brain-computer interfaces were introduced in 1970, and the classification of EEG signals captured by these interfaces began in 1988. The scientific community's interest in this research field began in late 1999 and early 2000. Since then, different approaches have been used for classifying electroencephalographic signals, where the primary approach used was the same as that used in pattern recognition systems. Currently, we find various investigations on the development of electroencephalographic signal classification systems that are implemented through the development of software in personal computers and that use machine learning algorithms and deep learning.

- The current methods for classifying EEG signals are complex, making their implementation difficult in embedded systems for real-time applications.
- Different investigations use few test subjects to obtain the performance metrics of machine learning algorithms for classifying EEG signals.

Proposed solution

This research developed a high-level graphical language application to carry out the pre-processing, processing, and extraction of features in the time domain in different frequency bands of electroencephalographic signals. The set of features extracted from the electroencephalographic signals is passed to different machine learning algorithms for their respective classification. These algorithms were developed in the Matlab 2021 development environment. One of the features of this version is that machine learning algorithms can be implemented in embedded development platforms such as Raspberry Pi 4 or NVIDIA Jason Nano. These platforms provide excellent reliability, portability, and multiple benefits compared to a computer.

Research objectives

The main research objective is to develop a methodology for classifying electroencephalographic signals through the extraction of different characteristics of the signals using machine learning algorithms and artificial neural networks.

Specific Research objectives

- Develop software that allows the reading of the database that contains the files of the electroencephalographic signals.

- Implement algorithms that allow segments of the electroencephalographic signals to be selected for their subsequent analysis.

- Design and develop algorithms that allow the preprocessing and processing of brain signals.

- Develop algorithms that allow the extraction of characteristics from electroencephalographic signals.

- Design and develop strategies to carry out the training of machine learning algorithms and artificial neural networks.

- Analyzing the performance metrics of the artificial neural network and machine learning algorithms used to classify electroencephalographic signals.

- Publish the research results in a high-impact JCR journal.

Chapter I

1. The brain

The most sophisticated structure in a human is the brain; it is considered to be a crucial part of the central nervous system and is situated inside the skull Savadkoohi et al. (2020). It is composed of 100 billion neurons on average Lent et al. (2012), which generate new interconnections between them when learning activities or new experiences are developed Mateos-Aparicio and Rodríguez-Moreno (2019).

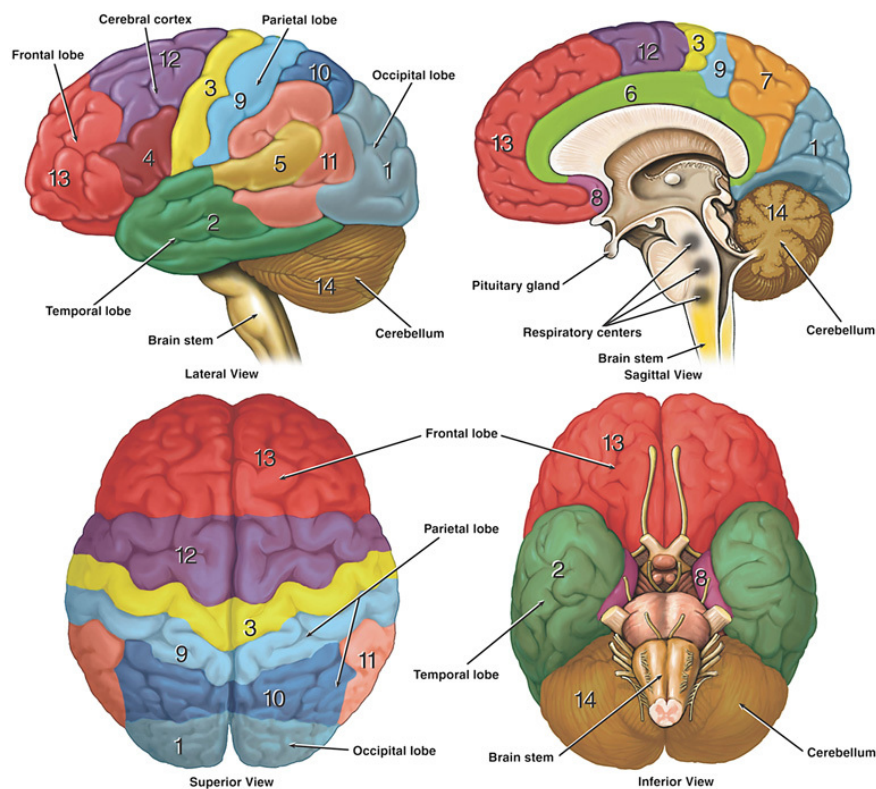


Figure 1: Anatomy and areas of the brain. Modified from source: Sulek (2019)

The human brain's main components include; the cerebrum, cerebellum, and brainstem. The cerebrum is an essential part, it is separated into the left and right hemispheres, where the right hemisphere is in charge of regulating the muscular activity of the left side of the human body. In contrast, the left hemisphere governs the movement of the right side Carter (2019). Four areas known as lobes separate each hemisphere: the frontal lobe, parietal lobe, occipital lobe, and temporal lobe. Figure 1 shows the human brain's anatomy and different

functional areas. Table 1 presents the different lobes that make up the brain and the functions associated with each of these regions.

Table 1: Lobes of the brain and functions associated.

Brain lobe	Function
Occipital lobe	Liabile for processing and analyzing visual information.
Temporal lobe	The sound processing center includes language and some forms of memory.
Parietal lobe	Home of the somatosensory cortex, an area of the brain responsible for processing sensations and touch information and diverse factors of spatial processing.
Frontal lobe	The most significant and most complex part of the brain lobes is responsible for executive functions, reasoning, decision making, sensory integration, planning, and movement execution.

The cerebellum is comparable in structure to the cerebrum. It has two hemispheres, and it is sometimes called the little brain. The cerebellum receives visual, auditory, ventricular, and somatosensory information. It also receives information about individual muscle movements directed by the brain. Therefore, its primary function is to coordinate the actions of the body integrating the control of the muscles, including balance, posture, and equilibrium Carlson (2005).

1.1. Brain signals

Communication between neurons within the brain is through the sending of electrochemical signals from one cell to another. The electrical signal from an individual neuron is too small to be detected by an electrode placed on the brain's surface. However, when hundreds of neurons activate, each small electrical current's contribution causes a strong signal detected by an electronic sensor, such as an electroencephalogram. If a set of neurons is activated synchronously, the sum of the activity can result in a perceptible signal on the scalp. In contrast, if the neurons within the group fire asynchronously, the sum of the action results in a small and intermittent signal. Table 2 compares the frequency bands, properties, and cognitive activities related to each brain signal.

Table 2: Bands of frequency related to brain activity and associated cognitive task.

Type	Frequency range (Hz)	Mental Activity
Delta	1-4	Liabile for processing and analyzing visual information.
Theta	4-8	The sound processing center includes language and some forms of memory.
Alpha	8-12	Home of the somatosensory cortex, an area of the brain responsible for processing sensations and touch information and diverse factors of spatial processing.
Beta	12-30	The most significant and most complex part of the brain lobes is responsible for executive functions, reasoning, decision making, sensory integration, planning, and movement execution.

Investigators categorize these brain signals into distinguishing frequency ranges or frequency bands: Delta (1 – 4 Hz), Theta (4 – 8 Hz), Alpha (8 – 12 Hz), Beta (12 – 25 Hz), and Gamma (30Hz) Ramzan and Dawn (2019). Each wave type correlates with various mental states, internal factors, and external conditions Niedermeyer and da Silva (2005). The Delta brain wave is the slowest and the one with the most significant amplitude, and its frequency range is between 1 – 4 Hz. Delta signals are only present in deep sleep and alert states. The typical studies related to these waves are for diagnosing sleep disorders and indicators of diseases such as alcoholism. Theta waves oscillate in a range between 4 – 8 Hz Kahana et al. (1999). They are present in states of inspiration, deep meditation, moments of leisure, and creativity. It correlates with complex mental operations, such as attention, information taking, processing, and learning. The 8 - 12 Hz oscillations are defined as the Alpha rhythm. This wave is associated with relaxation, concentration, and sometimes attention. Typical studies on the Alpha wave are meditation, biofeedback training, and attention. The Beta band oscillates between 12 – 25 Hz. It becomes stronger when we plan or execute movements Sleight et al. (2009). It is also related to alertness, thinking, and active concentration. Studies

of activity and alert induction use this wave as a reference. The somatosensory cortex exhibits the Gamma band. It can be shown in the ability to identify noises, objects, and tactile experiences. The Figure 2, shows the differences between five types of brainwaves.

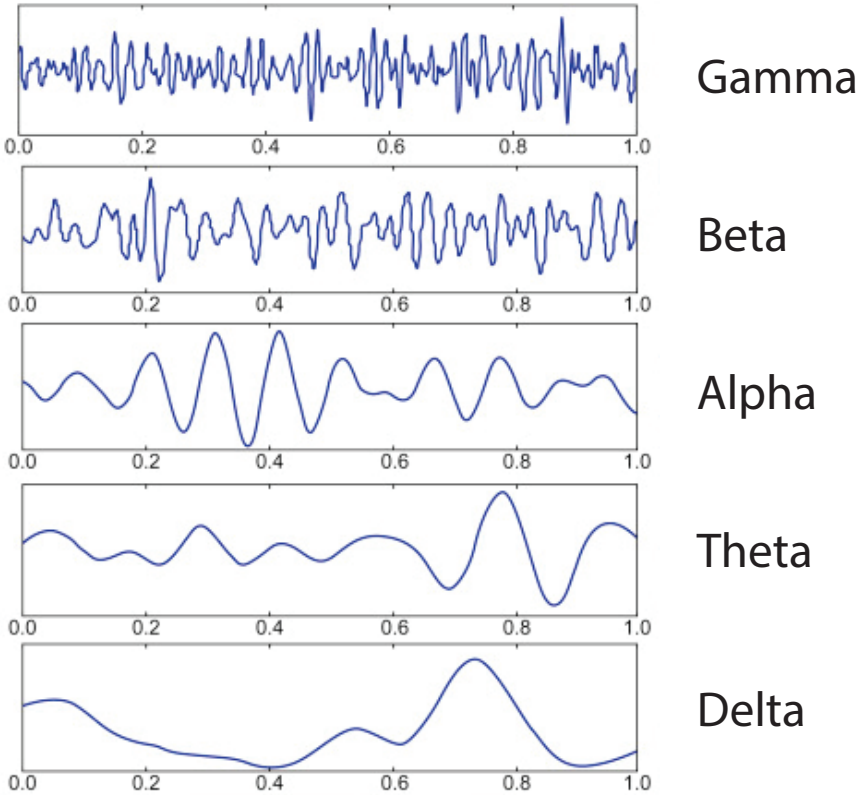


Figure 2: Brain wave sample of different band of frequencies. Modified from source Abhang et al. (2016)

1.2. Neuroimaging methods

Researchers have developed and used different neuroimaging techniques to measure and register the brain’s electrical activity and blood flow resulting from thoughts or physical movements. Among the most common methods are: Magnetoencephalography (MEG), Electro-corticography (ECoG), Magnetic Resonance Imaging (MRI), Functional near-infrared spectroscopy (fNRI), Positron emission tomography (PET), Single photon emission computed tomography (SPECT), electroencephalography (EEG). Table 3 summarizes the benefits and weaknesses of each method, and Table 4 offers us a comparison between these methods.

Table 3: Neuroimaging methods advantages and disadvantages.

Neuroimaging Method	Advantages	Disadvantages
Magnetoencephalography (MEG)	<ul style="list-style-type: none"> ▪ Excellent temporal resolution and better spatial resolution than EEG. ▪ Helps in the focus identification in some brain diseases. 	<ul style="list-style-type: none"> ▪ Equipment very expensive . ▪ Detects magnetic field in parallel.
Electrocorticography (ECoG)	<ul style="list-style-type: none"> ▪ Direct measurements. ▪ Better precision and sensitivity than EEG. 	<ul style="list-style-type: none"> ▪ It required surgery. ▪ The signal might be affected by anesthetics.
Magnetic Resonance Imaging (MRI)	<ul style="list-style-type: none"> ▪ It does not involve radiation exposure. ▪ Valid for the scanning and detecting of irregularities in soft tissue structures, including the brain. 	<ul style="list-style-type: none"> ▪ High installation, operation, and maintenance costs. ▪ Scanning is done indoors and generates quite a bit of noise.
Functional near-infrared spectroscopy (fNRI)	<ul style="list-style-type: none"> ▪ Good spatial and temporal resolution. ▪ Relatively inexpensive compared with PET. 	<ul style="list-style-type: none"> ▪ Temporal resolution poor compared to other methods. ▪ The information is limited by the temporal dynamics.
Positron emission tomography (PET) and single photon emission computed tomography (SPECT)	<ul style="list-style-type: none"> ▪ Most of the brain activities can be detected, for an efficient diagnosing. ▪ Good spatial and temporal resolution. 	<ul style="list-style-type: none"> ▪ No brain image can be retrieved. ▪ Not provided location of the diseases or injuries.
Electroencephalography (EEG)	<ul style="list-style-type: none"> ▪ Inexpensive. ▪ Efficient in diagnosing some brain diseases. 	<ul style="list-style-type: none"> ▪ Does nos provide an image for determination of brain injuries.

Table 4: Neuroimaging methods differences.

Method	Invasiveness	Signal	Temporal	Spacial	Portability
EEG	No	Electronic	Medium	Low	Yes
ECoG	Yes	Electronic	High	High	Yes
MEG	No	Magnetic	Medium	Medium	No
PET	No	Metabolic	High	High	No
SPECT	No	Metabolic	High	High	No
MRI	No	Metabolic	High	High	No
fMRI	No	Metabolic	High	High	No
fNRI	No	Metabolic	Medium	Medium	Yes

1.2.1. Magnetoencephalography (MEG)

It is a technique that measures the magnetic fields produced by electrical currents that occur naturally in the brain Sosa et al. (2011). Through the use of this technique, it is possible

to measure even small magnetoencephalographic signals through the use of superconducting quantum interference (SQUIR) devices . This technique requires a particular setting in laboratories because other magnetic fields can interfere with MEG signals, such as the earth's magnetic field He et al. (2013). Figure 3 shows a MEG machine used for brain imaging. The signals are less distorted by the cranial layer compared to magnetic fields; however, this advantage does not present a considerable improvement in performance and training time compared to other techniques Abdulkader et al. (2015a).



Figure 3: MEG device used for captures brain signals. From source: Proudfoot et al. (2014)

1.2.2. Electrocorticography (ECoG)

A technique that allows measuring the brain's electrical activity through the implantation of meshes or strips of electrodes on the cerebral cortex. The spatial resolution of the signal is better than other techniques, and the signal-to-noise ratio it presents is superior due to its proximity to the origin of neuronal activity Tiwari et al. (2018). This technique has various drawbacks, among which the area of the brain where the position of the electrodes is exposed makes it impossible to use this technique outside the operating room ref. Figure 4 presents the grid of sensor used in ECoG .

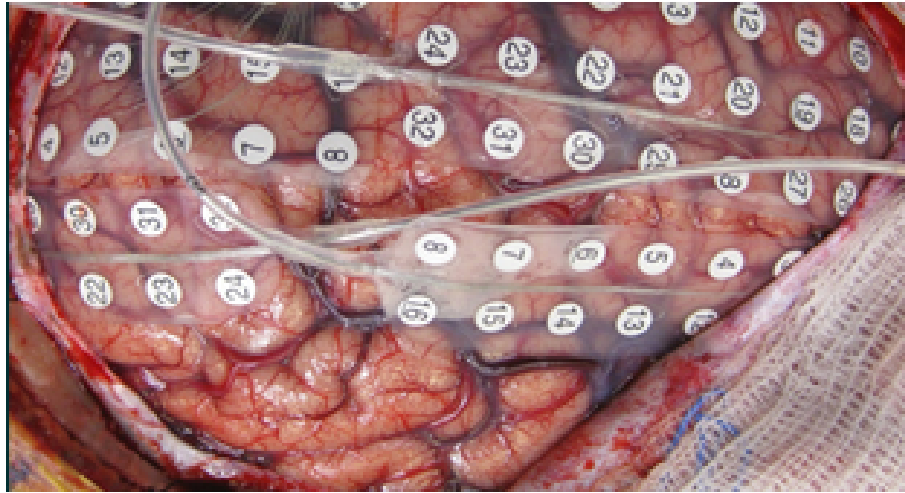


Figure 4: Grid of sensor used in the neuroimage method of ECoG. Modified from source: Greiner et al. (2016)

1.2.3. Magnetic Resonance Imaging (MRI)

Neuroimaging procedure employs magnetic fields and radio waves to provide detailed brain images. MRI helps find abnormalities in the brain and what causes them. This technique can contrast both hemispheres of the brain to determine the anomalies are located on which side. This neuroimaging technique provides better results than computed tomography due to its high-contrast images Balafar et al. (2010). Figure 5 presents a MRI device to acquired brain signals.



Figure 5: Magnetic resonance imaging scanner. Taken from source: Cohen Medical Centers (2022)

1.2.4. Functional Magnetic Resonance Imaging (fMRI)

This neuroimaging technique records changes in blood flow associated with neural activity. The increased neuronal activity requires oxygen, which is transported through the blood. The magnetic effects of oxygenated blood are distinct from those of deoxygenated blood. These properties are measured by fMRI as a distribution of the magnetic field generated by the protons Sitaram et al. (2008). The fMRI technique presents an excellent spatial resolution, while the characteristics of temporal resolution are low. However, fMRI makes it possible to capture information from deep brain parts that cannot be observed by measuring electric or magnetic fields. Figure 6 shows a fMRI scanner from SIEMENS company.

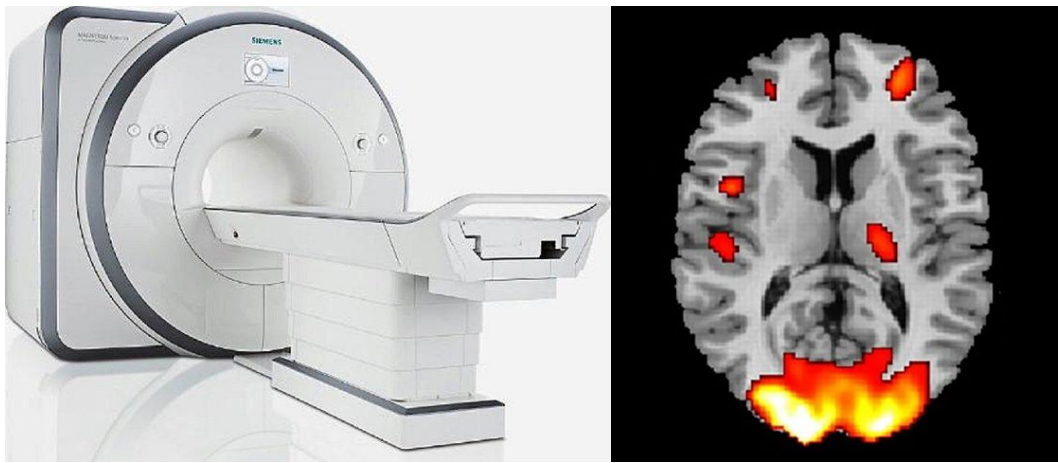


Figure 6: Function magnetic resonance imaging scanner. Taken from source: Romanowski et al. (2019)

1.2.5. Functional near-infrared spectroscopy (fNIRS)

fNIRS is a non-invasive neuroimaging method that measures blood dynamics in the brain to detect neural activity. It uses near-infrared light to determine blood flow Bunce et al. (2006). This technique projects infrared light into the brain to measure changes in diverse wavelengths as the light is reflected. fNIRS usually detects shifts in blood volume and oxygenation. fNIRS is a less helpful method compared to MRI or fMRI. One of the outstanding advantages of this technique is its portability, lower cost, and feasible alternative for medical studies and practical applications Saikia et al. (2021). Figure 7 presents a fNIRS system.



Figure 7: Function near-infrared spectroscopy system. Modified from source: Saikia et al. (2021)

1.2.6. Positron emission tomography (PET)

This technique monitors and detects any irregularity within the metabolic processes of the different organs of the human body, including the brain. An injection of radionuclides in patients is necessary to emit positrons interacting with electrons in the monitored area Ramadan and Vasilakos (2017). The interaction generates gamma rays, which can be used to construct an image. One of the significant disadvantages registered by different studies of this neuroimaging technique is the operation and maintenance cost Pfurtscheller et al. (2010). Figure 8 shows a PET scanner device.

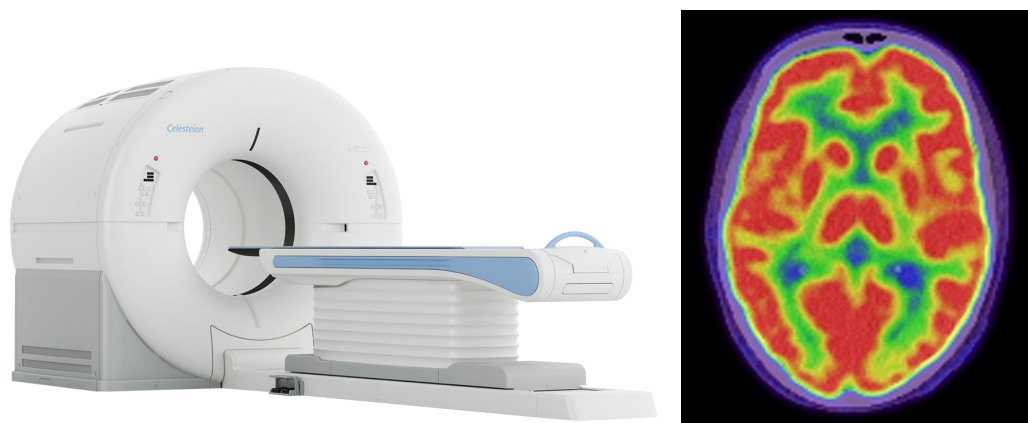


Figure 8: PET scanner. Taken from source: Cannon Medical Systems (2022)

1.2.7. Single Photon Emission Computed Tomography (SPECT)

SPECT is a nuclear tomography imaging neuroimaging technique that employs gamma rays produced by radioactive isotopes. The introduction of isotopes into the human body is by injection. SPECT devices produce two-dimensional images Roarke et al. (2008). This technique utilizes a set of 2D images to create a three-dimensional image. SPECT has a spatial resolution of about 1 cm and several seconds in terms of temporal resolution Castermans et al. (2013). Figure 9 shows a SPECT scanner from the company SIEMENS.



Figure 9: SPECT scanner. Taken from source: Siemens Healthineers (2022)

1.2.8. Electroencephalography EEG

EEG is recording electrical activity through the scalp through voltage fluctuations caused by the activity of neurotransmitters within the brain. Electrodes are placed on a cap-type device or directly on the scalp surface, as shown in Figure 10.

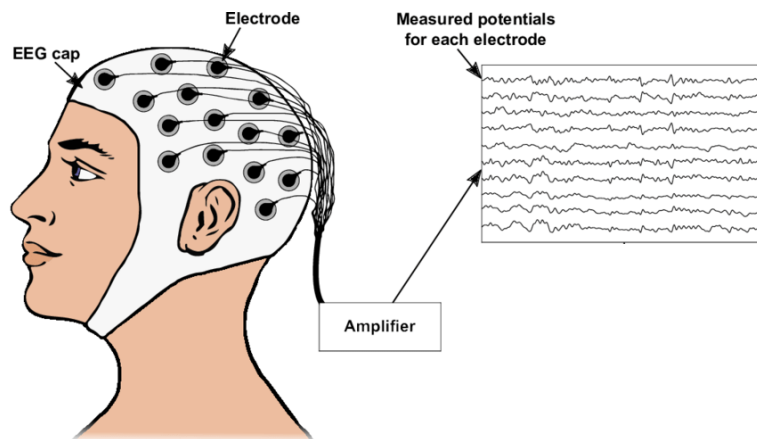


Figure 10: The EEG method for measuring brain. Taken and modified from source: Worldshapers Health (2022)

This method has a unique usability advantage over different methods for recording neural activity. It is an easy method to use, has excellent portability, and is economical. EEG recordings provide high temporal resolution Biasiucci et al. (2019). This method’s main challenges are the signal-to-noise ratio and spatial resolution. Several techniques were proposed to improve the localization of the signals and their spatial resolution. Using up to 256 electrodes is the most significant, along with creating various standards for electrode location, including 10-20, 10-10, and 10-5 Jurcak et al. (2007).

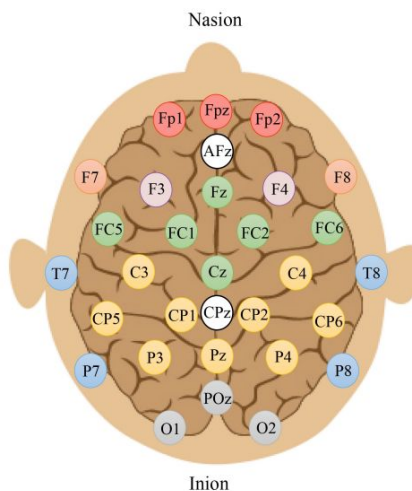


Figure 11: 10-20 system for EEG electrode placement. Taken and modified from source: Chai et al. (2019)

The image in figure 11 shows the 10-20 positioning standard, where the adjacent distance between the pair of electrodes must be between 10 or 20 of the skull diameter. Using passive and active electrodes increases the signal-to-noise ratio. Passive electrodes require an external amplifier to amplify the measured signals, while active electrodes have built-in amplifiers. Whether using passive or active electrodes, what is sought is to reduce ambient noise, line noise, and signal weakness due to cable movement. Using gel or saline solution to lower the impedance of the electrode’s contact with the skin is another disadvantage of EEG. Dry electrodes are currently the best solution for this issue Zander and Kothe (2011).

The EEG neuroimaging method is the preferred method for developing Brain–Computer Interfaces (BCIs), both in the academic community and the private sector. Historically, BCI has been clinically applied for understanding motor impairment, both in verbal communication Neuper et al. (2003), limb movement Bartur et al. (2019), as well as cognitive impairment Sergeev et al. (2021), and offer a great advantage over electromyography pattern recognition

Samuel et al. (2017b) due to the lack of neuromuscular signals under amputation conditions.

1.3. Brain Computer Interface

Brain-computer interfaces are complete systems that include hardware and software that manipulate signals from the human brain to control computers and different communication devices Ramadan and Vasilakos (2017). However, we can find other definitions in the literature; some of these are the following:

- BCI technology is a powerful communication mechanism between users and systems. It does not demand the intervention of any external device or muscles to send commands and achieve interactions Abdulkader et al. (2015a).
- A BCI employs the signals to establish a link between the person's mental state and a computer-based signal processing system, which analyzes the signals Aggarwal and Chugh (2019).
- BCI can improve collaboration between the brain and a device, which allows direct electrical signals from neurons to external devices such as a computer or a robotic arm Mudgal et al. (2020).
- BCI, also known as Human Machine Interface, includes the recording and decoding brain signals to control external devices Kant et al. (2020).

A BCI must possess the following qualities to qualify as such:

- Take direct measurements of brain activity.
- Deliver user feedback.
- Work online.

Depend on the control intent (that is, users must select to perform a mental task to send a message or command every time they want to use the BCI) Pfurtscheller et al. (2010).

1.3.1. Stages BCI

BCI generally consists of three stages: signal acquisition, signal processing, and application. Figure 12 shows the components of the BCI and their relations.

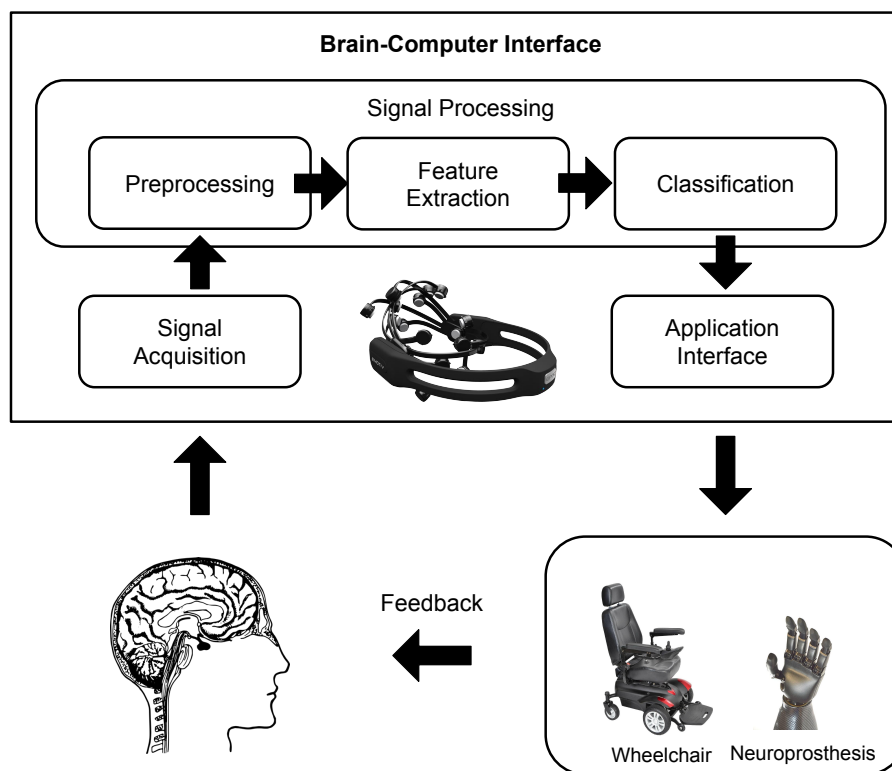


Figure 12: Components of BCI system. Modified from source: Aggarwal and Chugh (2019)

1.3.2. Signal acquisition

The brain signals acquired by electrodes are placed in different configurations on the scalp or over the brain's surface. The acquired signals should ideally be free of noise and artifacts. The most commonly used method inside the BCI is EEG due to its lower cost, easy implementation, lower cost, and temporal resolution.

1.3.3. Signal processing

This module is divided into different phases, among which are: preprocessing, feature extraction, and classification.

- Preprocessing: the assignment of this phase is to prepare the recorded signal for processing by improving the signal-to-noise ratio. Part of the electrical signal acquired by

the EEG electrodes is related to eye and head muscle movements. It does not include knowledge related to the electrical signal from the brain. These signals that do not provide information, but are part of the signal, are considered artifacts and should not be processed but eliminated to obtain the relevant information from the EEG signal. Carrying out an adequate preprocessing of the EEG signals is of great relevance to obtaining high results in classification accuracy.

- Feature extraction: After preprocessing the signals, the signals are analyzed by one or more feature extraction algorithms. In this phase, the most relevant characteristics of the signal in the time, frequency, and time-frequency domain are extracted. A wide variety of feature extraction methods are used within BCI systems. These methods include amplitude measurements, power bands, parameters or coefficients of some transform, autoregressive models, wavelets, and spatial filters.
- Classification: Once the relevant characteristics of the signals have been extracted, it is necessary to classify these components of brain patterns. Classification algorithms may be able to use linear and non-linear methods.

1.4. BCI Scenarios

The applications of BCIs can be pretty broad, as well as the different areas they can impact. Nevertheless, experts in this area propose six possible application scenarios. These scenarios are in the Figure 13, and listed below:

1. Replace the loss of any body member due to illness or accident is a field application of the BCI. Some examples include speech synthesis systems, assisted environments, and wheelchair control.
2. Restoring the loss of motor functions, such as the movement of arms and hands, allows the control of robotic neuroprostheses.
3. Enhance the body response is another possible application scenario for BCIs. Among the possible application examples, we find increasing the immersion experience in video games and education when performing specific tasks such as driving, reading, or writing.
4. Supplementing the human body with other robotic arms or being able to carry out remote control of mobile robots will allow more complex tasks to be carried out.

5. Improve the human body's response to processes such as rehabilitation by providing feedback to the patient on their progress.

6. Research tool is a scenario that will allow investigating the functions of the central nervous system to know the brain functions in clinical and non-clinical studies.

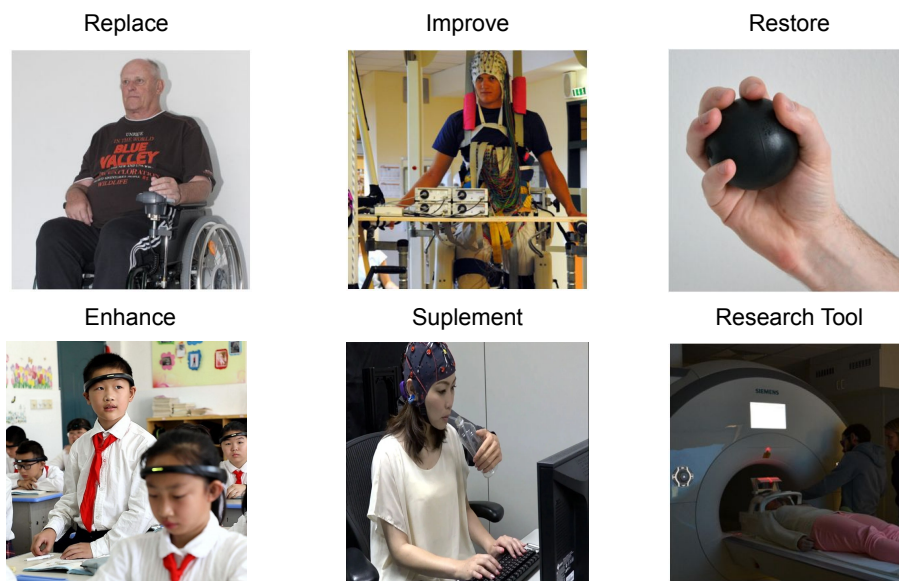


Figure 13: Brain computer interface possible application scenarios. Modified from source: Brunner et al. (2015)

1.5. State of the Art of BCI Applications

The type of applications that our work seeks to develop, once a robust methodology for processing and classifying EEG signals has been generated and developed, is the control of electromechanical devices or control systems with different degrees of freedom. The typical application of the BCI is the selection of objectives, letters, or icons on a computer screen, which has allowed the development of applications such as speech and writing assistants, as well as intelligent environments. Table 5 presents some of the different applications where we intend to apply the results obtained from our work in the medium term.

Table 5: BCI robotics and control applications.

Publication	Application	Output Commands	Used Electrodes
Hortal et al. (2015)	Industrial robot	Right Hand, Left Hand, Countdown and Alphabet back	Fz, FC5, FC1, FCz, FC2, FC6, C3, Cz, C4, CP5, CP1, CP2, CP6, P3, Pz, P4.
Lee et al. (2017)	Exoskeleton	Turn left, walk front, and turn right	FC3, FC1, FCz, FC2, FC4, C3, C1, Cz, C2, C4, CP3, CP1 CPz, CP2 and CP4
Bousseta et al. (2018)	Custom robotic arm	Right, left, up and down	AF3, AF4, F3 and F4
Liu et al. (2019)	Dual robotic arm	Lift and drop	C3 and C4
Xu et al. (2020)	Custom robotic arm	Left hand, right hand, both hand and relaxation	C3, FC3, CP3, C5, C4, FC4, CP4, and C6
Herath and de Mel (2021)	Robot hand	Resting, idle, flexion, hold flexion and extension	FC3, FC4, C1, C2, C3, C4, Cz, and CPz
Dumitrescu et al. (2021)	Virtual drone	Right and left	CP3, CP4, P3, C3, Pz, C4, P4 and Cz
Arshad et al. (2022)	Custom robotic arm	Left arm, right arm, and no movement	AF3, F7, F3, FC5, T7, P7, O1, O2, P8, T8, FC6, F4, F8, and AF4
Chen et al. (2022)	Electric wheelchair	Backward, forward, left and right and end orientation	O1, O2 and Pz
Quiles et al. (2022)	Industrial robot	Up, center, right and left	O1, O2, Oz, PO3, PO4, Pz, Cz, and Fz

Chapter II

2. Classification Methods

After the pertinent EEG signal parameters have been retrieved, it is necessary to perform signal processing to translate them into control commands or some instructions. Classification algorithms are used to do this task, which have proven efficient, effective, and accurate in developing brain-computer interface systems. It is worth mentioning that these signal parameters represent some motor or imaginary action of movement by the person. Classification is a process of predicting different classes from a given input. The classification process is carried out through a classification model. For the construction of the model, it is necessary to train it by employing a learning algorithm to adjust the parameters of the model. The same model is used in the training, validation, and testing stages to obtain a particular output and performance metrics. Figure 14 shows the process for training the ML and DL algorithms.

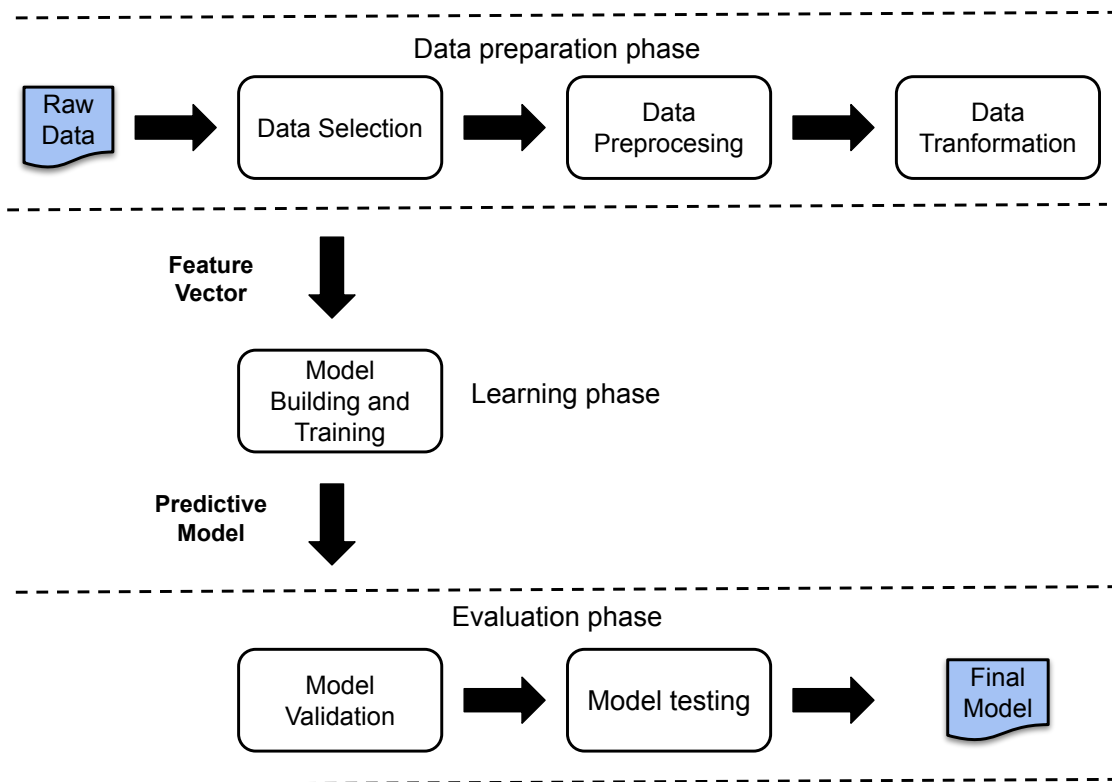


Figure 14: Construction process of a classification model. Modified from source: Pramanik et al. (2021)

Different classification methods have been explored within brain-computer interface sys-

tems. Figure 15 shows the main categories of classification algorithms.

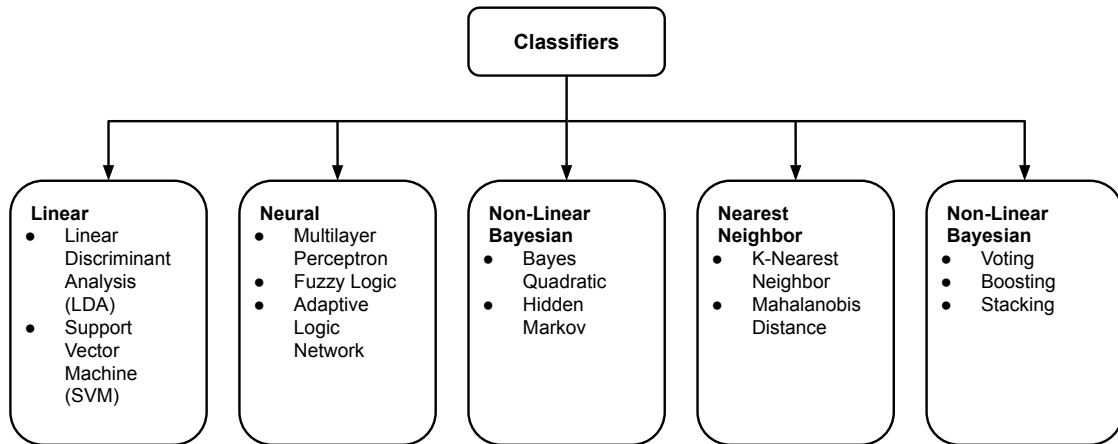


Figure 15: Categories of most common algorithms for classification task.

For the development of the methodology presented in this work, the five machine learning algorithms and four artificial neural networks listed below were used, which will be discussed in more detail in the next sections.

- Linear discriminant analysis (LDA).
- Decision trees (DT).
- K-neasted neighbors (kNN).
- Naive Bayes (NB).
- Support vector machines (SVM).
- Narrow Artificial neural network (Narrow-ANN).
- Medium Artificial neural network (Medium-ANN).
- Wide Artificial neural network (Wide-ANN).
- Bilayered Artificial neural networks (Bilayered-ANN).

2.1. Machine Learning Algorithms

2.1.1. Linear discriminant analysis

Linear discriminant analysis is the most widely used classifier in classifying EEG data and signals, where the Fisher distance is used to discriminate the data Duda et al. (2012); Kirby (2001). The LDA algorithm aims to project the original data array into a lower dimensional space. Three steps are needed to archive this. First step is to obtain the separability between the different classes. The second is to calculate the distance between the mean and the samples of each class. The third is to construct the space of least dimension to maximize the variance between classes and minimize the variance within the class. The Figure 16 shows the steps to calculate a lower dimensional subspace with the LDA technique Tharwat et al. (2017).

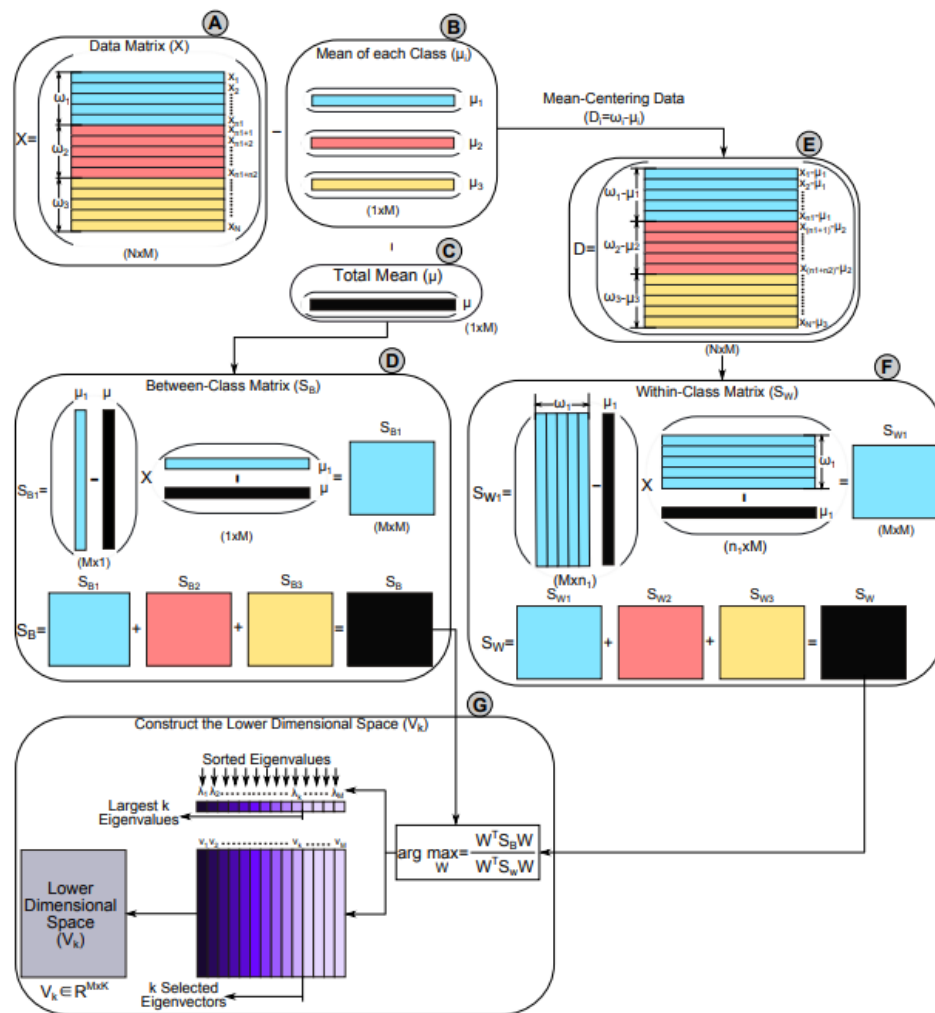


Figure 16: Steps of the LDA technique. Taken from source:Tharwat et al. (2017)

The next lines describe the different steps of the LDA algorithm.

- A. Given a dataset of N samples $[x_i]_{i=1}^N$, each sample represent a row of length M , and $X(N \times M)$.

$$X = \begin{bmatrix} x_{(1,1)} & x_{(1,2)} & \cdots & x_{(1,M)} \\ x_{(2,1)} & x_{(2,2)} & \cdots & x_{(2,M)} \\ \vdots & \vdots & \ddots & \vdots \\ x_{(N,1)} & x_{(N,2)} & \cdots & x_{(N,M)} \end{bmatrix}$$

- B. Compute the mean of each class $\mu_i(1 \times M)$.
- C. Compute the total mean of all data $\mu(1 \times M)$.
- D. Calculate between-class matrix $S_B(M \times M)$

$$S_B = \sum_{i=1}^c n_i (\mu_i - \mu)(\mu_i - \mu)^T \quad (1)$$

- E. Compute within-class $S_W(M \times M)$

$$S_W = \sum_{j=1}^c \sum_{i=1}^{n_j} (x_{ij} - \mu_j)(x_{ij} - \mu_j)^T \quad (2)$$

- F. The matrix that maximizing Fisher's distance is calculated as follow, . The eigenvalues and eigenvectors are then calculated $W = S_W^{-1} S_B$. The eigenvalues (λ) and eigenvectors (V) of W are then calculated.
- G. Sorting eigenvectors in descending order according to their corresponding eigenvalues. The first k are used as a lower dimensional space, to project all original samples onto the lower dimensional space of LDA.

2.1.2. Decision trees

An approach for supervised learning called a decision tree allows us to perform classification and regression tasks. A decision tree follows the principle of iteratively partitioning data by asking questions Li et al. (2022). The answers to the questions are crucial to creating the decision tree. Two primary methods for determining a split question's quality are entropy Shannon (1948) and Gini impurity Gini (1921). With more query information, the prediction model performs better. Gini impurity is mathematically formulated as

$$GI = \sum_{i=1}^N P(i)(1 - P(i)) \quad (3)$$

where N_C is the total number of classes and $P(i)$ is the probability of the i th class in the current dataset. By weighing the impurities in each branch, the split quality can be determined by

$$GI_{split} = \sum_{i=1}^N w_i GI_i \quad (4)$$

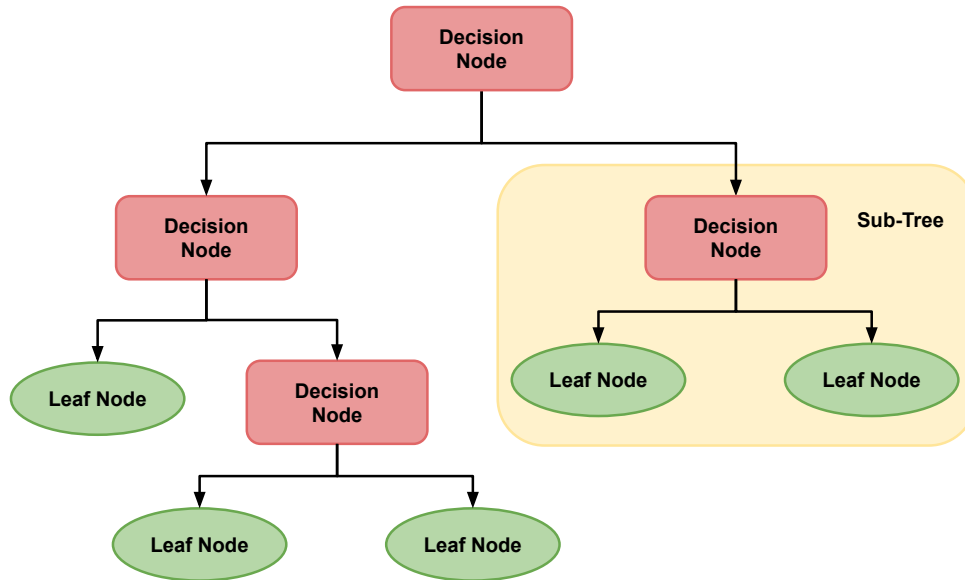


Figure 17: General example of a Decision Tree. Modified from source: Datacamp (2022)

2.1.3. K-Nearest Neighbor (KNN)

The KNN classifier is a component of unsupervised algorithms. The primary characteristic of these classifiers is that the feature vector is given to the k neighborhood's closest distance class. Methods for calculating distances include Euclidian, Manhattan, Minkowski and Hamming algorithms Walters-Williams and Li (2010). The Euclidean calculation that is most frequently employed is defined by

$$\delta = \sqrt{\sum_{i=1}^m (x_{1,i} - x_{2,i})^2} \quad (5)$$

where δ is the distance, x_1 and x_2 are two arbitrary data neighbors, and m is the input dimension. After analyzing the neighboring classes, the KNN uses a majority vote to assign the class based on query data. The Figure 18 shows the different step in the KNN algorithm.

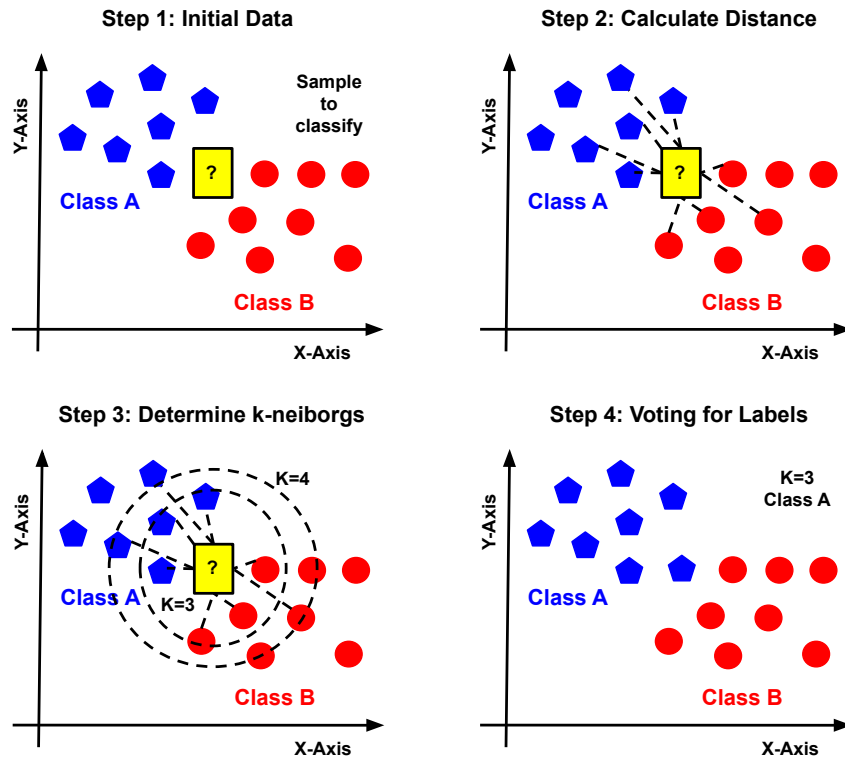


Figure 18: Steps of the KNN algorithm. Modified from source: Chakure (2021)

The main advantage of this algorithm is its simple and flexible Li et al. (2022). However, its sensitivity is considered one of its primary weaknesses, affecting BCI systems' performance Abdulkader et al. (2015a).

2.1.4. Naive Bayes

Statistical classifiers include Bayesian classifiers. They can forecast class probabilities and the likelihood that a given sample will belong to a specific class. The Bayes theorem provides the basis for the Bayesian classifier. The Naive Bayes classifier assumes that an attribute's impact on a particular class is unrelated to the values of the other characteristics. Conditional class independence is the term used to describe this principle. This assumption is called conditional class independence. It is viewed as naive since it is done to simplify the computations required.

Take $X = \{x_1, x_2, \dots, x_n\}$ as an sample, whose elements represent judgments made in relation to a set of n attributes. X is regarded as evidence in the Bayesian sense. Let H stand for some hypothesis, saying that the data X is a part of a particular class. When dealing with classification issues, we aim to figure out $P(H | X)$, or the probability that hypothesis H is true, given the evidence from the observed data sample X . In other words, given that we are aware of the attribute description of sample X , we are attempting to determine the likelihood that sample X belongs to class C . $P(H | X)$ is the posteriori probability of H conditioned on X , it is based on more information. $P(H)$ is the a priori probability of H , which is independent of X . The Bayes theorem Berrar (2018), express that the probability of $P(H | X)$ can be expressed in term of probabilities $P(H)$, $P(X | H)$, and $P(X)$ as

$$P(H | X) = \frac{P(X | H)P(H)}{P(X)} \quad (6)$$

and the available information can be used to determine these probability. Here is how the naive Bayes classifier operates Leung (2007):

1. Let T be a training set of samples, each with their class labels. There are k classes, C_1, C_2, \dots, C_k . Each sample is represented by an n -dimensional vector, $X = \{x_1, x_2, \dots, x_n\}$, depicting n measured values of the n attributes, A_1, A_2, \dots, A_n , respectively.
2. Given a sample X , the classifier will predict that X belongs to the class having the highest a posteriori probability, conditioned on X . That is X is predicted to belong to the class C_i if and only if

$$P(C_i | X) > P(C_j | X) \quad \text{for } 1 \leq j \leq m, j \neq i. \quad (7)$$

Thus we find the class that maximizes $P(C_i | X)$. The class C_i for which $P(C_i | X)$ is called the maximum posteriori hypothesis. By Bayes theorem

$$P(C_i | X) = \frac{P(X | C_i)P(C_i)}{P(X)} \quad (8)$$

3. As $P(X)$ is the same for all classes, only $P(X | C_i)P(C_i)$ need be maximized. If the class a priori probabilities, $P(C_i)$, are not known, then it is commonly assumed that the classes are equally likely, that is, $P(C_1) = P(C_2) = \dots P(C_k) = \dots$, and we would therefore maximize $P(X | C_i)$. Otherwise we maximize $P(X | C_i)P(C_i)$. Note that the class a priori probabilities may be estimated by $P(C)_i = \text{freq}(C_i, T) / |T|$.
4. Given dataset with many attributes, it would be computationally expensive to compute Compute within-class $P(X | C_i)$. In order to reduce computation in evaluating $P(X | C_i)P(C_i)$, the naive assumption of class conditional independence is made. This presumes that the values of the attributes are conditionally independent of one another, given the class label of the sample. Mathematically this means that

$$P(X | C_i) \approx \prod_{k=1}^n P(x_k | C_i) \quad (9)$$

The probabilities $P(x_1 | C_i), P(x_2 | C_i), \dots, P(x_n | C_i)$, can be easily be estimated from the training set. Recall that here x_k refers to the value of attribute A_k for sample X .

- (a) If A_k is categorical, then $P(x_k | C_i)$ is the number of samples of the class C_i in T having the values x_k for attribute A_k divided by $\text{freq}(C_i, T)$ the number of class C_i in T .
- (b) If A_k is a continuous-valued, then we typically assume that the values have a Gaussian distribution with mean μ and standard deviation σ defined by

$$g(x, \mu, \sigma) = \frac{1}{\sqrt{2\pi}\sigma} \exp - \frac{(x - \mu)^2}{2\sigma^2} \quad (10)$$

so that

$$p(x_k | C_i) = g(x_k, \mu_{C_i}, \sigma_{C_i}) \quad (11)$$

We need to compute μ_{C_i} and σ_{C_i} , which are the mean and standard deviation of values of attribute A_k for training samples of class C_i .

5. In order to predict the class label of X , $P(X | C_i)P(C_i)$ is evaluated for each class C_i .

The classifier predicts that the class label X of is C_i if only it is the class that maximizes $P(X | C_i)P(C_i)$.

According to comparative studies of classification methods, the Naive Bayes classifier is comparable in performance to decision tree classifiers and artificial neural networks. Bayesian classifiers have also demonstrated great accuracy and speed when used on large databases Daniela et al. (2009).

2.1.5. Support vector machines

Support vector machines are supervised algorithms employed in classification and regression tasks in applications related to medical signal processing, natural language processing, image recognition, and EEG signal classification applications. The classification and regression tasks are completed by building hyperplanes within the model's response space Hearst et al. (1998). The model aims to find a hyperplane that, to the best possible degree, separates one class's data points from another. The best hyperplane is defined as the most extended margin between two classes, as shown in Figure 19.

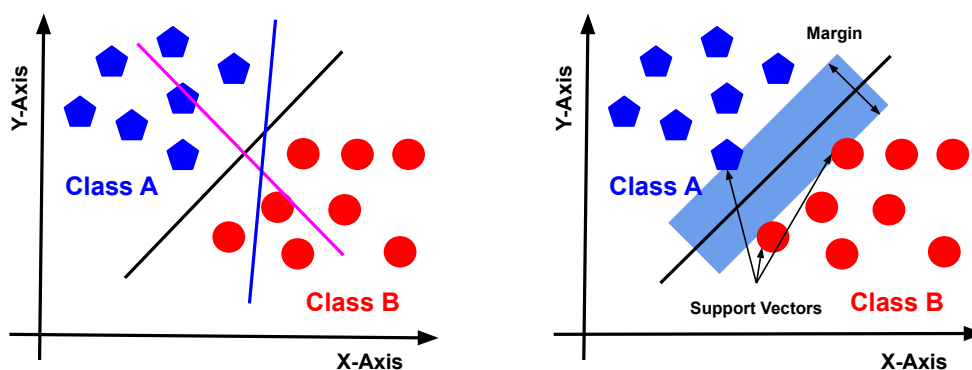


Figure 19: Classification by support vector machine. Modified from source: Ippolito (2021)

Vector supports refer to a subset of training observations identifying the positions of the separating hyperplane. The standard brackets machine algorithm is formulated for binary classification problems, reducing multiclass issues to a series of binary problems.

The support vector machine is called a support vector classifier for classification problems Cervantes et al. (2020). Given n training data $X \in \mathfrak{R}$ and corresponding two class categories $Y \in [-1, 1]$, the goal is determine the parameter $w \in \mathfrak{R}^m$ and $b \in \mathfrak{R}$ and predict the correct sign of $w^T \phi(x) + b$ for the most samples. Therefore, the SVC primal problem is:

$$\min_{u,b,\zeta} \frac{1}{2} w^T w + C \sum_{i=1}^n \zeta_i, \quad (12)$$

subject to

$$y_i(w^T \phi(x_i) + b) \geq 1 - \zeta_i, \quad (13)$$

$$\zeta_i \geq 0, i = 1, \dots, n. \quad (14)$$

In this formulation, the penalty $C \sum_{i=1}^n \zeta_i$ and $w^T w$ are minimized in order to maximize the margin. In more detail, the constant C determines the strength of the penalty and the positive-value ζ_i adds a penalty to the objective function above if the i th sample is inside the bounds of the hyperplane or is misclassified. The SVC primal problem is made easier by the Lagrangian duality principle as

$$\min_{\alpha} \frac{1}{2} \alpha^T Q \alpha - e^T \alpha \quad (15)$$

subject to

$$y^T \alpha = 0, \quad (16)$$

$$0 \leq \alpha_i \leq C, i =, \dots, n, \quad (17)$$

where e is the vector of all ones, Q is an n by n positive semi-definite matrix, $Q_{i,j} = y_i y_j K(x_i, x_j)$, $K(x_i, x_j) = \phi(x_i^T) \phi(x_j)$, is the kernel, and ϕ is a dual coefficient vector upper-bounded by C . The dual problem is a quadratic function subject to linear constrains, which quadratic programming algorithms can solve efficiently Rong et al. (2022). Once we construct the SVC by solving the above optimization problem, the predicted classification on a given sample x' becomes:

$$y' = \sum_{i \in SV} y_i \alpha_i K(x_i, x') + b \quad (18)$$

where SV is the support vector set. We only need to sum over the support vectors because the dual coefficients α are zero from the other training data.

2.2. Artificial neural network

Artificial neural networks are popular machine learning methods that mimic the workings of learning beings. Neurons are a type of cell found in the human nervous system. Axons and dendrites connect neurons, and the areas where these two structures meet are known as synapses. Figure 20 shows an illustration of these linkages presented in a biological neural network.

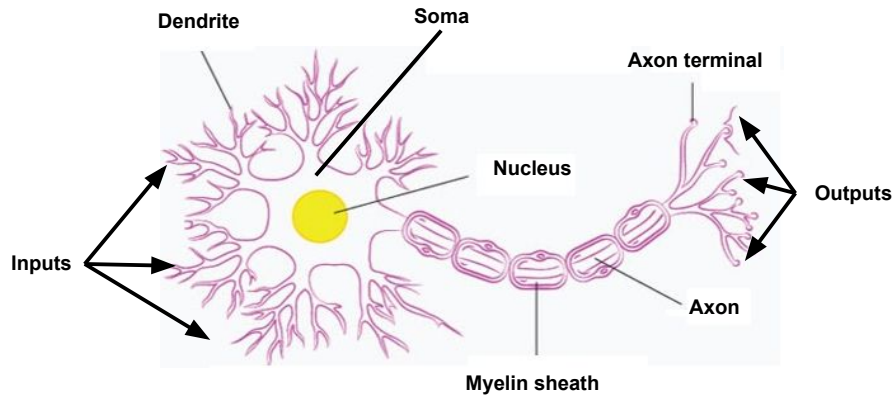


Figure 20: Biological neural network.

Learning occurs similarly in living organisms. Artificial neural networks, which include processing units referred to as neurons, imitate the biological mechanism. Weights are used to connect computing units, serving a similar purpose as synaptic connection strengths in biological organisms. As shown in Figure 22, each input to a neuron is scaled with a weight, which has an impact on the function computed at that unit. By transmitting computed values from the input neurons to the output neurons and utilizing the weights as intermediate parameters, an artificial neural network computes a function of the inputs. The weights holding the neurons together are modified during learning. Similar to how biological organisms require external stimuli for learning, artificial neural networks also require external stimuli. The training data, which contains examples of input-output pairings for the function to

be trained, serves as the external stimulus in these networks. The purpose of adjusting the weights is to alter the computed function such that predictions made in subsequent iterations are more accurate. In order to lower the calculation error on that example, the weights are changed carefully in a way that is supported by mathematics.

Even though the initial artificial neural network mathematical model was put forth in 1943, it was not until the 1960s and 1980s that the study and scope of what is now called artificial neural networks spread Michie et al. (1994). Figure 21 shows us the model of an artificial neural network.

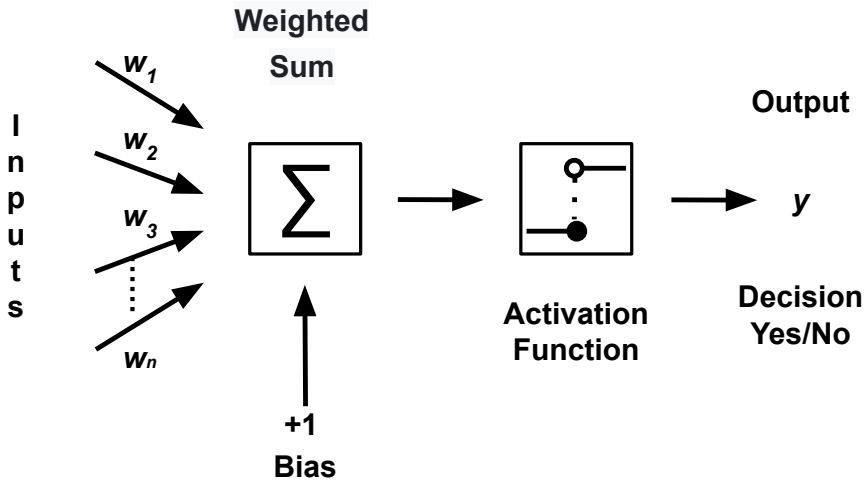


Figure 21: Artificial Neural Network.

We can interpret the above graphic as a function of the form:

$$f(w_0 + w_1x_1 + w_2x_2 + \dots + w_mx_m) = y \tag{19}$$

Therefore, the generic definition of an artificial neuron is given as a simple calculation device, which from an input vector coming from the outside or other neurons, provides a single output response Aggarwal (2018). The Figure 22 shows the generic model of an artificial neural network.

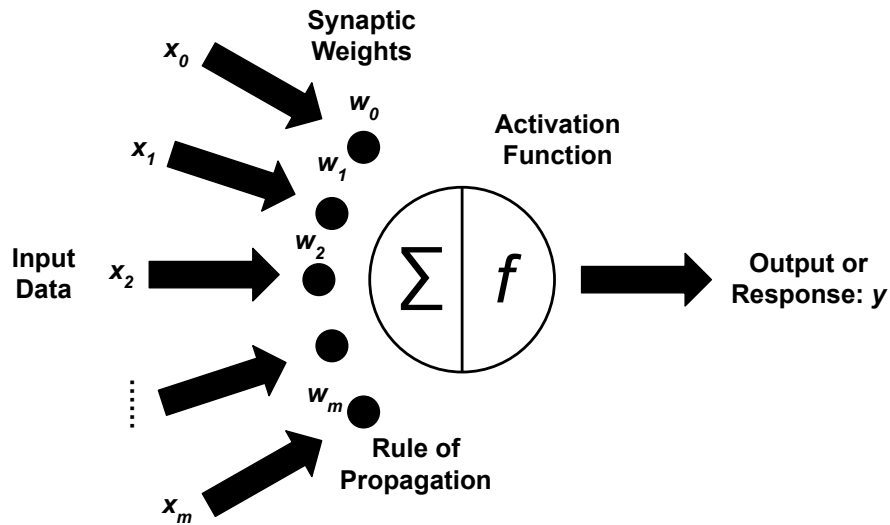


Figure 22: Artificial neural network, generic model.

The matrix product, often known as the inner product of two vectors, represents the propagation rule.

$$t = \vec{w}_j^T w_j = \sum_{j=0}^m w_j x_j = \sum_{j=1}^m w_j x_j + w_0 \quad (20)$$

The step function is assumed to be the activation function in its most basic form. We can say that with the step function, the activation threshold is 0.

$$y = f(t) \begin{cases} +1, & \text{if } t > 0 \\ 0, & \text{if } t \leq 0 \end{cases} \quad (21)$$

2.2.1. Activation function

The artificial neuron processes the information distributed throughout the network using the activation function. Numerous activation functions exist Ding et al. (2018); Apicella et al. (2021), some of which are shown in Figure 23.

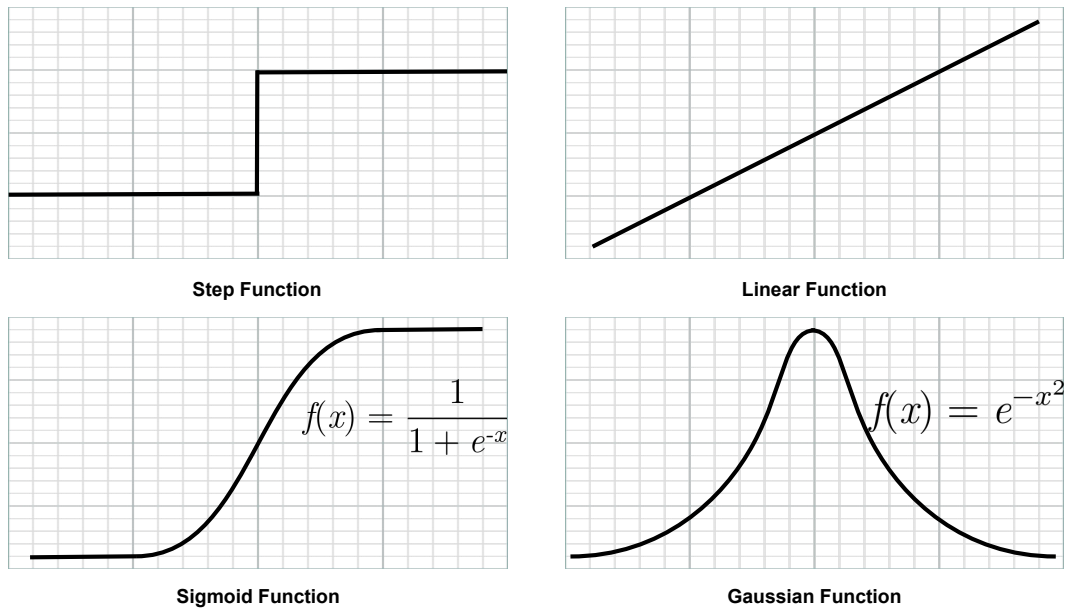


Figure 23: Examples of activation function used inside the artificial neural network.

2.2.2. Network topology

Despite the fact that there are many different types of architecture today. We can point to the shared following three fundamental qualities:

1. The number of layers in the network: input layer, output layer, and hidden layers.
2. The way information propagates within the network: feed-forward, feedback and back-propagation.
3. The number of nodes or neurons in each layer.

The Figure 24 shows the generic topology of an artificial neural network. The number of neurons in the input layer is determined by the same number of variables considered in the input data plus the threshold neuron. The number of neurons in the output layer is determined by the prediction variable of the problem, whether it is regression or classification. Although there are a few guidelines, there is no universal rule for calculating the optimal number of neurons to place in the hidden layers Fekiač et al. (2011). A theorem regarding the scope of artificial neural networks tells us that a forward-propagating neural network, with a single hidden layer and enough neurons in that layer, is sufficient to solve almost any machine-learning problem in real life.

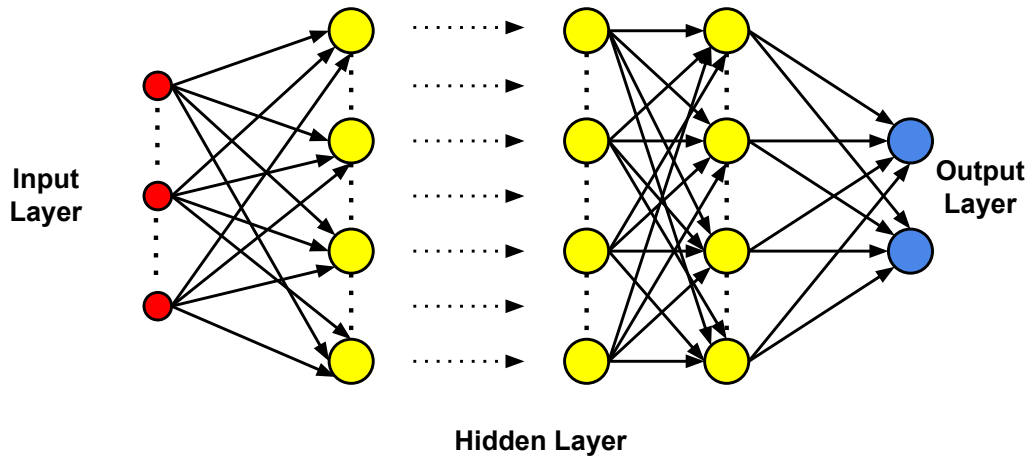


Figure 24: General topology of artificial neural network.

2.3. Classification methods used in robotics

In BCI research, neural networks (NN) and linear classifiers are the two types of classifiers that are most frequently utilized. In Bi et al. (2013), different tables indicate the classifiers used to classify the EEG signals, as well as with commands generated to control the related application. It can be seen that the use of linear classifiers, LDA, SVM, and ANN, are the main classifiers used. The precision mentioned in the different works ranges between 60 and 90 accuracy. Zhang and Wang (2021) presents similar tables showing the classifier used, the control object, and the output commands. This work shows that linear classifiers are the most widely used together with artificial neural networks. The accuracy of the different results presented is 10 and 95; it is because some applications include exoskeletons where the accuracy is drastically affected. In Aggarwal and Chugh (2019) work, different linear classifiers, artificial neural networks, and deep neural networks for the classification of EEG signals are mentioned in different databases related to validating signal processing and classification methods for BCIs. Table 6 presents various robotic application works and the classifier used.

Table 6: Classifier used in robotics and control applications.

Publication	Application	Classification
Hortal et al. (2015)	Industrial robot	SVM
Lee et al. (2017)	Exoskeleton	D.T.
Bousseta et al. (2018)	Custom robotic arm	SVM
Liu et al. (2019)	Dual robotic arm	SVM
Xu et al. (2020)	Custom robotic arm	ANN
Herath and de Mel (2021)	Robot hand	SVM
Dumitrescu et al. (2021)	Virtual drone	ANN
Arshad et al. (2022)	Custom robotic arm	KNN, D.T
Chen et al. (2022)	Electric wheelchair	SVM
Quiles et al. (2022)	Industrial robot	LDA

Chapter III

3. Methodology

A typical system for EEG signal classification is conceptually divided into signal acquisition, preprocessing, feature extraction, and classification Hosseini et al. (2021); Aggarwal and Chugh (2019). The EEG signals are acquired by electrodes located on the scalp's surface that transfer information on the electrical neuronal activity to the data acquisition system. In preprocessing, line noise and muscle artifacts are removed from EEG signals. Feature extraction uses several digital signal processing techniques to obtain feature vectors. These vectors are used to train the ML or DL algorithms to classify the EEG signals. The result of the algorithms is a specific class, as illustrated in Figure 25. The following subsections describe the procedure in detail.

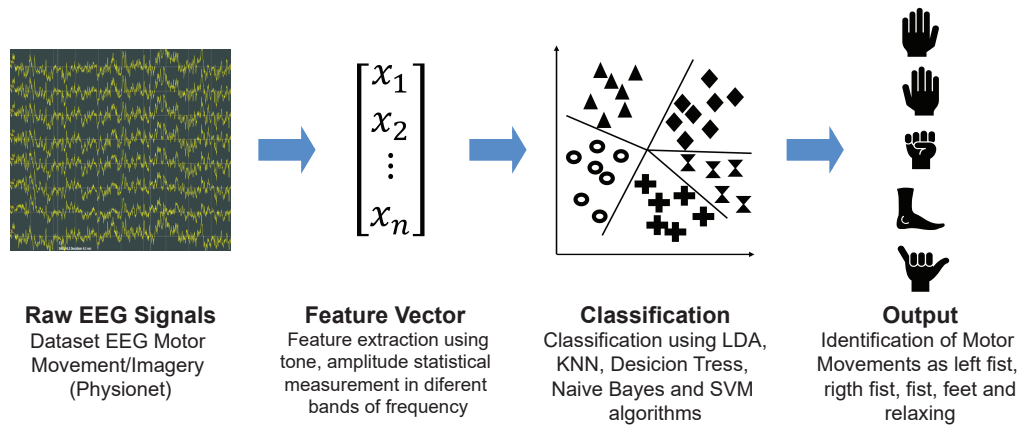


Figure 25: Proposed method for classifying EEG signals.

3.1. Hardware and Software

The hardware used for the implementation of the proposed method had the following specifications: Microsoft Windows 10 Pro operating system, System Model OptiPlex 3070, System type x64-based PC, Processor Intel Core i5-9500 at 3.00 GHz, 6 Cores, 6 Logical Processors, Memory (RAM) of 16.0 GB DDR4 2666 MHz (2 X 8 GB), and NVIDIA GeForce GT 1030 GDDR5 2 GB PCI-Express x16. The software used for reading the EEG signals, electrode selection, signal segmentation, preprocessing, analysis, feature extraction, and pre-

paration of the dataset was LabVIEW 2015. Furthermore, the following libraries, which are part of the development environment of LabVIEW, were used: Biomedical Toolkit and Signal Express. The MATLAB 2021a version was used for training and testing the different ML algorithms, which are part of the Statistics, Machine Learning and Deep Learning Toolbox.

3.2. Input data

The dataset used for EEG signal classification was developed by Schalk and colleagues at Nervous System Disorders Laboratory and is publicly available on Physionet Goldberger et al. (2000). The data consist of more than 1500 EEG recordings of 1–2 min in length from 109 subjects. Patients performed 14 tasks (experiments) while 64 electrodes acquired and recorded the EEG signals through the BCI2000 system G. Schalk et al. (2004). The data are in EDF+ format Kemp and Olivari (2003), and they contain 64 EEG signals, each displayed at a rate of 160 samples per second, and an annotation channel, which refers to the actions performed during the task. Table 7 shows the protocol of the Schalk agreement experiment. The diagram of the position of the electrodes used to record the data is the standard 10-10 placement. The dataset consists of 109 folders, and each folder contains 28 files, where 14 of these have the **.edf* extension, and the other 14 have the **.edf.event* extension. The files that contain the EEG signals are those that contain the **.edf* extension. The **.edf.event* files refer to the events during the development of the different tasks. Although the original set of recorded data consists of continuous multichannel data, and the number of users that comprise it is extensive, we only used the EEG signals of 30 randomly selected subjects and the tasks that are related to the real movements that take place in tasks 3, 5, 7, 9, 11, and 13. In tasks 3, 7, and 11, real movements related to the right and left fists and relaxation are carried out, while in tasks 5, 9, and 13, real movements of both fists and both feet are carried out. Table 7 summarizes the dataset used in the proposed approach.

Table 7: Tasks presented in the dataset to train the ML algorithms for EEG signal classification.

Task	Real Movement	Imaginary Movement	To	T1	T2	Duration
1	Open Eyes	-	Relaxing	-	-	1 min
2	Close Eyes	-	Relaxing	-	-	1 min
3	Fist	-	Relaxing	Left	Right	2 min
4	-	Fist	Relaxing	Left	Right	2 min
5	Fist/Feet	-	Relaxing	Fist	Feet	2 min
6	-	Fist/Feet	Relaxing	Fist	Feet	2 min
7	Fist	-	Relaxing	Left	Right	2 min
8	-	Fist	Relaxing	Left	Right	2 min
9	Fist/Feet	-	Relaxing	Fist	Feet	2 min
10	-	Fist/Feet	Relaxing	Fist	Feet	2 min
11	Fist	-	Relaxing	Left	Right	2 min
12	-	Fist	Relaxing	Left	Right	2 min
13	Fist/Feet	-	Relaxing	Fist	Feet	2 min
14	-	Fist/Feet	Relaxing	Fist	Feet	2 min

3.3. Proposed Method for EEG Signal Processing

Figure 26 depicts the proposed method for EEG signal processing, described in detail in the following subsections.

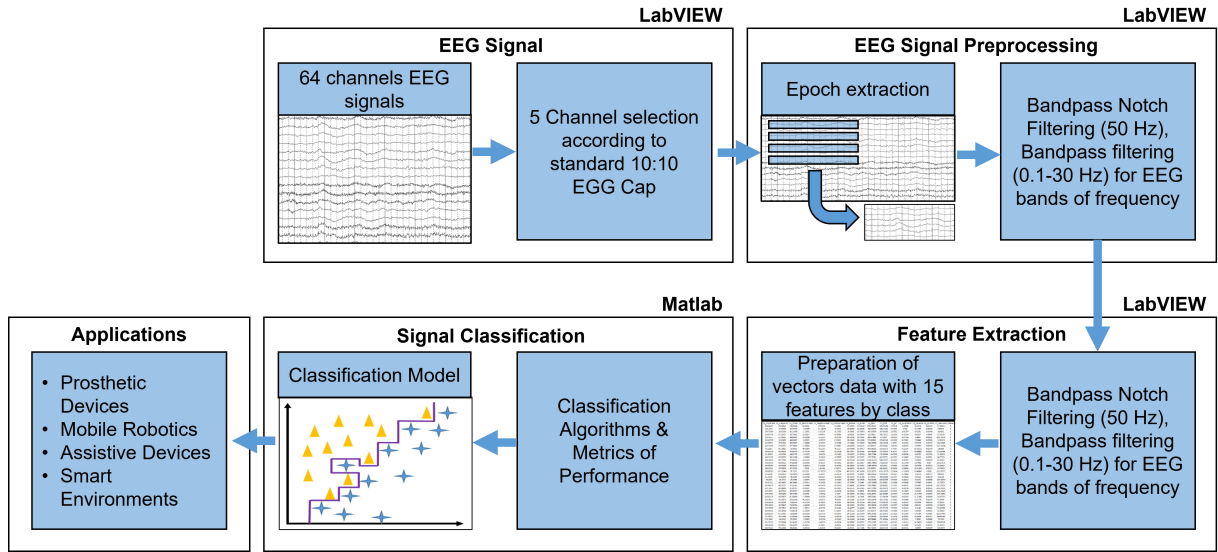


Figure 26: Proposed method for EEG signal classification.

3.3.1. EEG Signal Acquisition and Channel Selection

The LabVIEW software 2015 version was employed as the development platform, while the Biomedical Toolkit was used to import the EEG signals, due to the signals being in EDF format. The selected electrodes are shown in Figure 27(b). These electrodes present neuronal activity correlated to the execution of the left- and right-hand movements (contained in electrodes C3, C4, and CZ Neuper and Pfurtscheller (2001); Deecke et al. (1982)) the neuronal activity related to the movement of both feet (contained in electrodes C1 and C2 Hashimoto and Ushiba (2013)); because the different EEG channels tend to represent redundant information, as mentioned in Sleight et al. (2009), electrodes C3, C1, CZ, C2, and C4 were selected in our study. The selected electrodes were located around the center of the skull, within the motor cortex area; their characteristic is that these electrodes are the least affected by different artifacts Lee et al. (2017), which allows the reliable extraction of features to be obtained.

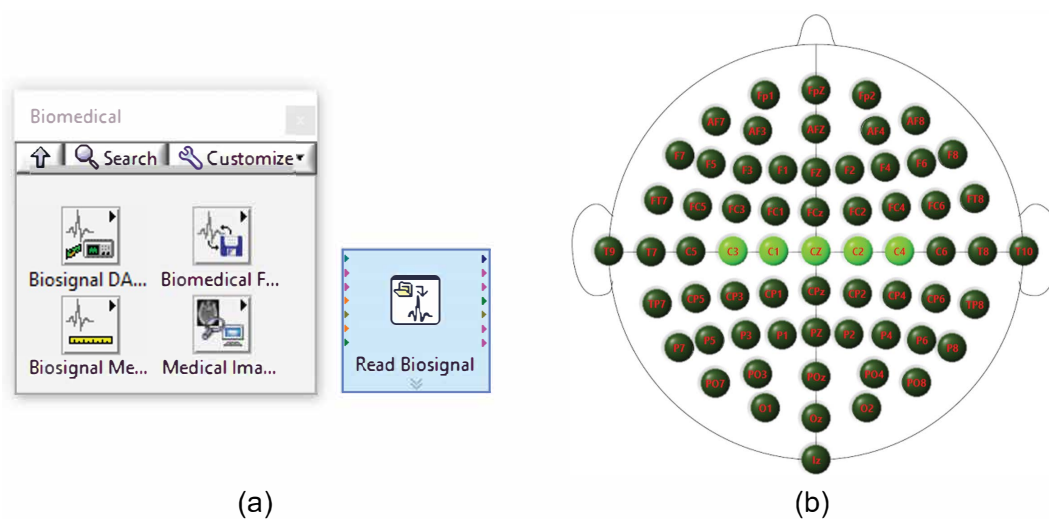


Figure 27: Selected electrodes for EEG signal classification. (a) Biomedical toolkit and (b) electrodes selected.

3.3.2. Pre-processing

The EEG signals used, with a sampled frequency of 160 samples per second, are available online Goldberger et al. (2000). Bandpass filters were required to select only the frequencies of interest and eliminate line noise and some other interferences. For this study, we processed the EEG signals through an IIR bandpass filter, with third-order Butterworth topology from

0.1 to 50 Hz. After this, a 50 Hz Notch filter was applied to the signals to eliminate noise from the signal power line. Figure 28 shows the original readings of the electrodes used before and after applying the different filters related to the signal pre-processing operations.

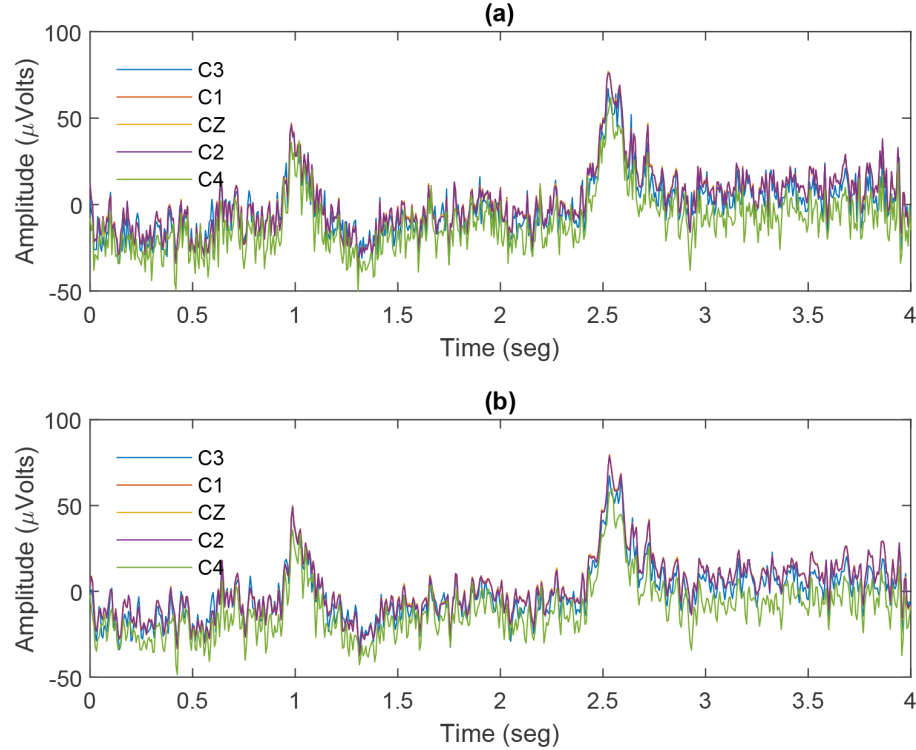


Figure 28: EEG signals acquired from electrodes C3, C1, CZ, C2, and C4. (a) Original EEG signal and (b) filtered EEG signal.

3.3.3. EEG Band Separation

Within EEG signal analysis, it is common to separate a signal into different frequency bands, including Delta (1-4 Hz), Theta (4-8 Hz), Alpha (8-12 Hz), Beta (12-30 Hz), and Gamma (30-50 Hz). As shown in Table 8, third-order bandpass Butterworth IIR filters with different cut-off frequencies were used to carry out this separation.

Table 8: Cut-off frequencies of bandpass filters for band extraction of EEG signals.

Band of EEG Signal	Low Cut-off Frequency	High Cut-off frequency
Delta	0.0 Hz	4.0 Hz
Theta	4.0 Hz	8.0 Hz
Alpha	8.0 Hz	12.0 Hz
Beta	12.0 Hz	30.0 Hz
Gamma	30.0 Hz	50.0 Hz

3.3.4. Feature Extraction

The features of the EEG rhythm can be obtained by using several digital signal processing techniques. These features were used for training the nine ML algorithms. These analysis techniques included measurements of tone, amplitude, and level, as well as statistical analyses. Table 9 shows the type of measurements and features obtained when these techniques were applied to the EEG signal epochs.

3.3.5. Signal Analysis

- Tone measurements. The tone measurements carried out in the EEG signal epochs were the following: amplitude, frequency, and phase.
- Level measurements. The level measurements implemented in the EEG signal epochs were the following: peak-to-peak, negative peak, and positive peak.
- Statistical features. The statistical measurements applied to the different signal epochs were the following:
 - *Median*, is the value separating the higher half from the lower half in the set Naik (2012)Stancin et al. (2021):

$$Median = \begin{cases} \frac{(N+1)}{2}, & \text{when N is odd} \\ \frac{N}{2} + \frac{(N+1)}{2}, & \text{when N is even} \end{cases} \quad (22)$$

- *Mode*, is the number that occurs most frequently in the set;
- *Mean*, is the average of the set Zwillinger and Kokoska (1999):

$$\tilde{x} = \frac{1}{N} \sum_{i=1}^N x_i \quad (23)$$

- *Root mean square (RMS)*, the arithmetic mean of the squares of a given set Zwillinger and Kokoska (1999):

$$RMS = \sqrt{\frac{1}{N} \sum_{i=1}^N x_i^2} \quad (24)$$

- *Standard deviation*, is a measure of how dispersed the set is in relation to the mean Zwillinger and Kokoska (1999):

$$S = \sqrt{\frac{1}{N} \sum_{i=1}^N (x_i - \tilde{x})^2} \quad (25)$$

- *Summation*, is the addition of the samples in the set:

$$\sum_{i=1}^N x_i \quad (26)$$

- *Variance*, is a measure of variability of the set from the mean Zwillinger and Kokoska (1999):

$$S^2 = \frac{1}{N} \sum_{i=1}^N (x_i - \tilde{x})^2 \quad (27)$$

where \tilde{x} is the mean;

- *Kurtosis*, is a metric that assesses how heavy-tailed or light-tailed the data are in comparison to a normal distribution Zwillinger and Kokoska (1999):

$$Kurtosis = \sum_{i=1}^N \frac{(x_i - \tilde{x})^4}{(N - 1)s^4} \quad (28)$$

- *Skewness*, is a measurement of the distortion of symmetrical distribution or asymmetry in a data set Zwillinger and Kokoska (1999):

$$Skewness = \sum_{i=1}^N \frac{(x_i - \tilde{x})^3}{(N - 1)s^3} \quad (29)$$

3.3.6. Dataset Preparation

The data vectors consist of 15 features, 3 features for each electrode; the electrodes correspond to positions C3, C1, Cz, C2, and C4, which are related to motor movements, and these belong to one of the five classes of *Relaxation*, *Right hand*, *Left hand*, and *Fist* and *Feet*. The dataset has 2,792 samples, where 558 samples correspond to the relaxation class, 567 to the right hand, 555 to the left hand, 561 to both fists, and 547 to the feet. On average, there are 557 samples per class, which preserves the balance among the classes. Figure 38 in

Appendix A shows a fragment of the dataset created by processing EEG signals when different users performed different motor tasks. Figure 39 in Appendix B depicts the graphic user interface (GUI) of the software (App) developed for the feature extraction process. The proposed App allows features to be extracted in different frequency bands, where each frequency band corresponds to a different class. Table 9 shows the features obtained for training the different ML algorithms. Each line represents a vector of features consisting of 5 electrodes. Three different measurements were made for each electrode, which resulted in a vector with 15 different characteristics used for the training and testing of the ML and DL models. It can be observed that the feature vector is labeled with its respective class. For each of the five classes, 15 different features were obtained in 5 different frequency bands to improve the classification accuracy of the ML algorithms Jatupaiboon et al. (2013); Al-Ani and Al-Sukker (2006).

Table 9: Features of the EEG signal used to train the ML algorithms.

Features of the channels for the different electrode positions																
Band	C3	C3	C3	C1	C1	C1	Cz	Cz	Cz	C2	C2	C2	C4	C4	C4	Class
Delta	Amplitude	Frequency	Phase	Peak to Peak	Neg.Peak	Pos.Peak	Median	Mode	Mean	RMS	S.D.	Summation	Variance	Kurtosis	Skewness	Relaxing
Theta	Amplitude	Frequency	Phase	Peak to Peak	Neg.Peak	Pos.Peak	Median	Mode	Mean	RMS	S.D.	Summation	Variance	Kurtosis	Skewness	Left Hand
Alpha	Amplitude	Frequency	Phase	Peak to Peak	Neg.Peak	Pos.Peak	Median	Mode	Mean	RMS	S.D.	Summation	Variance	Kurtosis	Skewness	Right Hand
Beta	Amplitude	Frequency	Phase	Peak to Peak	Neg.Peak	Pos.Peak	Median	Mode	Mean	RMS	S.D.	Summation	Variance	Kurtosis	Skewness	Fist
Gamma	Amplitude	Frequency	Phase	Peak to Peak	Neg.Peak	Pos.Peak	Median	Mode	Mean	RMS	S.D.	Summation	Variance	Kurtosis	Skewness	Feet

3.3.7. Machine Learning Algorithm Training

In this paper, we selected nine ML algorithms to evaluate their performance in the classification of EEG signals related to the motor movements of right hand, left hand, both fists, feet, and relaxation. The nine selected algorithms are: naive Bayes (N.B.), k-nearest neighbors (KNN), decision tree (D.T.), support vector machine (SVM), linear discriminant analysis (LDA), Narrow-ANN, Medium-ANN, Wide-ANN, and Bilayered-ANN. These ML algorithms are part of the statistical and machine learning toolbox of MATLAB, which has various tools that can be used for both the pre- and post-processing of data.

Figure 29 shows the block diagram to train, test and evaluate the selected ML algorithms. First, the dataset is loaded; the chosen dataset is constituted of more than 1500 EEG recordings from 109 subjects that become between 1 and 2 minutes long and can be found in Physio-net Goldberger et al. (2000). In this study, 30 people were randomly chosen to train, test, and validate the proposed method. subsequently, the data are normalized between 0 and 1 to obtain better results. Next, we randomly split the dataset into 80% for training and 20% for testing. Then, the ML model is trained. The next step is to obtain the performance metrics of the ML models (for example, using the confusion matrix), i.e., the performance metrics to evaluate the ML algorithms, such as the area under the curve (AUC) and accuracy, among others.

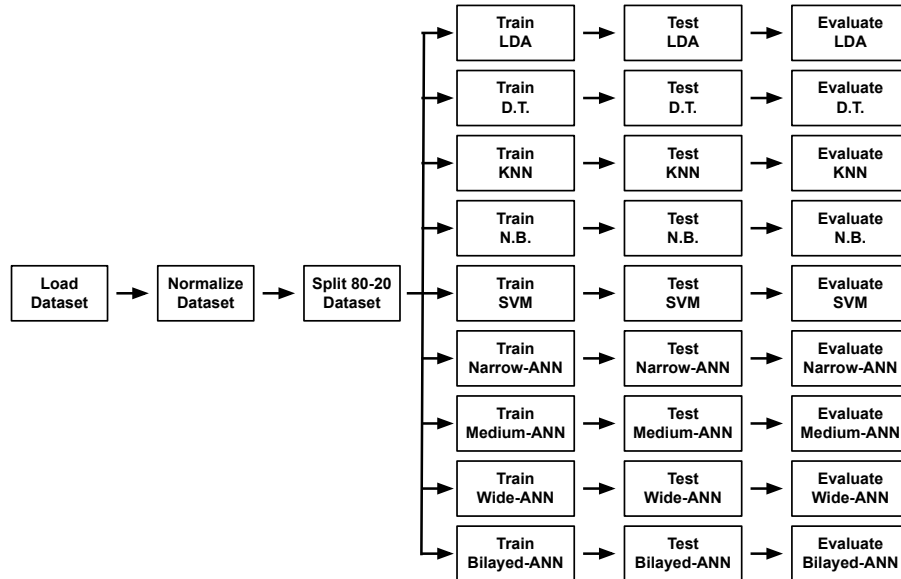


Figure 29: Block diagram for training, testing, and evaluating the ML algorithms.

Chapter IV

4. Experimental results

4.1. Results obtained by the classification algorithms

This chapter compares the different algorithms used for classifying EEG signals using the proposed methodology, in which the characteristics of the EEG signals were extracted through a customizing application developed in the LabVIEW development platform. The algorithms of ML and ANN were implemented in the Matlab programming environment for PC. Table 10 shows the list of ML algorithms and ANN networks used to classify EEG signals.

Table 10: List of algorithm used for EEG classification.

Machine Learning	Artificial Neural Network
LDA	Narrow-ANN
D.T.	Medium-ANN
KNN	Wide-ANN
N.B.	Bilayed-ANN
SVM	

4.1.1. Matrix of confusion

The confusion matrix is a popular measure used in solving problems of classification. Both multiclass problems and binary classification issues can benefit from this. Other authors define the confusion matrix as a table used to define a classification algorithm's performance. The Figure 30 shows the scheme of the confusion matrix for binary classification.

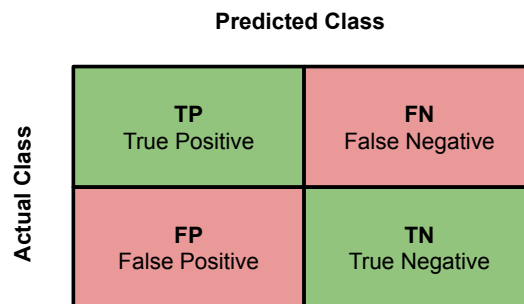


Figure 30: Scheme of the confusion matrix for binary classification.

The Figure 31 shows the confusion matrix (CM) of the four ANN algorithms trained for the classification of EEG signals related to the state off relaxation, right hand, left hand, both hands, and booth feet. The Figure 31(a) shows the CM of the Narrow-ANN algorithm. The Figure 31(b) shows the CM of the Medium-ANN algorithm. The Figure 31(c) shows the CM of the Wide-ANN algorithm. The Figure 31(d) shows the CM of the Bilayered-ANN algorithm.

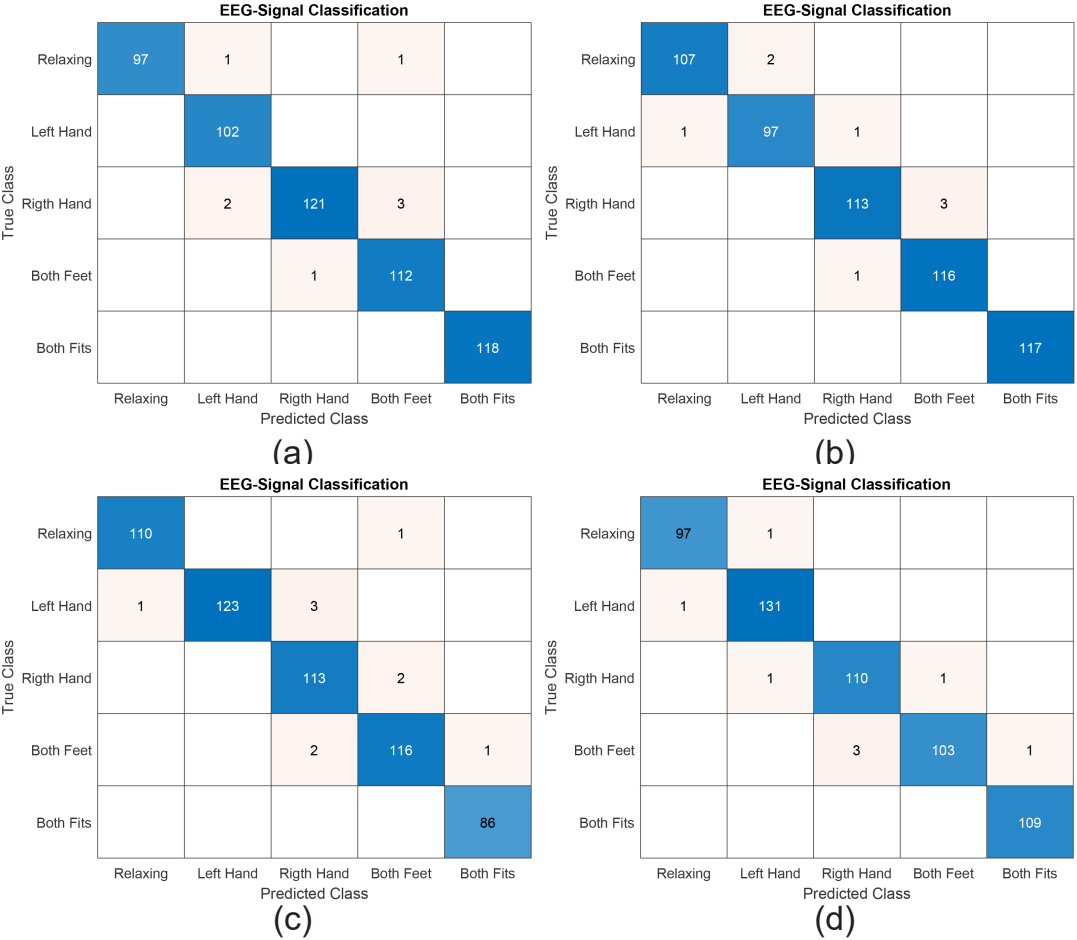


Figure 31: The confusion matrix (CM) of the four ANN algorithms trained for EEG signals classification, related to the movements of hands and feet: (a) CM of the Narrow-ANN algorithm, (b) CM of the Medium-ANN algorithm, (c) CM of the Wide-ANN algorithm, and (d) CM of the Bilayered-ANN algorithm.

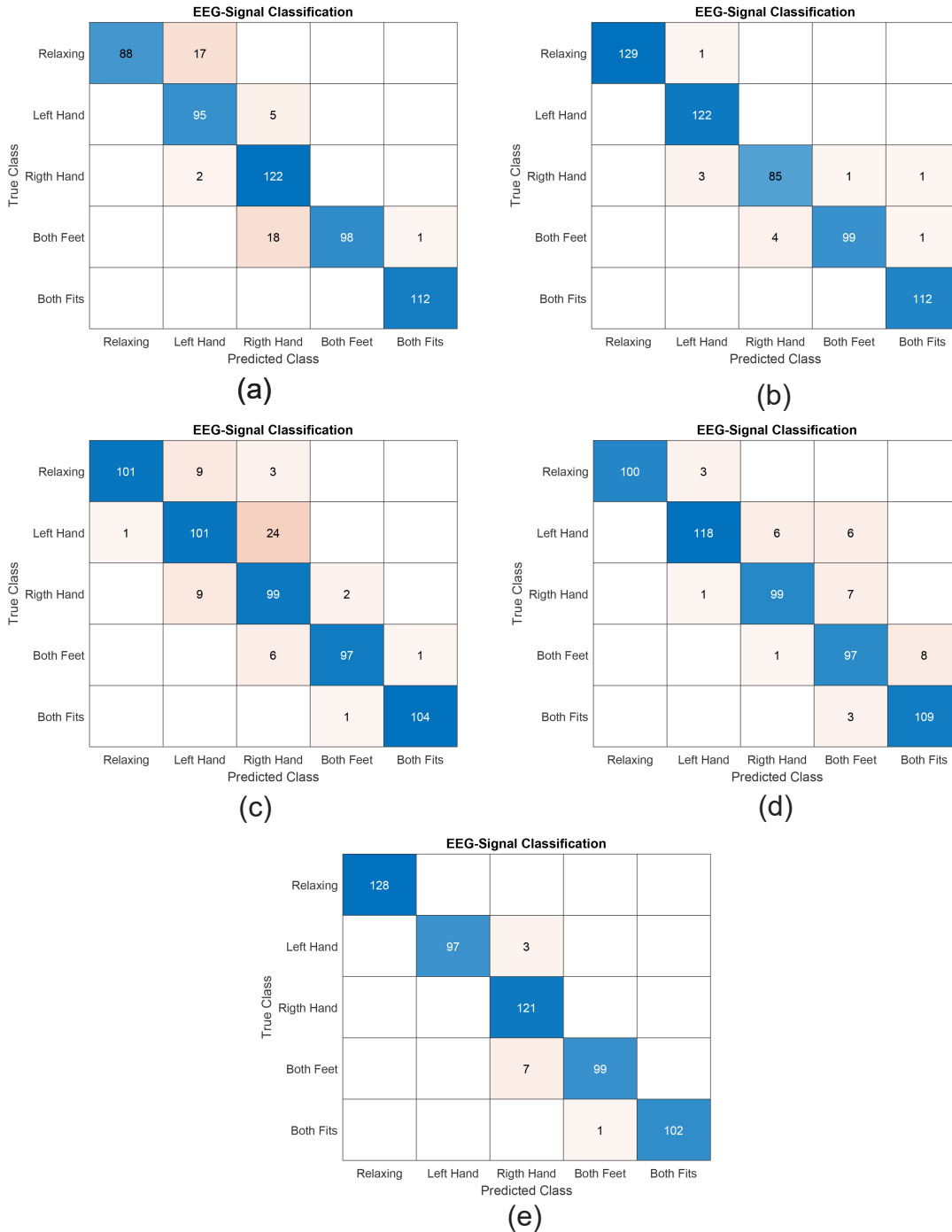


Figure 32: The confusion matrix (CM) of the five ML algorithms trained for EEG signals classification, related to the movements of hands and feet: (a) CM of the LDA algorithm, (b) CM of the D.T. algorithm, (c) CM of the KNN algorithm, and (d) CM of the N.B. algorithm, CM of the SVM algorithm.

Figure 32 shows the CM of the five ML algorithms trained for the classification off the EEG signal related to the different classes. Figure 32(a) shows the CM of the LDA algorithm. Figure 32(b) shows the CM of the D.T. algorithm. Figure 32(c) shows the CM of the KNN

algorithm. Figure 32(d) shows the CM of the N.B. algorithm. Figure 32(e) shows the CM of the SVM algorithm. We notice that artificial neural networks produce the best results. The fundamental reason is that artificial neural networks can classify, correlate, and recognize hidden patterns in data, because during training, the network is trained to associate the output with the input patterns.

4.2. Scoring metrics

To evaluate the performance of the ML algorithms, we used the following scoring metrics: Accuracy, Error, Recall, Specificity, Precision and F1-Score. The performance evaluation of the proposed ML was initiated by calculating Sensitivity, Specificity, Precision and Accuracy Sadrawi et al. (2018); Guang-Hui et al. (2017). Sensitivity, also known as Recall Guang-Hui et al. (2017), measures the proportion of positives that are correctly identified as such; it can be calculated by (30). Similarly, Specificity measures the proportion of negatives that are correctly identified as such; it can be calculated by (31). Precision is the proportion of true positives among the positive predictions; it can be calculated by (32). Accuracy is the proportion of the total number of predictions that were correct Sharma et al. (2022); it can be calculated by (33).

$$Recall = \frac{TruePositives}{FalseNegative + TruePositives}, \quad (30)$$

$$Specificity = \frac{TrueNegatives}{FalsePositives + TrueNegatives}, \quad (31)$$

$$Precision = \frac{TruePositives}{TruePositives + FalsePositives}, \quad (32)$$

$$Accuracy = \frac{TruePositives + TrueNegatives}{TruePositives + FalsePositives + TrueNegatives + FalseNegatives}. \quad (33)$$

F1-Score is a method for combining *Precision* and *Recall* into a single measure that includes both Castro et al. (2020). Neither *Accuracy* nor *Recall* can analyze the complete situation on their own. We might have outstanding *Precision* but poor *Recall*, or vice versa, poor *Precision* but good *Recall*. With *F1-Score*, one can represent both concerns with a single

score Grandini et al. (2020). Once *Accuracy* and *Recall* for a binary or multiclass classification task have been computed, the two scores may be combined to calculate the *F1-Score* metric; it can be calculated by (34):

$$F1 - Score = \frac{2 * Precision * Recall}{Precision + Recall}. \quad (34)$$

The precision and recall balance is expressed in F1 scores Singh et al. (2021). The test accuracy is also gauged by the F1 score. It is defined as the weighted mean of the precision and recall. Its worst value is 0, while its maximum value is 1 Arjaria et al. (2021). Equations (30)–(34) are valid for binary and multiclass classification; however, when used for multiclass problems, they must be calculated for each class and then averaged to obtain each metric per model.

Table 11 shows the average scores obtained in each performance metrics by the nine ML algorithms selected in this study. The first parameter analyzed was Accuracy, where the LDA model presented an Accuracy score of 0.9229; D.T. obtained 0.9803; KNN obtained 0.8996; N.B. obtained 0.9373; SVM obtained 0.9803; Narrow-ANN, Medium-ANN, and Bilayered-ANN obtained 0.9857; finally, Wide-ANN obtained 0.9821. The Narrow-ANN, Medium-ANN, and Bilayered-ANN models obtained the best Accuracy score (0.9857). Regarding the Error metric, we can see that the LDA, D.T., N.B., SVM, Narrow-ANN, Medium-ANN, Wide-ANN, and Bilayered-ANN algorithms achieved a score less than 0.1, while the KNN model obtained an Error greater than 0.1; therefore, the models with the lowest Error were Narrow-ANN, Medium-ANN, and Bilayered-ANN (0.0143). Considering the Recall parameter, we observed that the Narrow-ANN algorithm presented the highest score of 0.9863, while the KNN algorithm obtained the lowest score of 0.9037. Regarding the Specificity metric, all the algorithms achieved a score greater than 0.9; the ML models with the best results were the Narrow-ANN, Medium-ANN, and Bilayered-ANN models, all scoring 0.9964. Regarding the Precision metric, the Bilayered-ANN algorithm is the one that presented the best result, with 0.9859, while the KNN algorithm presented the lowest score, with 0.9099. Regarding the F1-Score parameter, the LDA, D.T., N.B., SVM, Narrow-ANN, Medium-ANN, Wide-ANN, and Bilayered-ANN algorithms achieved scores greater than 0.91, while the KNN model obtained a score below 0.91. The algorithm that presented the best F1-Score result was Narrow-ANN, with 0.9859.

Table 11: The average score parameters of the EEG classification algorithms.

Average scoring parameters						
ML Algorithm	Accuracy	Error	Recall	Specificity	Precision	F1-Score
LDA	0.9229	0.0771	0.9219	0.9807	0.9332	0.9228
D.T.	0.9803	0.0197	0.9777	0.9951	0.9792	0.9783
KNN	0.8996	0.1004	0.9037	0.9747	0.9099	0.9047
N.B.	0.9373	0.0627	0.9384	0.9844	0.9382	0.9378
SVM	0.9803	0.0197	0.9789	0.9950	0.9827	0.9803
Narrow-ANN	0.9857	0.0143	0.9863	0.9964	0.9857	0.9859
Medium-ANN	0.9857	0.0143	0.9854	0.9964	0.9856	0.9855
Wide-ANN	0.9821	0.0179	0.9834	0.9955	0.9824	0.9828
Bilayered-ANN	0.9857	0.0143	0.9854	0.9964	0.9859	0.9856

4.3. Performance Metrics

The metrics used to evaluate the performance of the ML and ANN algorithms were the area under the average curve (AUC average), Cohen’s Kappa coefficient Vieira et al. (2010), Matthews correlation coefficient Matthews (1975), and model loss. The receiver operating characteristics (ROC) curve is the plot between sensitivity and the FP rate for various threshold values. The AUC is the area under this ROC curve; it is used to measure the quality of the classification model Sharma et al. (2022). Figure 33 shows the ROC curves of the four DL algorithms (neural networks) trained for the classification of EEG signals. These algorithms are Narrow-ANN, Medium-ANN, Wide-ANN, and Bilayered-ANN. The algorithm that presented the best performance metrics was Medium-ANN, with an AUC average of 0.9998; it was the closest to the upper-left corner of the ROC space. Figure 34 shows the ROC curves of the top four ML algorithms trained for the classification of EEG signals related to the state of relaxation, right hand, left hand, both hands, and both feet. These algorithms are LDA, SVM, D.T and N.B. The algorithm that presented the best performance metrics was SVM, with an AUC average of 0.9988. The ROC curves showed a compromise between Sensitivity and Specificity. The SVM algorithm was the closest to the upper-left corner of the ROC space, while the D.T. model was closer to the 45-degree diagonal. Classifiers that obtain curves closer to the upper-left corner indicate better performance, while classifiers with ROC curves closer to the 45-degree diagonal of the ROC space are less accurate.

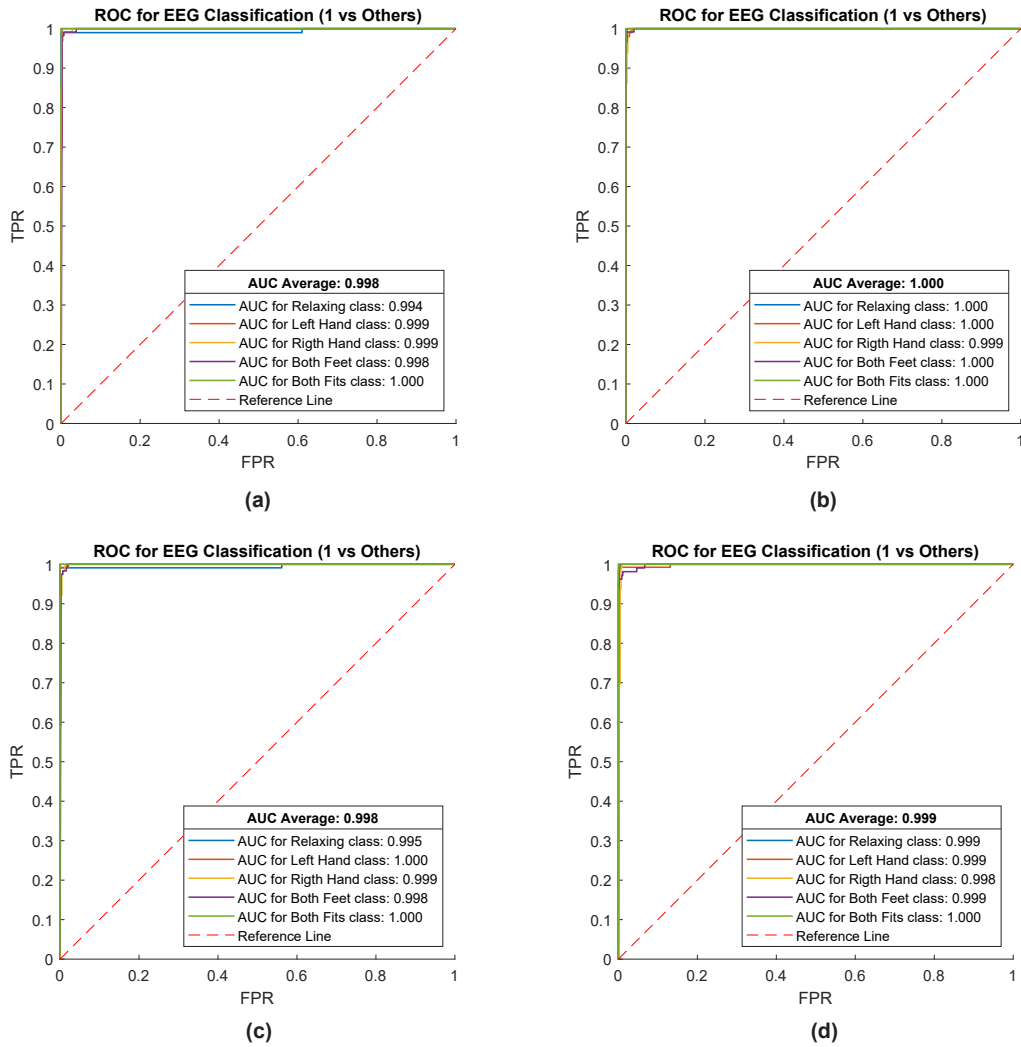


Figure 33: The receiver operating characteristic (ROC) curves of the four ANN algorithms trained for EEG signals classification, related to the movements of hands and feet: (a) ROC curves of the Narrow-ANN algorithm, (b) ROC curves of the Medium-ANN algorithm, (c) ROC curves of the Wide-ANN algorithm, and (d) ROC curves of the Bilayered-ANN algorithm.

Concerning the AUC average metric, all algorithms achieved a score greater than 0.90, where the top three ML models were the SVM, Medium-ANN, and Bilayered-ANN models, which obtained the highest scores (AUC scores).

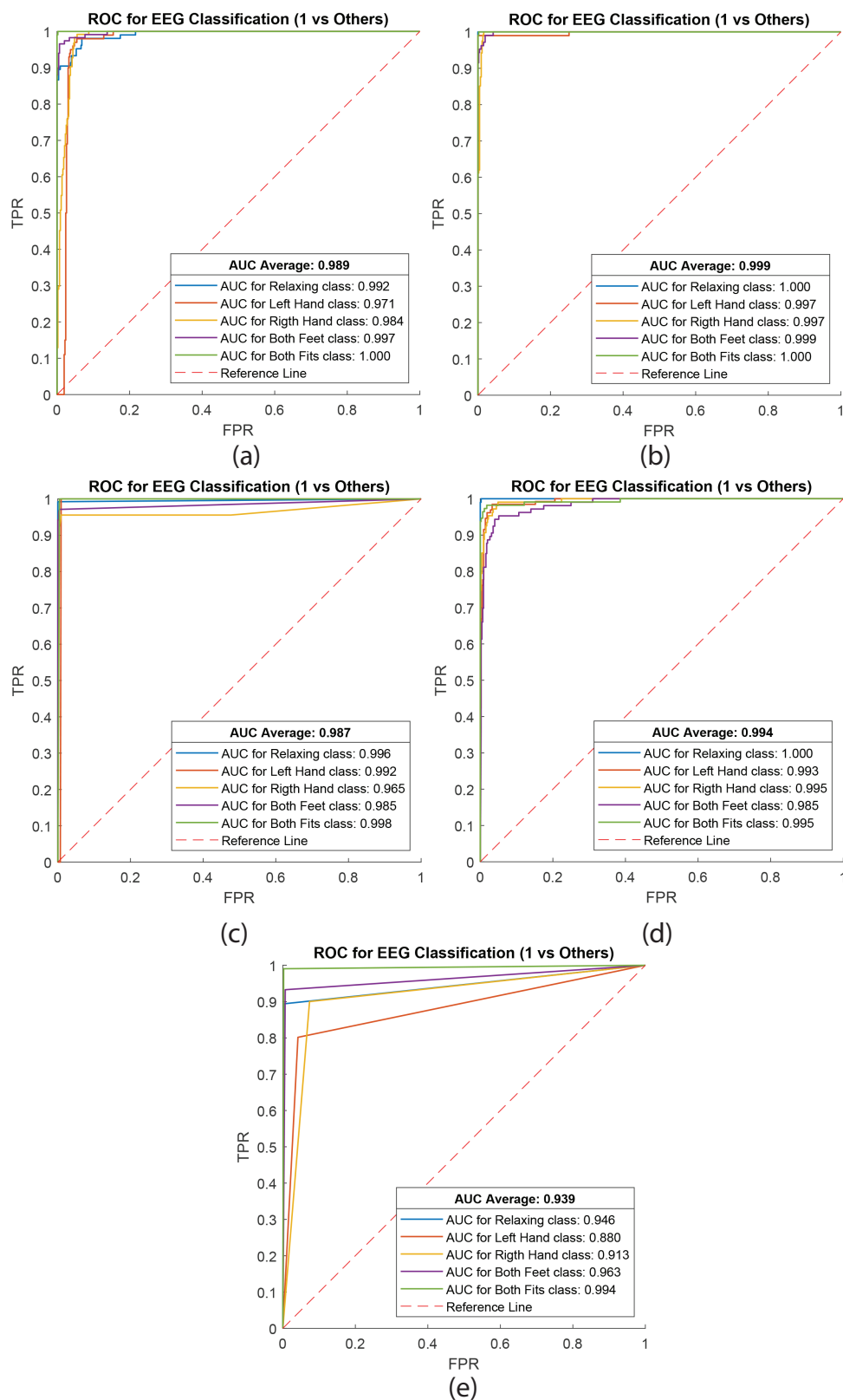


Figure 34: The receiver operating characteristic (ROC) curves of the top four ML algorithms trained for EEG signals classification, related to the movements of hands and feet: (a) ROC curves of the LDA algorithm, (b) ROC curves of the SVM algorithm, (c) ROC curves of the D.T. algorithm, and (d) ROC curves of the N.B. algorithm.

Regarding Cohen’s Kappa coefficient, a score above 0.8 indicates exemplary commitment, while zero or less indicates poor commitment. The LDA and KNN algorithms obtained Cohen’s Kappa coefficients less than 0.80 but greater than zero. While the D.T., N.B., SVM, Narrow-ANN, Medium-ANN, Wide-ANN, and Bilayered-ANN algorithms achieved Cohen’s Kappa coefficients of 0.9384, 0.8040, 0.9384, 0.9552, 0.9552, 0.9440, and 0.9552, respectively, where the Narrow-ANN, Medium-ANN, and Bilayered-ANN algorithms achieved the highest scores. In addition, we used the Matthews correlation coefficient, which has been widely used as a performance metric for ML algorithms since 2000. The best scores obtained were presented by the D.T, N.B., SVM, Narrow-ANN, Medium-ANN, Wide-ANN, and Bilayered-ANN models (0.9736, 0.9225, 0.9757, 0.9824, 0.9819, 0.9783, and 0.9820, respectively), with Narrow-ANN obtaining the best score, while the KNN algorithm achieved the lowest score of 0.8810. The ML model with the lowest loss was Narrow-ANN, with 0.0136, followed by the Medium-ANN and Bilayered-ANN models, both with 0.0147, while the ML algorithm with the highest loss was KNN. Table 12 presents the performance metrics achieved by each ML algorithm.

Table 12: Performance metrics of the nine ML algorithms trained for EEG signal classification.

Performance Metrics				
ML Algorithm	AUC Average	Cohen’s Kappa Coefficient	Matthews Correlation Coefficient	Loss
LDA	0.9889	0.7592	0.9072	0.0787
D.T.	0.9873	0.9384	0.9736	0.0229
KNN	0.9392	0.6864	0.8810	0.0961
N.B.	0.9935	0.8040	0.9225	0.0616
SVM	0.9988	0.9384	0.9757	0.0217
Narrow-ANN	0.9982	0.9552	0.9824	0.0136
Medium-ANN	0.9998	0.9552	0.9819	0.0147
Wide-ANN	0.9984	0.9440	0.9783	0.0165
Bilayered-ANN	0.9988	0.9552	0.9820	0.0147

4.4. Comparative analysis of ML and ANN with ConfusionVis

In machine learning, the presumably best model is chosen from a collection of model candidates obtained by evaluating various model types, hyperparameters, or feature subsets, among others. In this paper, it is proposed to use ConfusionVis, a model-agnostic technique for evaluating and comparing multiclass classifiers based on their confusion matrices Theissler et al. (2022). Figure 35 depicts the ConfusionVis achieved for the nine ML models chosen for EEG signal classification. Figure 35(a) shows the average Accuracy score per ML model, where it can be observed that Narrow-ANN had the best Accuracy score. Figure 35(b) illustrates the Confusion Matrix Similarity results, where it can be seen that the D.T., SVM, Narrow-ANN, and Medium-ANN models obtained the best similarity. Figure 35(c) depicts the Error by Class scores, where it can be observed that Medium-NN and Narrow-ANN achieved the lowest Error score in most classes of movements classified from the EEG signals. Figure 35(d) shows the Error by Model scores, where it can also be seen that Medium-ANN obtained the lowest Error score, followed by Bilayered-NN, Narrow-ANN, and decision tree (D.T.).

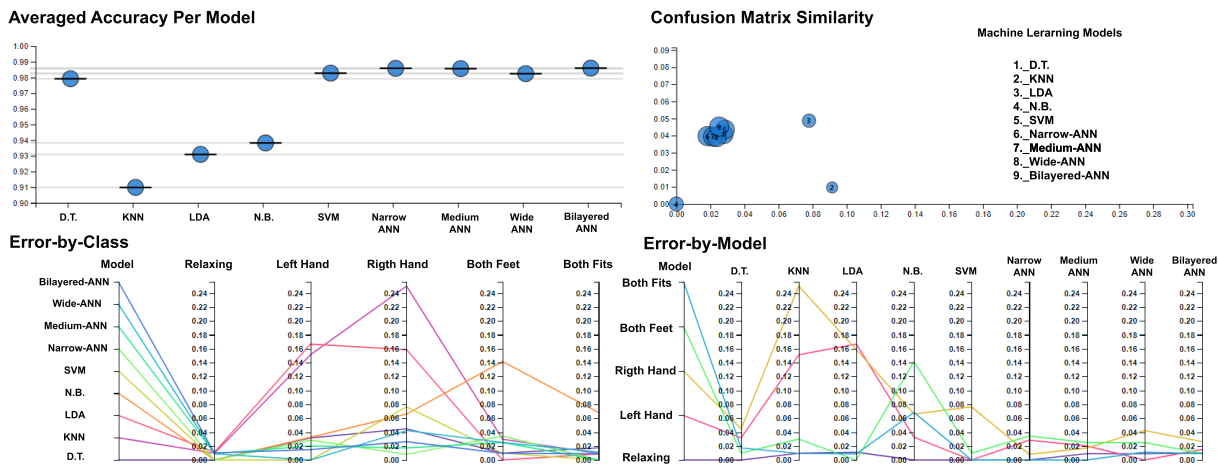


Figure 35: ConfusionVis Theissler et al. (2022): Comparative evaluation of the multiclass classifiers based on confusion matrices. (a) Averaged Accuracy per model, (b) Confusion Matrix Similarity, (c) Error by class, and (d) Error by Model.

4.5. Training time metrics

Figure 36 shows the training time of the nine ML algorithms tested, with N.B., LDA, and KNN having the shortest training time. However, the results shown in Tables 11 and 12 show that these algorithms had the lowest performance metrics, with the exception of D.T. In contrast, the SVM, Narrow-ANN, Medium-ANN, Wide-ANN, and Bilayered-ANN algorithms had the most considerable training times of 0.13546, 0.37135, 0.16956, 0.36255, and 0.45722 s, respectively, with the Bilayered-ANN algorithm having the longest training time. However, these algorithms had the best performance metrics, as shown in Tables 11-12 and Figures 33-35. Therefore, the data science engineer or researcher must perform a cost-benefit analysis regarding Accuracy and processing time. In most circumstances, engineers favor Accuracy over training time, because training is only done a few times and only the trained ML model is employed. For this reason, in this study, it is more convenient to select the Narrow-ANN model.

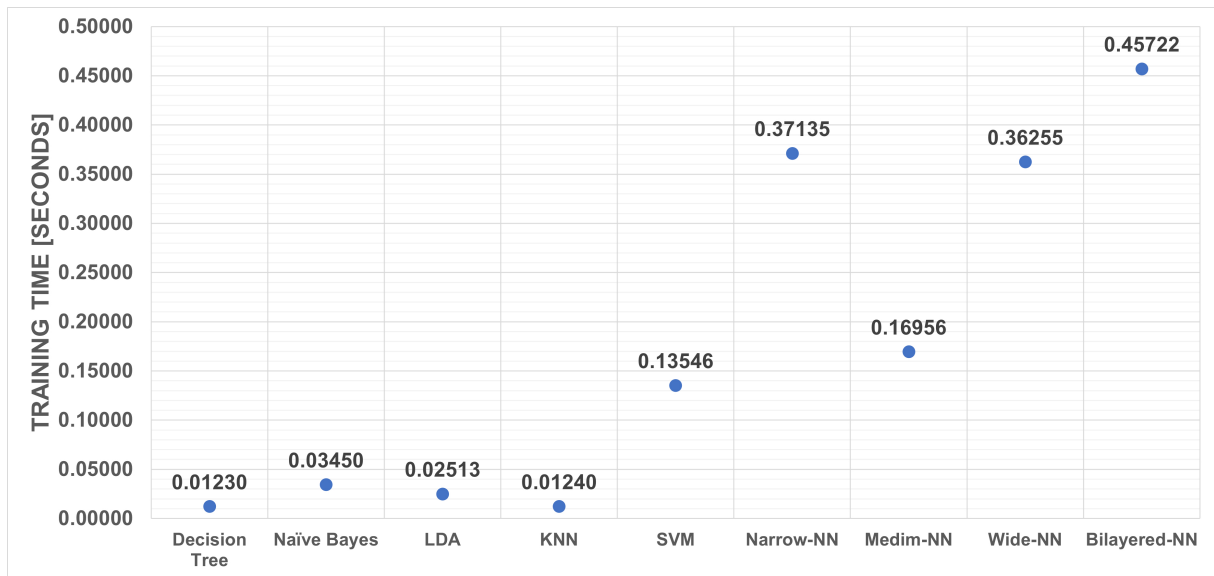


Figure 36: Training time of the nine ML models.

4.6. Discussion

In this study, we observed that the different features used were helpful for the classification of EEG signals, as proposed in our hypothesis. The presented features are based on the time domain: amplitude, frequency, phase, peak–peak value, negative peak, positive peak, median, mode, average, mean square error value, standard deviation, summation, variance, kurtosis, and skewness. We consider that they are good features for classifying EEG signals related to movements. Using these features, the ML model that achieved the best performance was Medium-ANN, with: average area under the curve of 0.9998, Cohen’s Kappa coefficient of 0.9552, Matthew correlation coefficient of 0.9819 and loss of 0.0147.

We observed that the performance metrics obtained from the nine machine learning algorithms were good. Using standard features in different frequency bands and related to a particular class allowed machine learning and deep learning algorithms to obtain excellent performance metrics, as shown in Tables 11-12 and Figures 34-35; this is because the proposed frequency bands and features improved the separability of the data, making the classification algorithms substantially better.

Regardless, the data science engineer/scientist is in charge of carrying out the corresponding analysis in terms of costs–benefits and precision concerning the information processing time. In most cases, ML models with better precision are chosen, and training time is usually sacrificed. Since the training of the ML algorithms is performed once, only the trained model is used for the assigned task. The Medium-ANN algorithm was selected for this reason and because its performance metrics were the best. Therefore, feature extraction is worth mentioning among the processes that improve relevant information acquisition and ensure better performance metrics when training EEG signal classification algorithms, as shown in different studies. Our results are consistent with other spectrogram methods implemented for identifying EEG patterns in persons with motor impairment using similar brain sources that were analyzed in this study Vrbancic and Podgorelec (2018). Many human behavior fields still a challenge for BCI’s, findings from this study may provide complementary data for other studies reporting findings from central nervous system’s damage with residuals of motor impairment of upper limb movement Bartur et al. (2019). In addition to limb paralysis, limb loss represents an obstacle to quality of life for which the results of this study offer a comprehensive and reliable technique for extracting electrical brain sources for

human movement programming. As in other research Samuel et al. (2017b), results of the present study provide consistent and accurate information for future controlling inputs for the adaptation of prosthesis. As reported elsewhere Samuel et al. (2017a), we conclude that it is necessary to increase movement classes in EEG features extraction for providing mechatronic systems controlled by means of BCI, suitable and reliable patterns corresponding for target movements.

4.7. Proposed Usage Scenario

The ML algorithms proposed in this research study could be implemented in high-performance embedded systems or edge computing devices as verified in previous studies Contreras-Luján et al. (2022); Aguirre-Castro et al. (2022). These act as the central control system, which is in charge of communicating with the BCI to acquire EEG signals. Likewise, the control system is in charge of carrying out the digital processing of the EEG signals, the extraction of features, the classification, and the translation (decoding and execution) of the control commands. The mechatronic control system would have a trained ML model which would allow a user with some motor disability to perform some motor activities, such as opening and closing the right fist, left fist, or both fists through the classification of EEG signals.

Figure 37 depicts a conceptual diagram of the prospective mechatronic control system. We could consider this model the first step in developing intelligent prostheses that integrate the system's several components. The future characteristics to be developed are lower cost, size, portability, low power consumption, and reliable communication with the BCI.

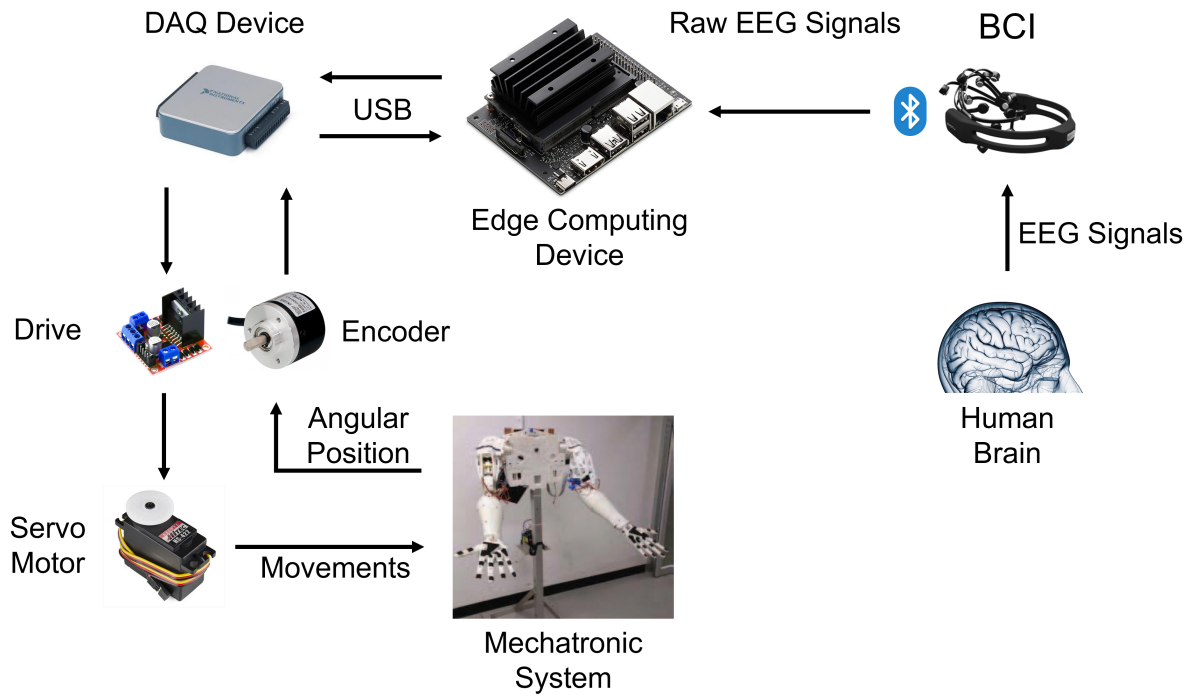


Figure 37: Suggested usage scenario for an application of mechatronic control system.

Chapter V

5. Conclusions

The methodology presented for classifying motor movements through the processing of EEG signals from 30 users showed satisfactory results due to the performance metrics obtained from the different machine learning models and artificial neural networks. The classification of EEG signals is related to movements of the left hand, right hand, both hands, feet, and relaxation. As a result of EEG signal processing, a dataset with custom metrics or features was created and used for training machine learning algorithms and artificial neural networks. The data set was obtained by reading files in EDF+ formats containing 64 EEG signals, with approximately 2 minutes and 160 samples per second. Electrodes in positions C3, C1, CZ, C2, and C4, which are under the international system 10-10, and are related to the motor cortex of the human brain, were selected. The EEG signals were then divided into segments, line noise was removed through preprocessing, each signal associated with a particular position was filtered in a distinct frequency band, and three characteristics were retrieved in the temporal domain. The signal analysis results are a vector of 15 features in the time domain, with their respective label to the corresponding class. The custom dataset was created to train and evaluate the performance metrics of five machine learning algorithms and four artificial neural network algorithms for classifying EEG signals related to motor movements. From the different generated models, the Medium-ANN model achieved the best performance metrics, with an average AUC of 0.9819, a Cohen's Kappa coefficient of 0.9552, a Matthews correlation coefficient of 0.9819, and a loss of 0.0147. It is worth mentioning that with the proposed methodology, eight of the nine trained models obtained an accuracy above 90 percent, which is considered good. The model that failed to be above this threshold was the KNN, with an accuracy of 0.8996. These findings allow our approach to be applied in different scenarios, such as the implementation of robotic prostheses. In these types of applications, using physical quantities is an acceptable alternative when hardware resources are constrained, or in embedded systems or edge computing devices, which has the advantage of low cost, small size, portability, low power consumption, and reliable communication with BCIs. Therefore, with the proposed method, we can obtain quantifiable information about

the motor movements of the hands and feet that can be obtained through the extraction of features and performance metrics from machine learning algorithms and artificial neural networks. We also think that the proposed method can allow us to generate different data sets that can be used in future studies since the developed software can be easily customized to analyze EEG signals.

5.1. Future Work

The following is a list of potential improvements that could be included in the LabVIEW development environment as part of future work on feature extraction software advancements.

- Publish the current version of the developed software in a high-impact JCR journal.
- Upgrade the development platform version from LabVIEW 2015 to LabVIEW 2020, to implement the training process of ML and DL models with the Deep Learning Module.
- Add additional signal preprocessing techniques, including principal component analysis, muscle movement removal, and non-linear noise removal filters.
- Add feature extraction in the frequency domain, which is a fundamental piece to improving the performance metrics of classification algorithms, whether they are machine learning algorithms or artificial neural networks.
- Add feature extraction in the time-frequency domain; these metrics are a current trend because they allow deep learning and transfer learning algorithms.
- Software parallelization: a software update can be beneficial; carrying out parallel analysis and feature extraction of the different EEG signals coming from multiple electrodes can improve the efficiency and effectiveness of the system, taking advantage of multi-core processors.
- The implemented methodology can be conditioned to be used within the area of Robotics, particularly for the control of robotic arms and prostheses and wheelchairs, and mobile robots.
- Using feature extraction in the time-frequency domain will allow the use of pre-trained deep neural networks, which have shown outstanding results for pattern recognition and classification.

- Optimization of machine learning and deep learning algorithms and selection of the best characteristics.
- Finally, implementing the proposed methodology in embedded systems or edge computing devices such as MyRIO, RaspberryPi, and NVIDIA Jetson could be possible to carry out control strategies.

Appendix

A. Fragment of the dataset created for this study

C3 Amplitude	C3 Frequency	C3 Phase	C1 Peak to Peak	C1 Negative Peak	C1 Positive Peak	C4 Median	C4 Mode	C4 Mean	C2 RMS	C2 SD	C2 Summation	C4 Variance	C4 Kurtosis	C4 Skewness	Classes
100.86617	-29.32351	79.5466	0.26955	2.97256	1.51095	17.2037	17.2253	979.79113	285.73589	7.49178	1.69966	8.42745	0.01292	-57.88825	0
145.2712	-52.97355	92.29735	-1.91889	-11.14636	-0.38611	18.6683	18.46945	-543.63732	366.13252	5.55892	0.902	9.11897	0.00636	7.69257	0
100.73007	-38.61309	62.11688	-1.21691	0.21219	-0.23162	16.3806	16.38057	-951.47539	257.03075	3.80701	0.61077	8.92251	0.00794	24.5861	0
119.87798	-57.16337	62.71462	-1.66857	0.04493	-0.00493	19.4224	19.42449	18.93081	368.71271	3.19239	0.32758	8.63137	0.0046	-97.59919	0
125.2583	-57.15535	68.0694	-1.91489	-5.52267	-0.49701	19.50148	19.48865	-2956.4001	377.8044	3.11134	0.27458	8.8037	0.00691	-109.72719	0
125.67379	-57.61492	68.05837	-1.47821	-4.39237	0.02402	19.54563	19.54656	173.02883	379.61249	3.12059	0.25601	7.58664	0.00088	-37.67507	0
125.68931	-57.61504	68.07427	-1.74668	-4.33893	-0.02686	17.26488	17.26855	-284.69056	288.30936	3.5752	0.41033	6.55339	0.00025	150.20839	0
125.31995	-57.61533	67.70643	-1.70889	-4.66525	0.03645	16.42054	16.42135	213.89227	270.07081	3.84992	0.46781	5.07003	0.00898	-129.32524	0
60.11105	-26.70835	33.4072	-0.68864	-0.23313	-0.5557	13.09898	13.09817	-414.86556	162.42172	2.4878	0.25355	10.79111	0.01589	2.81889	0
150.91658	-95.88303	94.93355	-1.77143	-5.3341	-0.20248	20.87857	20.88366	-434.83338	437.30133	8.8172	0.0715	16.00605	0.00621	115.23688	0
81.42884	-35.41586	46.01297	-1.01522	-0.04502	-0.15462	13.66927	13.66939	-766.25766	193.38404	4.47048	0.48256	5.48752	0.01028	-51.56381	0
149.91035	-80.69967	69.21068	-1.06843	-9.09432	-0.07855	20.50509	20.50722	-237.70391	422.09271	4.16793	0.10647	8.36332	0.00551	140.77191	0
168.19124	-80.77541	87.41583	-1.01319	2.02131	-0.17725	22.09124	22.09226	-1142.61713	488.78057	4.06289	0.24355	9.24432	0.00595	10.96383	0
178.18338	-80.95155	97.23333	-1.91043	-1.48237	-0.38365	23.20017	23.19817	-2985.49963	542.32634	4.07673	0.37249	6.94932	0.007	124.32721	0
165.99797	-68.76335	97.23412	-1.88315	2.43568	-0.28765	24.48947	24.48931	-2400.00755	603.6636	4.07886	0.54094	8.45258	0.00216	21.81982	0
164.91541	-67.67808	97.23933	-1.7938	2.43564	0.06713	24.04032	24.04147	510.43337	585.46381	4.08828	0.56694	10.81424	0.00215	-45.78993	0
208.89663	-113.28443	95.5152	0.15291	-17.76571	3.27354	40.61923	40.51458	-2222.06571	1621.20376	3.28414	-0.15438	39.40843	0.0081	-115.65355	0
86.64714	-32.25059	54.39655	-1.58422	-1.6633	-0.34174	12.8235	12.82229	-690.91512	159.61514	4.44967	0.70882	7.62719	0.00757	200.835	0
85.27214	-36.61694	49.1102	-1.34702	0.03834	-0.03464	14.12175	14.51493	37.44572	206.20682	3.25947	0.48182	7.04131	0.00579	64.3528	0
96.2026	-48.3727	47.8229	-1.55971	-0.02817	-0.13303	14.57802	14.57878	-715.35163	207.82778	3.31905	0.48414	7.16151	0.00606	-119.52097	0
96.61122	-48.34633	48.28469	-2.07812	-3.30589	-0.16501	15.34706	15.3469	-1257.20839	232.66531	3.21864	0.47966	7.57887	0.00601	-81.37703	0
115.44138	-48.12757	67.31381	-1.68488	-4.53478	-0.09991	15.84409	15.84484	-758.99683	250.80891	3.38552	0.48671	8.80287	0.00606	-125.87036	0
107.7065	-40.38833	67.31767	-1.59927	-3.99952	-0.03227	16.32175	16.32665	-337.47932	264.43873	3.53177	0.60548	9.58213	0.00665	-106.34589	0
107.3927	-40.07533	67.31917	-1.59398	-5.44033	-0.08078	15.80524	15.8058	-657.09752	246.15637	3.57552	0.57687	7.56182	0.00606	-111.23568	0
129.15821	-78.83456	50.32365	2.54778	-1.73504	1.9225	25.30673	25.26614	1164.45591	642.38665	4.72333	-0.92255	10.21739	0.00855	-179.18551	0
105.01136	-43.05677	61.56459	-1.74764	-2.98789	-0.22264	18.15878	18.1624	-386.03301	313.94184	3.64993	0.43932	11.21388	0.00688	-49.82756	0
103.4699	-39.51072	63.59318	-0.33663	3.66172	-0.02689	16.65389	16.65356	-105.03978	262.7192	3.74805	0.45868	9.27786	0.00584	-9.21414	0
170.39639	-95.58504	74.81133	-1.27524	-2.79184	-0.1146	18.94103	18.94256	-642.32131	344.03532	4.73865	0.20333	8.07855	0.00629	43.58395	0
170.18116	-95.78412	74.39704	-1.66529	-3.58302	-0.05165	18.01691	18.01833	-322.99376	315.3292	5.12737	0.08568	8.99191	0.00726	-17.34837	0
132.33885	-66.59612	65.74274	-1.70012	-4.83305	-0.01402	16.44777	16.44836	-260.7329	272.77158	3.90803	0.30343	6.0148	0.00643	233.40587	0
140.09181	-66.24984	73.84196	-1.52839	-5.4838	0.03415	16.85112	16.85209	129.02571	289.59865	3.76946	0.33227	5.65945	0.00543	76.20641	0
129.81297	-55.97095	73.84203	-1.66338	-2.65789	-0.06647	16.31524	16.31593	-642.92732	267.56623	3.97121	0.52604	6.43784	0.0083	-185.97406	0
74.47038	-33.17593	41.29465	-1.06786	-5.44768	-0.00179	15.44494	15.4535	-117.89732	271.18465	3.20773	0.39781	9.42659	0.01214	206.93585	0
101.9468	-44.0935	57.5333	-1.57687	-3.03288	-0.19162	16.61635	16.61664	-497.86008	271.47894	4.08116	0.52031	7.4292	0.00666	-29.1921	0
161.79333	-97.88084	63.94869	-1.63274	-3.40556	-0.08394	20.68456	20.68752	-279.22265	416.11531	4.82303	-0.00011	14.74093	0.00469	156.0626	0
168.28902	-98.89957	69.29944	-2.26611	-4.3866	-0.0091	18.43838	18.44054	-121.97746	333.03526	5.78385	0.23606	8.07345	0.00565	34.34179	0
118.41162	-49.11881	69.29281	-1.80372	1.16639	-0.16257	15.47354	15.47356	-957.41073	238.87176	4.28831	0.82451	7.88934	0.00689	-169.0244	0

Figure 38: Fragment of the dataset created for this study.

B. Front panel (App) for EEG signal analysis

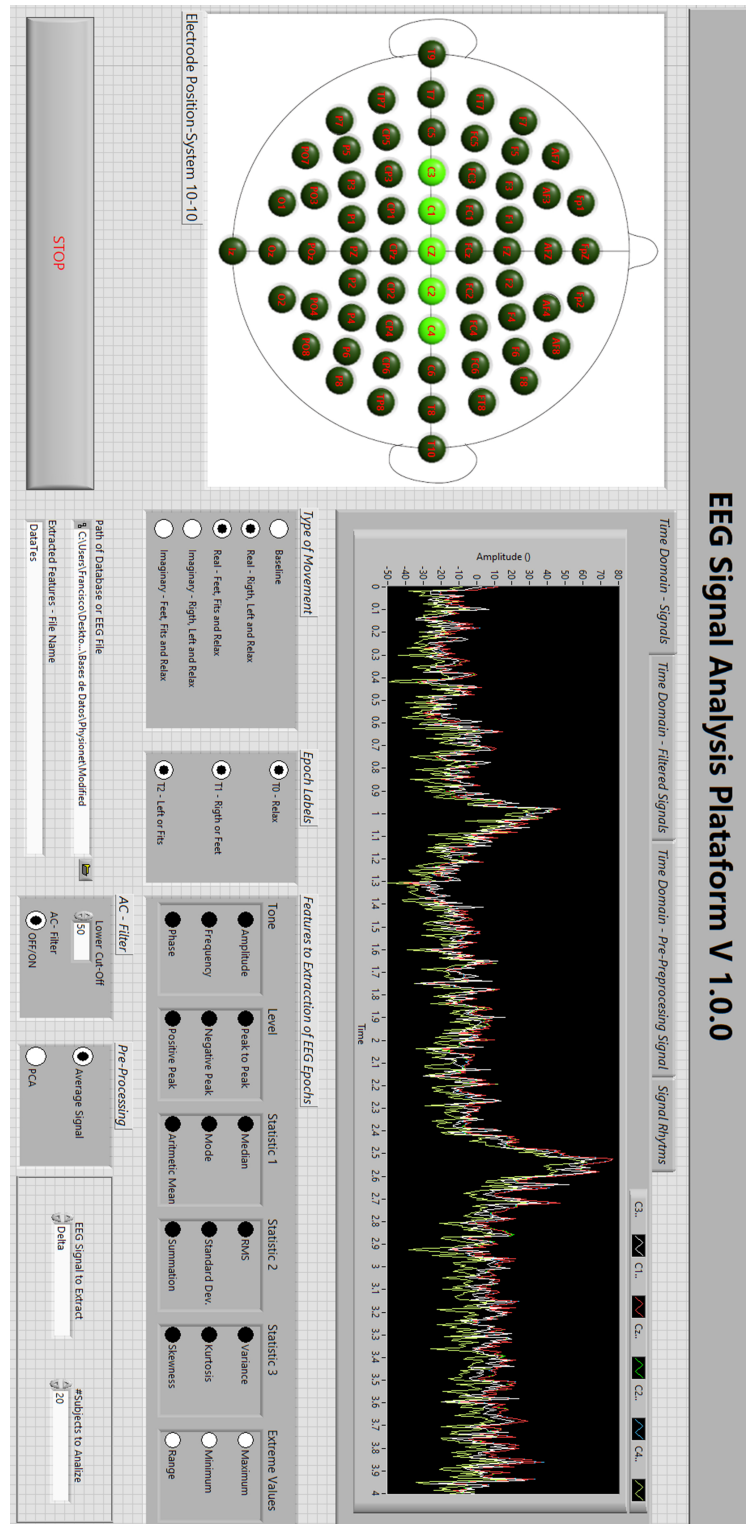


Figure 39: Front panel of software (App) developed for EEG signal analysis.

C. Matlab Code for LDA Algorithm

```
1 %Training of Lineal Discriminant Analysis Algorithm: ML
2 %Develop by: Francisco Javier Ramirez Arias
3
4 %Read of Data
5 %%%%%%%%%%%%%%%%%%%%%%%%%%%%%%%%%%%%%%%%%%%%%%%%%%%%%%%%%%%%%%%%%%%%%%%%%
6 data = ReadData("Dataset08_Balanced");
7 %%%%%%%%%%%%%%%%%%%%%%%%%%%%%%%%%%%%%%%%%%%%%%%%%%%%%%%%%%%%%%%%%%%%%%%%%
8
9 %Pre-processing
10 %%%%%%%%%%%%%%%%%%%%%%%%%%%%%%%%%%%%%%%%%%%%%%%%%%%%%%%%%%%%%%%%%%%%%%%%%
11 data.Classes = categorical(data.Classes);
12 data.Classes = renamecats(data.Classes, {'Relaxing', 'Left Hand', ...
13 'Rigth Hand', 'Both Feet', 'Both Fits'});
14 %%%%%%%%%%%%%%%%%%%%%%%%%%%%%%%%%%%%%%%%%%%%%%%%%%%%%%%%%%%%%%%%%%%%%%%%%
15
16 %Normalization
17 %%%%%%%%%%%%%%%%%%%%%%%%%%%%%%%%%%%%%%%%%%%%%%%%%%%%%%%%%%%%%%%%%%%%%%%%%
18 data{:,1:end-1} = normalize(data{:,1:end-1});
19 %%%%%%%%%%%%%%%%%%%%%%%%%%%%%%%%%%%%%%%%%%%%%%%%%%%%%%%%%%%%%%%%%%%%%%%%%
20
21 %Data for training and test
22 %%%%%%%%%%%%%%%%%%%%%%%%%%%%%%%%%%%%%%%%%%%%%%%%%%%%%%%%%%%%%%%%%%%%%%%%%
23 dp = cvpartition(size(data,1), "HoldOut", 0.2);
24 train = data(dp.training,:);
25 test = data(dp.test,:);
26 %%%%%%%%%%%%%%%%%%%%%%%%%%%%%%%%%%%%%%%%%%%%%%%%%%%%%%%%%%%%%%%%%%%%%%%%%
27
28 %Training of the model
29 %%%%%%%%%%%%%%%%%%%%%%%%%%%%%%%%%%%%%%%%%%%%%%%%%%%%%%%%%%%%%%%%%%%%%%%%%
30 mdl = fitcdiscr(train, "Classes");
31
32 %Prediction of the model
33 [lb,ss]=predict(mdl,test);
34 %%%%%%%%%%%%%%%%%%%%%%%%%%%%%%%%%%%%%%%%%%%%%%%%%%%%%%%%%%%%%%%%%%%%%%%%%
```

```

35
36 %Metrics of the model
37 %%%%%%%%%%%%%%%%%%%%%%%%%%%%%%%%%%%%%%%%%%%%%%%%%%%%%%%%%%%%%%%%%%%%%%%%%
38 cm = confusionchart(test.Classes,lb);
39 cm.Title = 'EEG-Signal Classification';
40 [m1,~] = confusionmat(test.Classes,lb);
41 [Result,ReferenceResult] = multiclass_metrics_special(m1)
42 %%%%%%%%%%%%%%%%%%%%%%%%%%%%%%%%%%%%%%%%%%%%%%%%%%%%%%%%%%%%%%%%%%%%%%%%%
43
44 %ROC Curves
45 %%%%%%%%%%%%%%%%%%%%%%%%%%%%%%%%%%%%%%%%%%%%%%%%%%%%%%%%%%%%%%%%%%%%%%%%%
46 figure(2)
47 hold on
48 Classes = categories mdl.ClassNames)
49 AUC = zeros(length mdl.ClassNames),1);
50 for i=1:length mdl.ClassNames)
51     [xr, yr, ~, auc] = perfcurve(test.Classes,ss(:, i),Classes{i});
52     plot(xr, yr, 'linewidth', 1)
53     legends{i} = sprintf('AUC for %s class: %.3f', Classes{i}, auc);
54     AUC(i,:) = auc;
55 end
56
57 AUCAverage = mean(AUC)
58 mdlloss = loss mdl,test,"Classes")
59
60 line([0 1], [0 1], 'linestyle', '--', 'color', 'r');
61 legends{6} = 'Reference Line';
62 lgd =legend(legends, 'location', 'southeast');
63 til = sprintf('AUC Average: %.3f',AUCAverage);
64 title(lgd,til)
65 xlabel('FPR'), ylabel('TPR');
66 title('ROC for EEG Classification (1 vs Others)');
67 axis square
68 %%%%%%%%%%%%%%%%%%%%%%%%%%%%%%%%%%%%%%%%%%%%%%%%%%%%%%%%%%%%%%%%%%%%%%%%%

```

D. Matlab Code for Tree Model

```
1 %Training of Lineal Discriminant Analysis Algorithm: ML
2 %Develop by: Francisco Javier Ramirez Arias
3
4
5 %Desarrollado por: Francisco Javier Ramirez Arias
6 %Asesor Everardo Inzunza Gonzalez
7 %Universidad Autonoma de Baja California
8 %Proyecto Doctoral
9
10 %Lectura de los datos
11 data = ReadData("Dataset08_Balanced");
12
13 %Preprocesamiento de la informacion
14 data.Classes = categorical(data.Classes);
15 data.Classes = renamecats(data.Classes, {'Relaxing', 'Left Hand', ...
16 'Rigth Hand', 'Both Feet', 'Both Fits'});
17
18 %Normalizacion
19 data{:, 1:end-1} = normalize(data{:, 1:end-1});
20
21 %Division de los datos de entrenamiento y de prueba
22 dp = cvpartition(size(data,1), "HoldOut", 0.2);
23 train = data(dp.training, :);
24 test = data(dp.test, :);
25
26 %Entrenamiento del modelo
27 mdl = fitctree(train, "Classes");
28
29 %Prediccion del modelo
30 [lb, ss]=predict(mdl, test);
31
32 %Graficas y metricas del modelo
33 cm = confusionchart(test.Classes, lb);
34 cm.Title = 'EEG-Signal Classification';
```

```

35 [m1, ~] = confusionmat(test.Classes, lb);
36 [Result, ReferenceResult] = multiclass_metrics_special(m1)
37
38 %Curvas ROC y Area Bajo la Curva
39 figure(2)
40 hold on
41 Classes = categories mdl.ClassNames)
42 AUC = zeros(length mdl.ClassNames), 1);
43 for i=1:length mdl.ClassNames)
44     [xr, yr, ~, auc] = perfcurve(test.Classes, ss(:, i), Classes{i});
45     plot(xr, yr, 'linewidth', 1)
46     legends{i} = sprintf('AUC for %s class: %.3f', Classes{i}, auc);
47     AUC(i, :) = auc;
48
49 end
50
51 AUCAverage = mean(AUC)
52 mdlloss = loss mdl, test, "Classes")
53
54 line([0 1], [0 1], 'linestyle', '--', 'color', 'r');
55 legends{6} = 'Reference Line';
56 lgd = legend(legends, 'location', 'southeast');
57 til = sprintf('AUC Average: %.3f', AUCAverage);
58 title(lgd, til)
59 xlabel('FPR'), ylabel('TPR');
60 title('ROC for EEG Classification (1 vs Others)');
61 axis square

```

E. Matlab Code for KNN Model

```
1
2
3
4 %%Desarrollado por: Francisco Javier Ramirez Arias
5 %%Asesor Everardo Inzunza Gonzalez
6 %%Universidad Autonoma de Baja California
7 %%Proyecto Doctoral
8
9 %Lectura de los datos
10 data = ReadData("Dataset08_Balanced");
11
12 %Preprocesamiento de la informacion
13 data.Classes = categorical(data.Classes);
14 data.Classes = renamecats(data.Classes,{'Relaxing','Left Hand',...
15 'Righth Hand','Both Feet','Both Fits'});
16
17 %Normalizacion
18 data{:,1:end-1} = normalize(data{:,1:end-1});
19
20 %Division de los datos de entrenamiento y de prueba
21 dp = cvpartition(size(data,1),"HoldOut",0.2);
22 train = data(dp.training,:);
23 test = data(dp.test,:);
24
25 %Entrenamiento del modelos
26 mdl = fitcknn(train,"Classes");
27
28 %Prediccion del modelo
29 [lb,ss]=predict(mdl,test);
30
31 %Graficas y metricas del modelo
32 cm = confusionchart(test.Classes,lb);
33 cm.Title = 'EEG-Signal Classification';
34 [m1,-] = confusionmat(test.Classes,lb);
```

```

35 [Result,ReferenceResult] = multiclass_metrics_special(m1)
36
37 %Curvas ROC y Area Bajo la Curva
38 figure(2)
39 hold on
40 Classes = categories mdl.ClassNames)
41 AUC = zeros(length mdl.ClassNames),1);
42 for i=1:length mdl.ClassNames)
43     [xr, yr, ~, auc] = perfcurve(test.Classes,ss(:, i),Classes{i});
44     plot(xr, yr, 'linewidth', 1)
45     legends{i} = sprintf('AUC for %s class: %.3f', Classes{i}, auc);
46     AUC(i,:) = auc;
47
48 end
49
50 AUCAverage = mean(AUC)
51 mdlloss = loss mdl,test,"Classes")
52
53 line([0 1], [0 1], 'linestyle', '--', 'color', 'r');
54 legends{6} = 'Reference Line';
55 lgd =legend(legends, 'location', 'southeast');
56 til = sprintf('AUC Average: %.3f',AUCAverage);
57 title(lgd,til)
58 xlabel('FPR'), ylabel('TPR');
59 title('ROC for EEG Classification (1 vs Others)');
60 axis square

```

F. Matlab Code for NB Model

```
1
2
3
4 %%Desarrollado por: Francisco Javier Ramirez Arias
5 %%Asesor Everardo Inzunza Gonzalez
6 %%Universidad Autonoma de Baja California
7 %%Proyecto Doctoral
8
9 %Lectura de los datos
10 data = ReadData("Dataset08_Balanced");
11
12 %Preprocesamiento de la informacion
13 data.Classes = categorical(data.Classes);
14 data.Classes = renamecats(data.Classes,{'Relaxing','Left Hand',...
15 'Righth Hand','Both Feet','Both Fits'});
16
17 %Normalizacion
18 data{:,1:end-1} = normalize(data{:,1:end-1});
19
20 %Division de los datos de entrenamiento y de prueba
21 dp = cvpartition(size(data,1),"HoldOut",0.2);
22 train = data(dp.training,:);
23 test  = data(dp.test,:);
24
25 %Entrenamiento del modelos
26 mdl = fitcnb(train,"Classes");
27
28 %Prediccion del modelo
29 [lb,ss]=predict(mdl,test);
30
31 %Graficas y metricas del modelo
32 cm = confusionchart(test.Classes,lb);
33 cm.Title = 'EEG-Signal Classification';
34 [m1,-] = confusionmat(test.Classes,lb);
```

```

35 [Result,ReferenceResult] = multiclass_metrics_special(m1)
36
37 %Curvas ROC y Area Bajo la Curva
38 figure(2)
39 hold on
40 Classes = categories(mdl.ClassNames)
41 AUC = zeros(length(mdl.ClassNames),1);
42 for i=1:length(mdl.ClassNames)
43     [xr, yr, ~, auc] = perfcurve(test.Classes,ss(:, i),Classes{i});
44     plot(xr, yr, 'linewidth', 1)
45     legends{i} = sprintf('AUC for %s class: %.3f', Classes{i}, auc);
46     AUC(i,:) = auc;
47
48 end
49
50 AUCAverage = mean(AUC)
51 mdlloss = loss(mdl,test,"Classes")
52
53 line([0 1], [0 1], 'linestyle', '--', 'color', 'r');
54 legends{6} = 'Reference Line';
55 lgd =legend(legends, 'location', 'southeast');
56 til = sprintf('AUC Average: %.3f',AUCAverage);
57 title(lgd,til)
58 xlabel('FPR'), ylabel('TPR');
59 title('ROC for EEG Classification (1 vs Others)');
60 axis square

```

G. Matlab Code for SVM Model

```
1
2
3
4 %%Desarrollado por: Francisco Javier Ramirez Arias
5 %%Asesor Everardo Inzunza Gonzalez
6 %%Universidad Autonoma de Baja California
7 %%Proyecto Doctoral
8
9 %Lectura de los datos
10 data = ReadData("Dataset08_Balanced");
11
12 %Preprocesamiento de la informacion
13 data.Classes = categorical(data.Classes);
14 data.Classes = renamecats(data.Classes,{'Relaxing','Left Hand',...
15 'Righth Hand','Both Feet','Both Fits'});
16
17 %Normalizacion
18 data{:,1:end-1} = normalize(data{:,1:end-1});
19
20 %Division de los datos de entrenamiento y de prueba
21 dp = cvpartition(size(data,1),"HoldOut",0.2);
22 train = data(dp.training,:);
23 test = data(dp.test,:);
24
25 %Entrenamiento del modelos
26 mdl = fitcecoc(train,"Classes");
27 %Prediccion del modelo
28 [lb,ss]=predict(mdl,test);
29
30 %Graficas y metricas del modelo
31 cm = confusionchart(test.Classes,lb);
32 cm.Title = 'EEG-Signal Classification';
33 [m1,-] = confusionmat(test.Classes,lb);
34 [Result,ReferenceResult] = multiclass_metrics_special(m1)
```

```

35
36 %Curvas ROC y Area Bajo la Curva
37 figure(2)
38 hold on
39 Classes = categories mdl.ClassNames)
40 AUC = zeros(length mdl.ClassNames),1);
41 for i=1:length mdl.ClassNames)
42     [xr, yr, ~, auc] = perfcurve(test.Classes,ss(:, i),Classes{i});
43     plot(xr, yr, 'linewidth', 1)
44     legends{i} = sprintf('AUC for %s class: %.3f', Classes{i}, auc);
45     AUC(i,:) = auc;
46
47 end
48
49 AUCAverage = mean(AUC)
50 mdlloss = loss mdl,test,"Classes")
51
52 line([0 1], [0 1], 'linestyle', '--', 'color', 'r');
53 legends{6} = 'Reference Line';
54 lgd =legend(legends, 'location', 'southeast');
55 til = sprintf('AUC Average: %.3f',AUCAverage);
56 title(lgd,til)
57 xlabel('FPR'), ylabel('TPR');
58 title('ROC for EEG Classification (1 vs Others)');
59 axis square

```

H. Matlab Code for Narrow-ANN Algorithm

```
1
2
3
4 %%Desarrollado por: Francisco Javier Ramirez Arias
5 %%Asesor Everardo Inzunza Gonzalez
6 %%Universidad Autonoma de Baja California
7 %%Proyecto Doctoral
8
9     clear all
10 %%Lectura de los datos
11     data = ReadData("Dataset08_Balanced");
12
13 %%Preprocesamiento de la informacion
14     data.Classes = categorical(data.Classes);
15     data.Classes = renamecats(data.Classes,{'Relaxing','Left Hand',...
16 'Rigth Hand','Both Feet','Both Fits'});
17
18 %%Normalizacion
19     data{:,1:end-1} = normalize(data{:,1:end-1});
20
21 %%Division de los datos de entrenamiento y de prueba
22     dp = cvpartition(size(data,1),"HoldOut",0.2);
23     train = data(dp.training,:);
24     test  = data(dp.test,:);
25
26 %%Entrenamiento del modelo
27     mdl = fitcnet(...
28         train, ...
29         "Classes", ...
30         'LayerSizes', 10, ...
31         'Activations', 'relu', ...
32         'Lambda', 0, ...
33         'IterationLimit', 1000, ...
34         'Standardize', true, ...
```

```

35     'ClassNames', categorical({'Relaxing'; 'Left Hand'; 'Rigth ...
        Hand';...
36     'Both Feet'; 'Both Fits'}), {'Relaxing' 'Left Hand' 'Rigth Hand'...
37     'Both Feet' 'Both Fits'}));
38
39 %Prediccion del modelo
40 [lb,ss]=predict(mdl,test);
41
42 %Graficas y metricas del modelo
43 cm = confusionchart(test.Classes,lb);
44 cm.Title = 'EEG-Signal Classification';
45 [m1,~] = confusionmat(test.Classes,lb);
46 [Result,ReferenceResult] = multiclass_metrics_special(m1)
47 %
48 % %Curvas ROC y Area Bajo la Curva
49 figure(2)
50 hold on
51 Classes = categories(mdl.ClassNames)
52 AUC = zeros(length(mdl.ClassNames),1);
53 for i=1:length(mdl.ClassNames)
54     [xr, yr, ~, auc] = perfcurve(test.Classes,ss(:, i),Classes{i});
55     plot(xr, yr, 'linewidth', 1)
56     legends{i} = sprintf('AUC for %s class: %.3f', Classes{i}, auc);
57     AUC(i,:) = auc;
58
59 end
60 %
61 AUCAverage = mean(AUC)
62 mdlloss = loss(mdl,test,"Classes")
63 %
64 line([0 1], [0 1], 'linestyle', '--', 'color', 'r');
65 legends{6} = 'Reference Line';
66 lgd = legend(legends, 'location', 'southeast');
67 til = sprintf('AUC Average: %.3f',AUCAverage);
68 title(lgd,til)
69 xlabel('FPR'), ylabel('TPR');
70 title('ROC for EEG Classification (1 vs Others)');
71 axis square

```

I. Matlab Code for Medium-ANN Algorithm

```
1
2
3 %%Desarrollado por: Francisco Javier Ramirez Arias
4 %%Asesor Everardo Inzunza Gonzalez
5 %%Universidad Autonoma de Baja California
6 %%Proyecto Doctoral
7
8     clear all
9 %Lectura de los datos
10    data = ReadData("Dataset08_Balanced");
11
12 %Preprocesamiento de la informacion
13    data.Classes = categorical(data.Classes);
14    data.Classes = renamecats(data.Classes,{'Relaxing','Left Hand',...
15 'Righth Hand','Both Feet','Both Fits'});
16
17 %Normalizacion
18    data{:,1:end-1} = normalize(data{:,1:end-1});
19
20 %Division de los datos de entrenamiento y de prueba
21    dp = cvpartition(size(data,1),"HoldOut",0.2);
22    train = data(dp.training,:);
23    test  = data(dp.test,:);
24
25 %Entrenamiento del modelo
26    mdl = fitcnet(...
27        train, ...
28        "Classes", ...
29        'LayerSizes', 25, ...
30        'Activations', 'relu', ...
31        'Lambda', 0, ...
32        'IterationLimit', 1000, ...
33        'Standardize', true, ...
34        'ClassNames', categorical({'Relaxing'; 'Left Hand';...
```

```

35         'Rigth Hand'; 'Both Feet'; 'Both Fits'}, {'Relaxing'...
36         'Left Hand' 'Rigth Hand' 'Both Feet' 'Both Fits'}));
37
38
39 %Prediccion del modelo
40 [lb,ss]=predict mdl,test);
41
42 %Graficas y metricas del modelo
43 cm = confusionchart(test.Classes,lb);
44 cm.Title = 'EEG-Signal Classification';
45 [m1,~] = confusionmat(test.Classes,lb);
46 [Result,ReferenceResult] = multiclass_metrics_special(m1)
47 %
48 % %Curvas ROC y Area Bajo la Curva
49 figure(2)
50 hold on
51 Classes = categories(mdl.ClassNames)
52 AUC = zeros(length(mdl.ClassNames),1);
53 for i=1:length(mdl.ClassNames)
54     [xr, yr, ~, auc] = perfcurve(test.Classes,ss(:, i),Classes{i});
55     plot(xr, yr, 'linewidth', 1)
56     legends{i} = sprintf('AUC for %s class: %.3f', Classes{i}, auc);
57     AUC(i,:) = auc;
58
59 end
60 %
61 AUCAverage = mean(AUC)
62 mdlloss = loss(mdl,test,"Classes")
63 %
64 line([0 1], [0 1], 'linestyle', '--', 'color', 'r');
65 legends{6} = 'Reference Line';
66 lgd =legend(legends, 'location', 'southeast');
67 til = sprintf('AUC Average: %.3f',AUCAverage);
68 title(lgd,til)
69 xlabel('FPR'), ylabel('TPR');
70 title('ROC for EEG Classification (1 vs Others)');
71 axis square

```

J. Matlab Code for Wide Model

```
1
2
3 %%Desarrollado por: Francisco Javier Ramirez Arias
4 %%Asesor Everardo Inzunza Gonzalez
5 %%Universidad Autonoma de Baja California
6 %%Proyecto Doctoral
7
8     clear all
9 %Lectura de los datos
10    data = ReadData("Dataset08_Balanced");
11
12 %Preprocesamiento de la informacion
13    data.Classes = categorical(data.Classes);
14    data.Classes = renamecats(data.Classes,{'Relaxing','Left Hand',...
15 'Righth Hand','Both Feet','Both Fits'});
16
17 %Normalizacion
18    data{:,1:end-1} = normalize(data{:,1:end-1});
19
20 %Division de los datos de entrenamiento y de prueba
21    dp = cvpartition(size(data,1),"HoldOut",0.2);
22    train = data(dp.training,:);
23    test  = data(dp.test,:);
24
25 %Entrenamiento del modelo
26    mdl = fitcnet(...
27        train, ...
28        "Classes", ...
29        'LayerSizes', 100, ...
30        'Activations', 'relu', ...
31        'Lambda', 0, ...
32        'IterationLimit', 1000, ...
33        'Standardize', true, ...
34        'ClassNames', categorical({'Relaxing'; 'Left Hand';...
```

```

35     'Rigth Hand'; 'Both Feet'; 'Both Fits'}},...
36     {'Relaxing' 'Left Hand' 'Rigth Hand' 'Both Feet' 'Both Fits'}));
37
38 %Prediccion del modelo
39 [lb,ss]=predict(mdl,test);
40
41 %Graficas y metricas del modelo
42 cm = confusionchart(test.Classes,lb);
43 cm.Title = 'EEG-Signal Classification';
44 [m1,~] = confusionmat(test.Classes,lb);
45 [Result,ReferenceResult] = multiclass_metrics_special(m1)
46 %
47 % %Curvas ROC y Area Bajo la Curva
48 figure(2)
49 hold on
50 Classes = categories(mdl.ClassNames)
51 AUC = zeros(length(mdl.ClassNames),1);
52 for i=1:length(mdl.ClassNames)
53     [xr, yr, ~, auc] = perfcurve(test.Classes,ss(:, i),Classes{i});
54     plot(xr, yr, 'linewidth', 1)
55     legends{i} = sprintf('AUC for %s class: %.3f', Classes{i}, auc);
56     AUC(i,:) = auc;
57
58 end
59 %
60 AUCAverage = mean(AUC)
61 mdlloss = loss(mdl,test,"Classes")
62 %
63 line([0 1], [0 1], 'linestyle', '--', 'color', 'r');
64 legends{6} = 'Reference Line';
65 lgd =legend(legends, 'location', 'southeast');
66 til = sprintf('AUC Average: %.3f',AUCAverage);
67 title(lgd,til)
68 xlabel('FPR'), ylabel('TPR');
69 title('ROC for EEG Classification (1 vs Others)');
70 axis square

```

K. Matlab Code for Bilayed Model

```
1
2
3 %%Desarrollado por: Francisco Javier Ramirez Arias
4 %%Asesor Everardo Inzunza Gonzalez
5 %%Universidad Autonoma de Baja California
6 %%Proyecto Doctoral
7
8     clear all
9 %Lectura de los datos
10    data = ReadData("Dataset08_Balanced");
11
12 %Preprocesamiento de la informacion
13    data.Classes = categorical(data.Classes);
14    data.Classes = renamecats(data.Classes,{'Relaxing','Left Hand',...
15 'Rigth Hand','Both Feet','Both Fits'});
16
17 %Normalizacion
18    data{:,1:end-1} = normalize(data{:,1:end-1});
19
20 %Division de los datos de entrenamiento y de prueba
21    dp = cvpartition(size(data,1),"HoldOut",0.2);
22    train = data(dp.training,:);
23    test  = data(dp.test,:);
24
25    inputTable = train;
26    predictorNames = {'C3_Amplitude', 'C3_Frequency', 'C3_Phase',...
27 'C1_PeakToPeak', 'C1_NegativePeak', 'C1_PositivePeak',...
28 'Cz_Median', 'Cz_Mode', 'Cz_Mean', 'C2_RMS', 'C2_SD',...
29 'C2_Summation', 'C4_Variance', 'C4_Kurtosis', 'C4_Skewness'};
30    predictors = inputTable(:, predictorNames);
31    response = inputTable.Classes;
32
33
34 %Entrenamiento del modelo
```

```

35
36 mdl = fitcnet(...
37 predictors, ...
38 response, ...
39 'LayerSizes', [10 10], ...
40 'Activations', 'relu', ...
41 'Lambda', 0, ...
42 'IterationLimit', 1000, ...
43 'Standardize', true, ...
44 'ClassNames', categorical({'Relaxing'; 'Left Hand';...
45 'Righth Hand'; 'Both Feet'; 'Both Fits'}),...
46 {'Relaxing' 'Left Hand' 'Righth Hand' 'Both Feet' 'Both Fits'}));
47
48 %Prediccion del modelo
49 [lb,ss]=predict(mdl,test);
50
51 %Graficas y metricas del modelo
52 cm = confusionchart(test.Classes,lb);
53 cm.Title = 'EEG-Signal Classification';
54 [m1,~] = confusionmat(test.Classes,lb);
55 [Result,ReferenceResult] = multiclass_metrics_special(m1)
56 %
57 % %Curvas ROC y Area Bajo la Curva
58 figure(2)
59 hold on
60 Classes = categories(mdl.ClassNames)
61 AUC = zeros(length(mdl.ClassNames),1);
62 for i=1:length(mdl.ClassNames)
63     [xr, yr, ~, auc] = perfcurve(test.Classes,ss(:, i),Classes{i});
64     plot(xr, yr, 'linewidth', 1)
65     legends{i} = sprintf('AUC for %s class: %.3f', Classes{i}, auc);
66     AUC(i,:) = auc;
67
68 end
69 %
70 AUCAverage = mean(AUC)
71 mdlloss = loss(mdl,test,"Classes")
72 %

```

```
73 line([0 1], [0 1], 'linestyle', '--', 'color', 'r');
74 legends{6} = 'Reference Line';
75 lgd =legend(legends, 'location', 'southeast');
76 til = sprintf('AUC Average: %.3f',AUCAverage);
77 title(lgd,til)
78 xlabel('FPR'), ylabel('TPR');
79 title('ROC for EEG Classification (1 vs Others)');
80 axis square
```

Referencias

- B. Abbasi and D. M. Goldenholz. Machine learning applications in epilepsy. *Epilepsia*, 60 (10):2037 – 2047, 2019. doi: 10.1111/epi.16333.
- S. N. Abdulkader, A. Atia, and M.-S. M. Mostafa. Brain computer interfacing: Applications and challenges. *Egyptian Informatics Journal*, 16(2):213–230, July 2015a. ISSN 1110-8665. doi: 10.1016/j.eij.2015.06.002. URL <http://www.sciencedirect.com/science/article/pii/S1110866515000237>.
- S. N. Abdulkader, A. Atia, and M.-S. M. Mostafa. Brain computer interfacing: Applications and challenges. *Egyptian Informatics Journal*, 16(2):213–230, July 2015b. ISSN 1110-8665. doi: 10.1016/j.eij.2015.06.002. URL <https://www.sciencedirect.com/science/article/pii/S1110866515000237>.
- P. A. Abhang, B. W. Gawali, and S. C. Mehrotra. Chapter 2 - Technological Basics of EEG Recording and Operation of Apparatus. In P. A. Abhang, B. W. Gawali, and S. C. Mehrotra, editors, *Introduction to EEG- and Speech-Based Emotion Recognition*, pages 19–50. Academic Press, Jan. 2016. ISBN 978-0-12-804490-2. doi: 10.1016/B978-0-12-804490-2.00002-6. URL <https://www.sciencedirect.com/science/article/pii/B9780128044902000026>.
- T. Aboneh, A. Rorissa, and R. Srinivasagan. Stacking-Based Ensemble Learning Method for Multi-Spectral Image Classification. *Technologies*, 10(1), 2022. ISSN 2227-7080. doi: 10.3390/technologies10010017.
- A. Affes, A. Mdhaftar, C. Triki, M. Jmaiel, and B. Freisleben. Personalized attention-based EEG channel selection for epileptic seizure prediction. *Expert Systems with Applications*, 206:117733, Nov. 2022. ISSN 09574174. doi: 10.1016/j.eswa.2022.117733. URL <https://linkinghub.elsevier.com/retrieve/pii/S0957417422010144>.
- C. C. Aggarwal. *Neural Networks and Deep Learning: A Textbook*. Springer International Publishing, Cham, 2018. ISBN 978-3-319-94462-3 978-3-319-94463-0. doi: 10.1007/978-3-319-94463-0. URL <http://link.springer.com/10.1007/978-3-319-94463-0>.

- S. Aggarwal and N. Chugh. Signal processing techniques for motor imagery brain computer interface: A review. *Array*, 1-2:100003, Jan. 2019. ISSN 2590-0056. doi: 10.1016/j.array.2019.100003. URL <https://www.sciencedirect.com/science/article/pii/S2590005619300037>.
- O. Aguirre-Castro, E. García-Guerrero, O. López-Bonilla, E. Tlelo-Cuautle, D. López-Mancilla, J. Cárdenas-Valdez, J. Olguín-Tiznado, and E. Inzunza-González. Evaluation of underwater image enhancement algorithms based on Retinex and its implementation on embedded systems. *Neurocomputing*, 494:148–159, 2022. ISSN 0925-2312. doi: 10.1016/j.neucom.2022.04.074.
- A. Al-Ani and A. Al-Sukker. Effect of Feature and Channel Selection on EEG Classification. In *2006 International Conference of the IEEE Engineering in Medicine and Biology Society*, pages 2171–2174, Aug. 2006. doi: 10.1109/IEMBS.2006.259833. ISSN: 1557-170X.
- M. H. Alomari, A. Samaha, and K. AlKamha. Automated Classification of L/R Hand Movement EEG Signals using Advanced Feature Extraction and Machine Learning. *International Journal of Advanced Computer Science and Applications*, 4(6), 2013. ISSN 2158107X, 21565570. doi: 10.14569/IJACSA.2013.040628. URL <http://arxiv.org/abs/1312.2877>. arXiv: 1312.2877.
- A. Apicella, F. Donnarumma, F. Isgrò, and R. Prevete. A survey on modern trainable activation functions. *Neural Networks*, 138:14–32, June 2021. ISSN 0893-6080. doi: 10.1016/j.neunet.2021.01.026. URL <https://www.sciencedirect.com/science/article/pii/S0893608021000344>.
- S. K. Arjaria, A. S. Rathore, and J. S. Cherian. Chapter 13 - Kidney disease prediction using a machine learning approach: A comparative and comprehensive analysis. In P. N, S. Kautish, and S.-L. Peng, editors, *Demystifying Big Data, Machine Learning, and Deep Learning for Healthcare Analytics*, pages 307–333. Academic Press, Jan. 2021. ISBN 978-0-12-821633-0. doi: 10.1016/B978-0-12-821633-0.00006-4. URL <https://www.sciencedirect.com/science/article/pii/B9780128216330000064>.
- J. Arshad, A. Qaisar, A.-U. Rehman, M. Shakir, M. K. Nazir, A. U. Rehman, E. T. Eldin, N. A. Ghamry, and H. Hamam. Intelligent Control of Robotic Arm Using Brain Computer

- Interface and Artificial Intelligence. *Applied Sciences*, 12(21):10813, Jan. 2022. ISSN 2076-3417. doi: 10.3390/app122110813. URL <https://www.mdpi.com/2076-3417/12/21/10813>. Number: 21 Publisher: Multidisciplinary Digital Publishing Institute.
- Y. Bai, J. He, X. Xia, Y. Wang, Y. Yang, H. Di, X. Li, and U. Ziemann. Spontaneous transient brain states in EEG source space in disorders of consciousness. *NeuroImage*, 240:118407, Oct. 2021. ISSN 10538119. doi: 10.1016/j.neuroimage.2021.118407. URL <https://linkinghub.elsevier.com/retrieve/pii/S1053811921006820>.
- M. A. Balafar, A. R. Ramli, M. I. Saripan, and S. Mashohor. Review of brain MRI image segmentation methods. *Artificial Intelligence Review*, 33(3):261–274, Mar. 2010. ISSN 1573-7462. doi: 10.1007/s10462-010-9155-0. URL <https://doi.org/10.1007/s10462-010-9155-0>.
- G. Bartur, H. Pratt, and N. Soroker. Changes in mu and beta amplitude of the eeg during upper limb movement correlate with motor impairment and structural damage in subacute stroke. *Clinical Neurophysiology*, 130(9):1644 – 1651, 2019. ISSN 13882457. URL <https://libcon.rec.uabc.mx:5471/login.aspx?direct=true&db=asn&AN=137872324&lang=es&site=ehost-live>.
- D. Berrar. Bayes’ theorem and naive bayes classifier. *Encyclopedia of Bioinformatics and Computational Biology: ABC of Bioinformatics*, 403, 2018. doi: 10.1016/B978-0-12-809633-8.20473-1.
- L. Bi, X. Fan, and Y. Liu. EEG-Based Brain-Controlled Mobile Robots: A Survey. *IEEE Transactions on Human-Machine Systems*, 43(2):161–176, Mar. 2013. ISSN 2168-2305. doi: 10.1109/TSMCC.2012.2219046. Conference Name: IEEE Transactions on Human-Machine Systems.
- A. Biasucci, B. Franceschiello, and M. M. Murray. Electroencephalography. *Current Biology*, 29(3):R80–R85, Feb. 2019. ISSN 0960-9822. doi: 10.1016/j.cub.2018.11.052. URL <https://www.sciencedirect.com/science/article/pii/S0960982218315513>.
- J. Bismuth, F. Vialatte, and J.-P. Lefaucheur. Relieving peripheral neuropathic pain by increasing the power-ratio of low- over high- activities in the central cortical region with EEG-

- based neurofeedback: Study protocol for a controlled pilot trial (SMRPain study). *Neurophysiologie Clinique*, 50(1):5–20, Feb. 2020. ISSN 09877053. doi: 10.1016/j.neucli.2019.12.002. URL <https://linkinghub.elsevier.com/retrieve/pii/S0987705320300022>.
- R. Bousseta, I. El Ouakouak, M. Gharbi, and F. Regragui. EEG Based Brain Computer Interface for Controlling a Robot Arm Movement Through Thought. *IRBM*, 39(2):129–135, Apr. 2018. ISSN 1959-0318. doi: 10.1016/j.irbm.2018.02.001. URL <https://www.sciencedirect.com/science/article/pii/S195903181830037X>.
- C. Brunner, N. Birbaumer, B. Blankertz, C. Guger, A. Kübler, D. Mattia, J. d. R. Millán, F. Miralles, A. Nijholt, E. Opisso, N. Ramsey, P. Salomon, and G. R. Müller-Putz. BNCI Horizon 2020: towards a roadmap for the BCI community. *Brain-Computer Interfaces*, 2(1):1–10, 2015. doi: 10.1080/2326263X.2015.1008956. URL <http://dx.doi.org/10.1080/2326263X.2015.1008956>.
- S. Bunce, M. Izzetoglu, K. Izzetoglu, B. Onaral, and K. Pourrezaei. Functional near-infrared spectroscopy. *IEEE engineering in medicine and biology magazine : the quarterly magazine of the Engineering in Medicine & Biology Society*, 25:54–62, July 2006. doi: 10.1109/MEMB.2006.1657788.
- P. E. t. P. |. C. M. Cannon Medical Systems. Oncology – PET/CT Scanner Technology | Celesteion PUREVISION Edition PET/CT | Canon Medical Systems USA, 2022. URL <https://us.medical.canon/products/molecular-imaging/celesteion/technology/>.
- N. R. Carlson. *Foundations of Physiological Psychology*. Pearson A and B, 2005. ISBN 978-0-205-42723-9. Google-Books-ID: BSijQgAACAAJ.
- R. Carter. *The Human Brain Book: An Illustrated Guide to its Structure, Function, and Disorders*. Penguin, Jan. 2019. ISBN 978-1-4654-9952-3. Google-Books-ID: s8bhDwAAQBAJ.
- A. Casey, H. Azhar, M. Grzes, and M. Sakel. BCI controlled robotic arm as assistance to the rehabilitation of neurologically disabled patients. *Disability and Rehabilitation: Assistive Technology*, 16(5):525–537, July 2021. ISSN 1748-3107. doi: 10.1080/17483107.2019.

1683239. URL <https://doi.org/10.1080/17483107.2019.1683239>. Publisher: Taylor & Francis _eprint: <https://doi.org/10.1080/17483107.2019.1683239>.
- T. Castermans, M. Duvinage, G. Cheron, and T. Dutoit. Towards Effective Non-Invasive Brain-Computer Interfaces Dedicated to Gait Rehabilitation Systems. *Brain Sciences*, 4: 1–48, Mar. 2013. doi: 10.3390/brainsci4010001.
- C. Castro, E. Vargas-Viveros, A. Sánchez, E. Gutiérrez-López, and D. Flores. Parkinson’s Disease Classification Using Artificial Neural Networks. In C. Springer, editor, *VIII Latin American Conference on Biomedical Engineering and XLII National Conference on Biomedical Engineering. CLAIB 2019. IFMBE Proceedings*, volume 75, 2020. doi: 10.1007/978-3-030-30648-9_137.
- M. Cerrada, L. Trujillo, D. E. Hernández, H. A. Correa Zevallos, J. C. Macancela, D. Cabrera, and R. Vinicio Sánchez. AutoML for Feature Selection and Model Tuning Applied to Fault Severity Diagnosis in Spur Gearboxes. *Mathematical and Computational Applications*, 27 (1):6, Feb. 2022. ISSN 2297-8747. doi: 10.3390/mca27010006. Number: 1 Publisher: Multidisciplinary Digital Publishing Institute.
- J. Cervantes, F. Garcia-Lamont, L. Rodríguez-Mazahua, and A. Lopez. A comprehensive survey on support vector machine classification: Applications, challenges and trends. *Neurocomputing*, 408:189–215, Sept. 2020. ISSN 0925-2312. doi: 10.1016/j.neucom.2019.10.118. URL <https://www.sciencedirect.com/science/article/pii/S0925231220307153>.
- M. Chai, H. U. Amin, L. Izhar, M. N. MOHAMAD SAAD, M. Rahman, A. Malik, and T. B. Tang. Exploring EEG Effective Connectivity Network in Estimating Influence of Color on Emotion and Memory. *Frontiers in Neuroinformatics*, 13:66, Oct. 2019. doi: 10.3389/fninf.2019.00066.
- A. Chakure. K-Nearest Neighbors (KNN) Algorithm, June 2021. URL <https://medium.datadriveninvestor.com/k-nearest-neighbors-knn-algorithm-bd375d14eec7>.
- W. Chen, S.-K. Chen, Y.-H. Liu, Y.-J. Chen, and C.-S. Chen. An Electric Wheelchair Manipulating System Using SSVEP-Based BCI System. *Biosensors*, 12(10):772, Oct. 2022. ISSN 2079-6374. doi: 10.3390/bios12100772. URL <https://www.mdpi.com/2079-6374/12/10/772>. Number: 10 Publisher: Multidisciplinary Digital Publishing Institute.

- J.-H. Cho, J.-H. Jeong, K.-H. Shim, D.-J. Kim, and S.-W. Lee. Classification of Hand Motions within EEG Signals for Non-Invasive BCI-Based Robot Hand Control. In *2018 IEEE International Conference on Systems, Man, and Cybernetics (SMC)*, pages 515–518, Oct. 2018. doi: 10.1109/SMC.2018.00097. ISSN: 2577-1655.
- M. R. I. M. |. C. M. Cohen Medical Centers. Magnetic Resonance Imaging (MRI), 2022. URL <https://www.cohencenters.com/treatments/magnetic-resonance-imaging-mri/>.
- E. E. Contreras-Luján, E. E. García-Guerrero, O. R. López-Bonilla, E. Tlelo-Cuautle, D. López-Mancilla, and E. Inzunza-González. Evaluation of Machine Learning Algorithms for Early Diagnosis of Deep Venous Thrombosis. *Mathematical and Computational Applications*, 27(2), 2022. ISSN 2297-8747. doi: 10.3390/mca27020024.
- S. Coyle, T. Ward, C. Markham, and G. Mcdarby. On the suitability of near-infrared (NIR) systems for next-generation brain-computer interfaces. *Physiological measurement*, 25:815–22, Sept. 2004. doi: 10.1088/0967-3334/25/4/003.
- A. Craik, Y. He, and J. L. Contreras-Vidal. Deep learning for electroencephalogram (EEG) classification tasks: A review. *Journal of Neural Engineering*, 16(3), 2019. doi: 10.1088/1741-2552/ab0ab5.
- X. Daniela, C. Hinde, and R. Stone. Naive Bayes vs. Decision Trees vs. Neural Networks in the Classification of Training Web Pages. *International Journal of Computer Science Issues*, 4, Sept. 2009.
- D. T. C. i. P. T. |. D. Datacamp. Python Decision Tree Classification Tutorial: Scikit-Learn DecisionTreeClassifier, 2022. URL <https://www.datacamp.com/tutorial/decision-tree-classification-python>.
- L. Deecke, H. Weinberg, and P. Brickett. Magnetic fields of the human brain accompanying voluntary movement: Bereitschaftsmagnetfeld. *Experimental Brain Research*, 48(1):144–148, 1982. ISSN 0014-4819. doi: 10.1007/BF00239582.
- B. Ding, H. Qian, and J. Zhou. Activation functions and their characteristics in deep neural networks. In *2018 Chinese Control And Decision Conference (CCDC)*, pages 1836–1841, June 2018. doi: 10.1109/CCDC.2018.8407425. ISSN: 1948-9447.

- R. Duda, P. Hart, and D. Stork. *Pattern Classification*. Wiley, 2012. ISBN 978-1-118-58600-6. URL <https://books.google.com.mx/books?id=Br33IRC3PkQC>.
- C. Dumitrescu, I.-M. Costea, and A. Semencescu. Using Brain-Computer Interface to Control a Virtual Drone Using Non-Invasive Motor Imagery and Machine Learning. *Applied Sciences*, 11(24):11876, Jan. 2021. ISSN 2076-3417. doi: 10.3390/app112411876. URL <https://www.mdpi.com/2076-3417/11/24/11876>. Number: 24 Publisher: Multidisciplinary Digital Publishing Institute.
- D. R. Edla, K. Mangalorekar, G. Dhavalikar, and S. Dodia. Classification of EEG data for human mental state analysis using Random Forest Classifier. *Procedia Computer Science*, 132:1523–1532, 2018. ISSN 1877-0509. doi: 10.1016/j.procs.2018.05.116. URL <https://www.sciencedirect.com/science/article/pii/S1877050918308482>.
- J. Enríquez Zárate, M. d. l. A. Gómez López, J. A. Carmona Troyo, and L. Trujillo. Analysis and Detection of Erosion in Wind Turbine Blades. *Mathematical and Computational Applications*, 27(1):5, Feb. 2022. ISSN 2297-8747. doi: 10.3390/mca27010005.
- J. J. Esqueda-Elizondo, R. Juárez-Ramírez, O. R. López-Bonilla, E. E. García-Guerrero, G. M. Galindo-Aldana, L. Jiménez-Beristáin, A. Serrano-Trujillo, E. Tlelo-Cuautle, and E. Inzunza-González. Attention Measurement of an Autism Spectrum Disorder User Using EEG Signals: A Case Study. *Mathematical and Computational Applications*, 27(2), 2022. doi: 10.3390/mca27020021.
- M. Z. A. Faiz and A. A. Al-Hamadani. Online Brain Computer Interface Based Five Classes EEG To Control Humanoid Robotic Hand. In *2019 42nd International Conference on Telecommunications and Signal Processing (TSP)*, pages 406–410, July 2019. doi: 10.1109/TSP.2019.8769072.
- J. Fekiač, I. Zelinka, and J. Burguillo. A Review Of Methods For Encoding Neural Network Topologies In Evolutionary Computation. *ECMS 2011 Proceedings*, June 2011. doi: 10.7148/2011-0410-0416.
- M. B. Fong-Mata, E. E. García-Guerrero, D. A. Mejía-Medina, O. R. López-Bonilla, L. J. Villarreal-Gómez, F. Zamora-Arellano, D. López-Mancilla, and E. Inzunza-González. An

- Artificial Neural Network Approach and a Data Augmentation Algorithm to Systematize the Diagnosis of Deep-Vein Thrombosis by Using Wells' Criteria. *Electronics*, 9(11):1810, Nov. 2020. ISSN 2079-9292. doi: 10.3390/electronics9111810. URL <https://www.mdpi.com/2079-9292/9/11/1810>. Number: 11 Publisher: Multidisciplinary Digital Publishing Institute.
- C. A. Fontanillo Lopez, G. Li, and D. Zhang. Beyond Technologies of Electroencephalography-Based Brain-Computer Interfaces: A Systematic Review From Commercial and Ethical Aspects. *Frontiers in Neuroscience*, 14, 2020. ISSN 1662-453X. URL <https://www.frontiersin.org/article/10.3389/fnins.2020.611130>.
- G. Schalk, D. J. McFarland, T. Hinterberger, N. Birbaumer, and J. R. Wolpaw. BCI2000: a general-purpose brain-computer interface (BCI) system. *IEEE Transactions on Biomedical Engineering*, 51(6):1034–1043, June 2004. ISSN 1558-2531. doi: 10.1109/TBME.2004.827072.
- P. Ghaderyan, F. Moghaddam, S. Khoshnoud, and M. Shamsi. New interdependence feature of EEG signals as a biomarker of timing deficits evaluated in Attention-Deficit/Hyperactivity Disorder detection. *Measurement*, 199:111468, Aug. 2022. ISSN 02632241. doi: 10.1016/j.measurement.2022.111468. URL <https://linkinghub.elsevier.com/retrieve/pii/S0263224122006959>.
- C. Gini. Measurement of Inequality of Incomes. *The Economic Journal*, 31(121):124–126, 1921. ISSN 0013-0133. doi: 10.2307/2223319. URL <https://www.jstor.org/stable/2223319>. Publisher: [Royal Economic Society, Wiley].
- A. L. Goldberger, L. A. N. Amaral, L. Glass, J. M. Hausdorff, P. C. Ivanov, R. G. Mark, J. E. Mietus, G. B. Moody, C.-K. Peng, and H. E. Stanley. PhysioBank, PhysioToolkit, and PhysioNet. *Circulation*, 101(23):e215–e220, June 2000. doi: 10.1161/01.CIR.101.23.e215. URL <https://www.ahajournals.org/doi/10.1161/01.CIR.101.23.e215>. Publisher: American Heart Association.
- M. Grandini, E. Bagli, and G. Visani. Metrics for Multi-Class Classification: an Overview, Aug. 2020. URL <http://arxiv.org/abs/2008.05756>. arXiv:2008.05756 [cs, stat].

- H. M. Greiner, P. S. Horn, J. R. Tenney, R. Arya, S. V. Jain, K. D. Holland, J. L. Leach, L. Miles, D. F. Rose, H. Fujiwara, and F. T. Mangano. Preresection intraoperative electrocorticography (ECoG) abnormalities predict seizure-onset zone and outcome in pediatric epilepsy surgery. *Epilepsia*, 57(4):582–589, 2016. ISSN 1528-1167. doi: <https://doi.org/10.1111/epi.13341>. URL <https://onlinelibrary.wiley.com/doi/abs/10.1111/epi.13341>. eprint: <https://onlinelibrary.wiley.com/doi/pdf/10.1111/epi.13341>.
- J. Gross. Magnetoencephalography in Cognitive Neuroscience: A Primer. *Neuron*, 104(2): 189–204, Oct. 2019. ISSN 0896-6273. doi: 10.1016/j.neuron.2019.07.001. URL <https://www.sciencedirect.com/science/article/pii/S0896627319305999>.
- F. Guang-Hui, X. Feng, Z. Bing-Yang, and Y. Lun-Zhao. Stable variable selection of class-imbalanced data with precision-recall criterion. *Chemometrics and Intelligent Laboratory Systems*, 171:241–250, 2017. doi: 10.1016/j.chemolab.2017.10.015.
- Y. Han, Y. Ma, L. Zhu, Y. Zhang, L. Li, W. Zheng, J. Guo, and Y. Che. Study on Mind Controlled Robotic Arms by Collecting and Analyzing Brain Alpha Waves. In *2018 2nd International Conference on Applied Mathematics, Modelling and Statistics Application (AMMSA 2018)*, pages 145–148. Atlantis Press, May 2018. ISBN 978-94-6252-529-0. doi: 10.2991/ammsa-18.2018.30. URL <https://www.atlantis-press.com/proceedings/ammsa-18/25898286>. ISSN: 1951-6851.
- R. Haque, N. Islam, M. Islam, and M. M. Ahsan. A Comparative Analysis on Suicidal Ideation Detection Using NLP, Machine, and Deep Learning. *Technologies*, 10(3), 2022. ISSN 2227-7080. doi: 10.3390/technologies10030057.
- Y. Hashimoto and J. Ushiba. EEG-based classification of imaginary left and right foot movements using beta rebound. *Clinical Neurophysiology*, 124(11):2153–2160, Nov. 2013. ISSN 13882457. doi: 10.1016/j.clinph.2013.05.006. URL <https://linkinghub.elsevier.com/retrieve/pii/S1388245713006457>.
- B. He, S. Gao, H. Yuan, and J. R. Wolpaw. Brain–Computer Interfaces. *Neural Engineering*, pages 87–151, 2013. doi: 10.1007/978-1-4614-5227-0_2. URL https://libcon.rec.uabc.mx:4476/chapter/10.1007/978-1-4614-5227-0_2. Publisher: Springer, Boston, MA.

- M. Hearst, S. Dumais, E. Osman, J. Platt, and B. Scholkopf. Support vector machines. *Intelligent Systems and their Applications, IEEE*, 13:18–28, Aug. 1998. doi: 10.1109/5254.708428.
- H. M. K. K. M. B. Herath and W. R. de Mel. Controlling an Anatomical Robot Hand Using the Brain-Computer Interface Based on Motor Imagery. *Advances in Human-Computer Interaction*, 2021:e5515759, Aug. 2021. ISSN 1687-5893. doi: 10.1155/2021/5515759. URL <https://www.hindawi.com/journals/ahci/2021/5515759/>. Publisher: Hindawi.
- E. Hortal, D. Planelles, A. Costa, E. Iáñez, A. Úbeda, J. M. Azorín, and E. Fernández. SVM-based Brain–Machine Interface for controlling a robot arm through four mental tasks. *Neurocomputing*, 151:116–121, Mar. 2015. ISSN 0925-2312. doi: 10.1016/j.neucom.2014.09.078. URL <https://www.sciencedirect.com/science/article/pii/S092523121401323X>.
- M.-P. Hosseini, A. Hosseini, and K. Ahi. A Review on Machine Learning for EEG Signal Processing in Bioengineering. *IEEE Reviews in Biomedical Engineering*, 14:204–218, 2021. ISSN 1941-1189. doi: 10.1109/RBME.2020.2969915. Conference Name: IEEE Reviews in Biomedical Engineering.
- N. F. Ince, F. Goksu, and A. H. Tewfik. ECoG Based Brain Computer Interface with Subset Selection. In A. Fred, J. Filipe, and H. Gamboa, editors, *Biomedical Engineering Systems and Technologies*, Communications in Computer and Information Science, pages 357–374, Berlin, Heidelberg, 2009. Springer. ISBN 978-3-540-92219-3. doi: 10.1007/978-3-540-92219-3_27.
- P. P. Ippolito. SVM: Feature Selection and Kernels, Sept. 2021. URL <https://towardsdatascience.com/svm-feature-selection-and-kernels-840781cc1a6c>.
- C. Janiesch, P. Zschech, and K. Heinrich. Machine learning and deep learning. *Electronic Markets*, 31(3):685–695, 2021a. doi: 10.1007/s12525-021-00475-2.
- C. Janiesch, P. Zschech, and K. Heinrich. Machine learning and deep learning. *Electronic Markets*, 31(3):685–695, Sept. 2021b. ISSN 1422-8890. doi: 10.1007/s12525-021-00475-2. URL <https://doi.org/10.1007/s12525-021-00475-2>.

- N. Jatupaiboon, S. Pan-ngum, and P. Israsena. Emotion classification using minimal EEG channels and frequency bands. In *The 2013 10th International Joint Conference on Computer Science and Software Engineering (JCSSE)*, pages 21–24, May 2013. doi: 10.1109/JCSSE.2013.6567313.
- J. Jeong. EEG dynamics in patients with Alzheimer’s disease. *Clinical Neurophysiology*, 115(7):1490–1505, July 2004. ISSN 1388-2457. doi: 10.1016/j.clinph.2004.01.001. URL <https://www.sciencedirect.com/science/article/pii/S138824570400015X>.
- V. Jurcak, D. Tsuzuki, and I. Dan. 10/20, 10/10, and 10/5 systems revisited: Their validity as relative head-surface-based positioning systems. *NeuroImage*, 34(4):1600–1611, Feb. 2007. ISSN 1053-8119. doi: 10.1016/j.neuroimage.2006.09.024. URL <http://www.sciencedirect.com/science/article/pii/S1053811906009724>.
- M. J. Kahana, R. Sekuler, J. B. Caplan, M. Kirschen, and J. R. Madsen. Human theta oscillations exhibit task dependence during virtual maze navigation. *Nature*, 399(6738): 781–784, June 1999. ISSN 1476-4687. doi: 10.1038/21645. URL <https://www.nature.com/articles/21645>. Number: 6738 Publisher: Nature Publishing Group.
- P. Kant, S. H. Laskar, J. Hazarika, and R. Mahamune. CWT Based Transfer Learning for Motor Imagery Classification for Brain computer Interfaces. *Journal of Neuroscience Methods*, 345:108886, Nov. 2020. ISSN 0165-0270. doi: 10.1016/j.jneumeth.2020.108886. URL <https://www.sciencedirect.com/science/article/pii/S0165027020303095>.
- D. Kaur, S. Uslu, K. J. Rittichier, and A. Durresi. Trustworthy Artificial Intelligence: A Review. *ACM Comput. Surv.*, 55(2), 2023. doi: 10.1145/3491209.
- A. Kazemi, M. J. McKeown, and M. S. Mirian. Sleep staging using semi-supervised clustering of EEG: Application to REM sleep behavior disorder. *Biomedical Signal Processing and Control*, 75:103539, May 2022. ISSN 17468094. doi: 10.1016/j.bspc.2022.103539. URL <https://linkinghub.elsevier.com/retrieve/pii/S1746809422000611>.
- B. Kemp and J. Olivan. European data format ‘plus’ (EDF+), an EDF alike standard format for the exchange of physiological data. *Clinical Neurophysiology*, 114(9):1755–1761, Sept. 2003. ISSN 1388-2457. doi: 10.1016/S1388-2457(03)00123-8. URL <https://www.sciencedirect.com/science/article/pii/S1388245703001238>.

- S. Khalid, T. Khalil, and S. Nasreen. A survey of feature selection and feature extraction techniques in machine learning. In *2014 Science and Information Conference*, pages 372–378, Aug. 2014. doi: 10.1109/SAI.2014.6918213.
- M. Kirby. *Geometric Data Analysis: An Empirical Approach to Dimensionality Reduction and the Study of Patterns*. Wiley, 2001. ISBN 978-0-471-23929-1. URL <https://books.google.com.mx/books?id=nRmFQgAACAAJ>.
- D. J. Kupfer, F. G. Foster, P. Coble, R. J. McPartland, and R. F. Ulrich. The application of EEG sleep for the differential diagnosis of affective disorders. *The American Journal of Psychiatry*, 135(1):69–74, Jan. 1978. ISSN 0002-953X. doi: 10.1176/ajp.135.1.69.
- V. J. Lawhern, A. J. Solon, N. R. Waytowich, S. M. Gordon, C. P. Hung, and B. J. Lance. EEGNet: A compact convolutional neural network for EEG-based brain-computer interfaces. *Journal of Neural Engineering*, 15(5), 2018. doi: 10.1088/1741-2552/aace8c.
- Y. LeCun, Y. Bengio, and G. Hinton. Deep learning. *Nature*, 521(7553):436–444, 2015. doi: 10.1038/nature14539.
- K. Lee, D. Liu, L. Perroud, R. Chavarriaga, and J. d. R. Millán. A brain-controlled exoskeleton with cascaded event-related desynchronization classifiers. *Special Issue on New Research Frontiers for Intelligent Autonomous Systems*, 90(Supplement C):15–23, Apr. 2017. ISSN 0921-8890. doi: 10.1016/j.robot.2016.10.005. URL <http://www.sciencedirect.com/science/article/pii/S0921889016304948>.
- L. Lei, K. Liu, Y. Yang, A. Doubriez, X. Hu, Y. Xu, and Y. Zhou. Spatio-temporal analysis of EEG features during consciousness recovery in patients with disorders of consciousness. *Clinical Neurophysiology*, 133:135–144, Jan. 2022. ISSN 13882457. doi: 10.1016/j.clinph.2021.08.027. URL <https://linkinghub.elsevier.com/retrieve/pii/S1388245721007628>.
- R. Lent, F. C. Azevedo, C. Andrade-Moraes, and A. Pinto. How many neurons do you have? Some dogmas of quantitative neuroscience under revision. *Eur J Neurosci*, 35(1):1–9, 2012. doi: 10.1111/j.1460-9568.2011.07923.x.
- K. M. Leung. Naive bayesian classifier. *Polytechnic University Department of Computer Science/Finance and Risk Engineering*, 2007:123–156, 2007.

- J. Li, X. Du, and J. R. R. A. Martins. Machine learning in aerodynamic shape optimization. *Progress in Aerospace Sciences*, 134:100849, Oct. 2022. ISSN 0376-0421. doi: 10.1016/j.paerosci.2022.100849. URL <https://www.sciencedirect.com/science/article/pii/S0376042122000410>.
- Y. Liu, W. Su, Z. Li, G. Shi, X. Chu, Y. Kang, and W. Shang. Motor-Imagery-Based Teleoperation of a Dual-Arm Robot Performing Manipulation Tasks. *IEEE Transactions on Cognitive and Developmental Systems*, 11(3):414–424, Sept. 2019. ISSN 2379-8939. doi: 10.1109/TCDS.2018.2875052. Conference Name: IEEE Transactions on Cognitive and Developmental Systems.
- F. Lotte, L. Bougrain, A. Cichocki, M. Clerc, M. Congedo, A. Rakotomamonjy, and F. Yger. A review of classification algorithms for EEG-based brain-computer interfaces: A 10 year update. *Journal of Neural Engineering*, 15(3), 2018. doi: 10.1088/1741-2552/aab2f2.
- M. Á. Luján, M. V. Jimeno, J. Mateo Sotos, J. J. Ricarte, and A. L. Borja. A Survey on EEG Signal Processing Techniques and Machine Learning: Applications to the Neurofeedback of Autobiographical Memory Deficits in Schizophrenia. *Electronics*, 10(23):3037, Jan. 2021. ISSN 2079-9292. doi: 10.3390/electronics10233037. URL <https://www.mdpi.com/2079-9292/10/23/3037>. Number: 23 Publisher: Multidisciplinary Digital Publishing Institute.
- M. B. Mahmoud, N. B. Ali, S. Fray, H. jamoussi, S. Chebbi, and M. Fredj. Utility of EEG on attention deficit–hyperactivity disorder (ADHD). *Epilepsy & Behavior*, 114:107583, Jan. 2021. ISSN 15255050. doi: 10.1016/j.yebeh.2020.107583. URL <https://linkinghub.elsevier.com/retrieve/pii/S1525505020307630>.
- I. Majidov and T. Whangbo. Efficient Classification of Motor Imagery Electroencephalography Signals Using Deep Learning Methods. *Sensors*, 19(7), 2019. ISSN 1424-8220. doi: 10.3390/s19071736.
- P. Mateos-Aparicio and A. Rodríguez-Moreno. The Impact of Studying Brain Plasticity. *Frontiers in Cellular Neuroscience*, 13, 2019. ISSN 1662-5102. URL <https://www.frontiersin.org/articles/10.3389/fncel.2019.00066>.

- B. W. Matthews. Comparison of the predicted and observed secondary structure of T4 phage lysozyme. *Biochimica et Biophysica Acta (BBA) - Protein Structure*, 405(2):442–451, Oct. 1975. ISSN 0005-2795. doi: 10.1016/0005-2795(75)90109-9. URL <https://www.sciencedirect.com/science/article/pii/0005279575901099>.
- D. Michie, D. J. Spiegelhalter, and C. C. Taylor. *Machine learning, neural and statistical classification*. Citeseer, 1994.
- F. Mormann, K. Lehnertz, P. David, and C. E. Elger. Mean phase coherence as a measure for phase synchronization and its application to the EEG of epilepsy patients. *Physica D: Nonlinear Phenomena*, 144(3):358–369, Oct. 2000. ISSN 0167-2789. doi: 10.1016/S0167-2789(00)00087-7. URL <https://www.sciencedirect.com/science/article/pii/S0167278900000877>.
- M. F. Mridha, S. C. Das, M. M. Kabir, A. A. Lima, M. R. Islam, and Y. Watanobe. Brain-Computer Interface: Advancement and Challenges. *Sensors*, 21(17):5746, Jan. 2021. ISSN 1424-8220. doi: 10.3390/s21175746. URL <https://www.mdpi.com/1424-8220/21/17/5746>. Number: 17 Publisher: Multidisciplinary Digital Publishing Institute.
- S. K. Mudgal, S. K. Sharma, J. Chaturvedi, and A. Sharma. Brain computer interface advancement in neurosciences: Applications and issues. *Interdisciplinary Neurosurgery*, 20:100694, June 2020. ISSN 2214-7519. doi: 10.1016/j.inat.2020.100694. URL <https://www.sciencedirect.com/science/article/pii/S2214751920300098>.
- G. R. Naik. *The Usefulness of Mean and Median Frequencies in Electromyography Analysis*. IntechOpen, Oct. 2012. ISBN 978-953-51-0805-4. doi: 10.5772/50639. URL <https://www.intechopen.com/chapters/40123>. Publication Title: Computational Intelligence in Electromyography Analysis - A Perspective on Current Applications and Future Challenges.
- A. Navarro-Espinoza, O. R. López-Bonilla, E. E. García-Guerrero, E. Tlelo-Cuautle, D. López-Mancilla, C. Hernández-Mejía, and E. Inzunza-González. Traffic Flow Prediction for Smart Traffic Lights Using Machine Learning Algorithms. *Technologies*, 10(1), 2022. ISSN 2227-7080. doi: 10.3390/technologies10010005.

- C. Neuper and G. Pfurtscheller. Evidence for distinct beta resonance frequencies in human EEG related to specific sensorimotor cortical areas. *Clinical Neurophysiology*, 112(11): 2084–2097, Nov. 2001. ISSN 1388-2457. doi: 10.1016/S1388-2457(01)00661-7. URL <https://www.sciencedirect.com/science/article/pii/S1388245701006617>.
- C. Neuper, G. Müller, A. Kübler, N. Birbaumer, and G. Pfurtscheller. Clinical application of an eeg-based brain–computer interface: a case study in a patient with severe motor impairment. *Clinical Neurophysiology*, 114(3):399, 2003. ISSN 13882457. URL <https://libcon.rec.uabc.mx:5471/login.aspx?direct=true&db=asn&AN=9658180&lang=es&site=ehost-live>.
- E. Niedermeyer and F. L. da Silva. *Electroencephalography: basic principles, clinical applications, and related fields*. Lippincott Williams & Wilkins, 2005.
- N. Padfield, J. Zabalza, H. Zhao, V. Masero, and J. Ren. EEG-based brain-computer interfaces using motor-imagery: Techniques and challenges. *Sensors (Switzerland)*, 19(6), 2019. doi: 10.3390/s19061423.
- H. Peng, B. Hu, Y. Qi, Q. Zhao, and M. Ratcliffe. An improved EEG de-noising approach in electroencephalogram (EEG) for home care. In *2011 5th International Conference on Pervasive Computing Technologies for Healthcare (PervasiveHealth) and Workshops*, pages 469–474, May 2011. doi: 10.4108/icst.pervasivehealth.2011.246021. ISSN: 2153-1641.
- G. Pfurtscheller, B. Z. Allison, G. Bauernfeind, C. Brunner, T. Solis Escalante, R. Scherer, T. O. Zander, G. Mueller-Putz, C. Neuper, and N. Birbaumer. The hybrid BCI. *Frontiers in Neuroscience*, 4, 2010. ISSN 1662-453X. doi: 10.3389/fnpro.2010.00003. URL <https://www.frontiersin.org/articles/10.3389/fnpro.2010.00003/full>. Publisher: Frontiers.
- O. Pinheiro, L. Alves, and J. Souza. EEG Signals Classification: Motor Imagery for Driving an Intelligent Wheelchair. *IEEE Latin America Transactions*, 16(1):254–259, Jan. 2018. ISSN 1548-0992. doi: 10.1109/TLA.2018.8291481. Conference Name: IEEE Latin America Transactions.
- P. K. D. Pramanik, S. Pal, M. Mukhopadhyay, and S. P. Singh. 1 - Big Data classification: techniques and tools. In A. Khanna, D. Gupta, and N. Dey, editors, *Applications of Big*

- Data in Healthcare*, pages 1–43. Academic Press, Jan. 2021. ISBN 978-0-12-820203-6. doi: 10.1016/B978-0-12-820203-6.00002-3. URL <https://www.sciencedirect.com/science/article/pii/B9780128202036000023>.
- M. Proudfoot, M. W. Woolrich, A. C. Nobre, and M. R. Turner. Magnetoencephalography. *Practical Neurology*, 14(5):336–343, Oct. 2014. ISSN 1474-7758, 1474-7766. doi: 10.1136/practneurol-2013-000768. URL <http://pn.bmj.com/lookup/doi/10.1136/practneurol-2013-000768>.
- E. Quiles, J. Dadone, N. Chio, and E. García. Cross-Platform Implementation of an SSVEP-Based BCI for the Control of a 6-DOF Robotic Arm. *Sensors*, 22(13):5000, Jan. 2022. ISSN 1424-8220. doi: 10.3390/s22135000. URL <https://www.mdpi.com/1424-8220/22/13/5000>. Number: 13 Publisher: Multidisciplinary Digital Publishing Institute.
- R. A. Ramadan and A. V. Vasilakos. Brain computer interface: control signals review. *Neurocomputing*, 223(Supplement C):26–44, Feb. 2017. ISSN 0925-2312. doi: 10.1016/j.neucom.2016.10.024. URL <http://www.sciencedirect.com/science/article/pii/S0925231216312152>.
- M. Ramzan and S. Dawn. A Survey of Brainwaves using Electroencephalography(EEG) to develop Robust Brain-Computer Interfaces(BCIs): Processing Techniques and Algorithms. In *2019 9th International Conference on Cloud Computing, Data Science Engineering (Confluence)*, pages 642–647, Jan. 2019. doi: 10.1109/CONFLUENCE.2019.8776890.
- M. C. Roarke, B. D. Nguyen, and B. A. Pockaj. Applications of SPECT/CT in Nuclear Radiology. *American Journal of Roentgenology*, 191(3):W135–W150, Sept. 2008. ISSN 0361-803X. doi: 10.2214/AJR.07.3564. URL <https://www.ajronline.org/doi/full/10.2214/AJR.07.3564>. Publisher: American Roentgen Ray Society.
- R. Romanowski, M. Lewicki, W. Ciechomski, E. Baron, B. Pierański, U. Garczarek-Bak, S. Białowas, and A. Szyszka. *Managing Economic Innovations - Methods and Instruments*. Bogucki Wydawnictwo Naukowe, Sept. 2019. ISBN 978-83-7986-277-1. doi: 10.12657/9788379862771.
- M. Rong, D. Zhang, and N. Wang. A Lagrangian dual-based theory-guided deep neural network. *Complex & Intelligent Systems*, 8, Apr. 2022. doi: 10.1007/s40747-022-00738-1.

- G. Roy, A. K. Bhoi, and S. Bhaumik. A Comparative Approach for MI-Based EEG Signals Classification Using Energy, Power and Entropy. *IRBM*, Mar. 2021. ISSN 1959-0318. doi: 10.1016/j.irbm.2021.02.008. URL <https://www.sciencedirect.com/science/article/pii/S1959031821000300>.
- C. Rudin. Stop explaining black box machine learning models for high stakes decisions and use interpretable models instead. *Nature Machine Intelligence*, 1(5):206–215, 2019. doi: 10.1038/s42256-019-0048-x.
- B. J. Ruijter, M. C. Tjepkema-Cloostermans, S. C. Tromp, W. M. van den Bergh, N. A. Foudraine, F. H. Kornips, G. Drost, E. Scholten, F. H. Bosch, A. Beishuizen, M. J. van Putten, and J. Hofmeijer. Platform Session – Electroencephalography/Epilepsy: EEG for the prediction of outcome within the first five days of postanoxic coma: A prospective multicenter cohort study. *Clinical Neurophysiology*, 129:e231–e232, May 2018. ISSN 13882457. doi: 10.1016/j.clinph.2018.04.595. URL <https://linkinghub.elsevier.com/retrieve/pii/S1388245718308940>.
- R. Sabharwal and S. J. Miah. An intelligent literature review: adopting inductive approach to define machine learning applications in the clinical domain. *Journal of Big Data*, 9(1), 2022. doi: 10.1186/s40537-022-00605-3.
- M. Sadrawi, W.-Z. Sun, M.-M. Ma, Y.-T. Yeh, M. Abbod, and J.-S. Shieh. Ensemble Genetic Fuzzy Neuro Model Applied for the Emergency Medical Service via Unbalanced Data Evaluation. *Symmetry*, 10(71), 2018. doi: 10.3390/sym10030071.
- M. Saeidi, W. Karwowski, F. V. Farahani, K. Fiok, R. Taiar, P. A. Hancock, and A. Al-Juaid. Neural Decoding of EEG Signals with Machine Learning: A Systematic Review. *Brain Sciences*, 11(11), 2021. ISSN 2076-3425. doi: 10.3390/brainsci11111525.
- M. J. Saikia, W. G. Besio, and K. Mankodiya. The Validation of a Portable Functional NIRS System for Assessing Mental Workload. *Sensors*, 21(11):3810, Jan. 2021. ISSN 1424-8220. doi: 10.3390/s21113810. URL <https://www.mdpi.com/1424-8220/21/11/3810>. Number: 11 Publisher: Multidisciplinary Digital Publishing Institute.
- O. W. Samuel, Y. Geng, X. Li, and G. Li. Towards efficient decoding of multiple classes of motor imagery limb movements based on eeg spectral and time domain descriptors. *Journal*

- of medical systems*, 41(12):194, 2017a. ISSN 1573-689X. URL <https://libcon.rec.uabc.mx:5471/login.aspx?direct=true&db=mdc&AN=29080913&lang=es&site=ehost-live>.
- O. W. Samuel, L. Xiangxin, G. Yanjuan, F. Pang, C. Shixiong, and L. Guanglin. Motor imagery classification of upper limb movements based on spectral domain features of eeg patterns. *Annual International Conference of the IEEE Engineering in Medicine and Biology Society. IEEE Engineering in Medicine and Biology Society. Annual International Conference*, 2017:2976 – 2979, 2017b. ISSN 2694-0604. URL <https://libcon.rec.uabc.mx:5471/login.aspx?direct=true&db=mdc&AN=29060523&lang=es&site=ehost-live>.
- A. S. Saragih, A. Pamungkas, B. Y. Zain, and W. Ahmed. Electroencephalogram (EEG) Signal Classification Using Artificial Neural Network to Control Electric Artificial Hand Movement. *IOP Conference Series: Materials Science and Engineering*, 938(1):012005, Oct. 2020. ISSN 1757-899X. doi: 10.1088/1757-899X/938/1/012005. URL <https://doi.org/10.1088/1757-899x/938/1/012005>. Publisher: IOP Publishing.
- M. Savadkoohi, T. Oladunni, and L. Thompson. A machine learning approach to epileptic seizure prediction using Electroencephalogram (EEG) Signal. *Biocybernetics and Biomedical Engineering*, 40(3):1328–1341, July 2020. ISSN 0208-5216. doi: 10.1016/j.bbe.2020.07.004. URL <https://www.sciencedirect.com/science/article/pii/S0208521620300851>.
- V. S. Selvam and S. Shenbagadevi. Brain tumor detection using scalp eeg with modified Wavelet-ICA and multi layer feed forward neural network. In *2011 Annual International Conference of the IEEE Engineering in Medicine and Biology Society*, pages 6104–6109, Aug. 2011. doi: 10.1109/IEMBS.2011.6091508. ISSN: 1558-4615.
- K. Sergeev, A. Runnova, M. Zhuravlev, O. Kolokolov, N. Akimova, A. Kiselev, A. Titova, A. Slepnev, N. Semenova, and T. Penzel. Wavelet skeletons in sleep eeg-monitoring as biomarkers of early diagnostics of mild cognitive impairment. *Chaos*, 31(7):1 – 9, 2021. ISSN 10541500. URL <https://libcon.rec.uabc.mx:5471/login.aspx?direct=true&db=iih&AN=151705221&lang=es&site=ehost-live>.
- C. E. Shannon. A mathematical theory of communication. *The Bell System Technical Journal*, 27(3):379–423, July 1948. ISSN 0005-8580. doi: 10.1002/j.1538-7305.1948.tb01338.x. Conference Name: The Bell System Technical Journal.

- D. K. Sharma, M. Chatterjee, G. Kaur, and S. Vavilala. 3 - Deep learning applications for disease diagnosis. In D. Gupta, U. Kose, A. Khanna, and V. E. Balas, editors, *Deep Learning for Medical Applications with Unique Data*, pages 31–51. Academic Press, Jan. 2022. ISBN 978-0-12-824145-5. doi: 10.1016/B978-0-12-824145-5.00005-8. URL <https://www.sciencedirect.com/science/article/pii/B9780128241455000058>.
- M. Shen, P. Wen, B. Song, and Y. Li. An EEG based real-time epilepsy seizure detection approach using discrete wavelet transform and machine learning methods. *Biomedical Signal Processing and Control*, 77:103820, Aug. 2022. ISSN 17468094. doi: 10.1016/j.bspc.2022.103820. URL <https://linkinghub.elsevier.com/retrieve/pii/S1746809422003421>.
- A. Shoeibi, D. Sadeghi, P. Moridian, N. Ghassemi, J. Heras, R. Alizadehsani, A. Khadem, Y. Kong, S. Nahavandi, Y.-D. Zhang, and J. M. Gorriz. Automatic Diagnosis of Schizophrenia in EEG Signals Using CNN-LSTM Models. *Frontiers in Neuroinformatics*, 15, 2021. ISSN 1662-5196. doi: 10.3389/fninf.2021.777977.
- S. P. E. C. T. S. | S. H. Siemens Healthineers. Siemens Healthineers introduces Symbia Pro.specta SPECT/CT scanner, 2022. URL <https://www.siemens-healthineers.com/press/releases/prospecta>.
- P. Singh, N. Singh, K. K. Singh, and A. Singh. Chapter 5 - Diagnosing of disease using machine learning. In K. K. Singh, M. Elhoseny, A. Singh, and A. A. Elngar, editors, *Machine Learning and the Internet of Medical Things in Healthcare*, pages 89–111. Academic Press, Jan. 2021. ISBN 978-0-12-821229-5. doi: 10.1016/B978-0-12-821229-5.00003-3. URL <https://www.sciencedirect.com/science/article/pii/B9780128212295000033>.
- R. Sitaram, N. Weiskopf, A. Caria, R. Veit, M. Erb, and N. Birbaumer. fMRI Brain-Computer Interfaces. *IEEE Signal Processing Magazine*, 25(1):95–106, 2008. ISSN 1558-0792. doi: 10.1109/MSP.2008.4408446. Conference Name: IEEE Signal Processing Magazine.
- J. Sleight, P. J. Pillai, and S. Mohan. Classification of Executed and Imagined Motor Movement EEG Signals, 2009. URL <https://www.semanticscholar.org/paper/Classification-of-Executed-and-Imagined-Motor-EEG-Sleight-Pillai/8a9d0ee78265cee260f1072f81f7819e0f752519>.

- R. Solís-Vivanco, M. Rodríguez-Violante, A. Cervantes-Arriaga, E. Justo-Guillén, and J. Ricardo-Garcell. Brain oscillations reveal impaired novelty detection from early stages of Parkinson's disease. *NeuroImage: Clinical*, 18:923–931, Jan. 2018. ISSN 2213-1582. doi: 10.1016/j.nicl.2018.03.024. URL <https://www.sciencedirect.com/science/article/pii/S2213158218300949>.
- J. Son, L. Ai, R. Lim, T. Xu, S. Colcombe, A. R. Franco, J. Cloud, S. LaConte, J. Lisinski, A. Klein, R. C. Craddock, and M. Milham. Evaluating fMRI-Based Estimation of Eye Gaze During Naturalistic Viewing. *Cerebral Cortex*, 30:1171–1184, 3 2020. ISSN 1047-3211. doi: 10.1093/CERCOR/BHZ157.
- O. A. P. Sosa, Y. Quijano, M. Doniz, and J. E. Chong-Quero. BCI: A historical analysis and technology comparison. In *2011 Pan American Health Care Exchanges*, pages 205–209, Mar. 2011. doi: 10.1109/PAHCE.2011.5871883. ISSN: 2327-817X.
- I. Stancin, M. Cifrek, and A. Jovic. A Review of EEG Signal Features and Their Application in Driver Drowsiness Detection Systems. *Sensors (Basel, Switzerland)*, 21(11):3786, May 2021. ISSN 1424-8220. doi: 10.3390/s21113786. URL <https://www.ncbi.nlm.nih.gov/pmc/articles/PMC8198610/>.
- M. Stylianou, N. Murphy, L. R. Peraza, S. Graziadio, R. Cromarty, A. Killen, J. T. O' Brien, A. J. Thomas, F. E. N. LeBeau, and J.-P. Taylor. Quantitative electroencephalography as a marker of cognitive fluctuations in dementia with Lewy bodies and an aid to differential diagnosis. *Clinical Neurophysiology*, 129(6):1209–1220, June 2018. ISSN 1388-2457. doi: 10.1016/j.clinph.2018.03.013. URL <https://www.sciencedirect.com/science/article/pii/S1388245718302670>.
- A. Subasi and M. Ismail Gursoy. EEG signal classification using PCA, ICA, LDA and support vector machines. *Expert Systems with Applications*, 37(12):8659–8666, Dec. 2010. ISSN 0957-4174. doi: 10.1016/j.eswa.2010.06.065. URL <https://www.sciencedirect.com/science/article/pii/S0957417410005695>.
- K. Sulek. *Neuroanatomy: The Basics*, 2019. URL <https://www.dana.org/article/neuroanatomy-the-basics/>.

- Z. Tang, S. Sun, S. Zhang, Y. Chen, C. Li, and S. Chen. A Brain-Machine Interface Based on ERD/ERS for an Upper-Limb Exoskeleton Control. *Sensors*, 16(12):2050, Dec. 2016. ISSN 1424-8220. doi: 10.3390/s16122050. URL <https://www.mdpi.com/1424-8220/16/12/2050>. Number: 12 Publisher: Multidisciplinary Digital Publishing Institute.
- M. Teplan. FUNDAMENTALS OF EEG MEASUREMENT. *MEASUREMENT SCIENCE REVIEW*, 2:11, 2002.
- A. Tharwat, T. Gaber, A. Ibrahim, and A. E. Hassanien. Linear discriminant analysis: A detailed tutorial. *AI Communications*, 30(2):169–190, May 2017. ISSN 18758452, 09217126. doi: 10.3233/AIC-170729. URL <https://www.medra.org/servlet/aliasResolver?alias=iospress&doi=10.3233/AIC-170729>.
- A. Theissler, M. Thomas, M. Burch, and F. Gerschner. ConfusionVis: Comparative evaluation and selection of multi-class classifiers based on confusion matrices. *Knowledge-Based Systems*, 247:108651, 2022. ISSN 0950-7051. doi: 10.1016/j.knosys.2022.108651.
- N. Tiwari, D. R. Edla, S. Dodia, and A. Bablani. Brain computer interface: A comprehensive survey. *Biologically Inspired Cognitive Architectures*, 26:118–129, Oct. 2018. ISSN 2212-683X. doi: 10.1016/j.bica.2018.10.005. URL <http://www.sciencedirect.com/science/article/pii/S2212683X18301142>.
- S. Tiwari and D. Arora. Diagnosis of sleep disorders in optimized time slot based machine learning techniques on EEG energy level patterns. *Materials Today: Proceedings*, 51:1179–1190, 2022. ISSN 22147853. doi: 10.1016/j.matpr.2021.07.204. URL <https://linkinghub.elsevier.com/retrieve/pii/S221478532105063X>.
- E. Tuncer and E. D. Bolat. Channel based epilepsy seizure type detection from electroencephalography (EEG) signals with machine learning techniques. *Biocybernetics and Biomedical Engineering*, 42(2):575–595, Apr. 2022. ISSN 02085216. doi: 10.1016/j.bbe.2022.04.004. URL <https://linkinghub.elsevier.com/retrieve/pii/S0208521622000365>.
- J. van Erp, F. Lotte, and M. Tangermann. Brain-Computer Interfaces: Beyond Medical Applications. *Computer*, 45(4):26–34, Apr. 2012. ISSN 1558-0814. doi: 10.1109/MC.2012.107. Conference Name: Computer.

- J. Vidal. Real-time detection of brain events in EEG. *Proceedings of the IEEE*, 65(5): 633–641, May 1977. ISSN 1558-2256. doi: 10.1109/PROC.1977.10542. Conference Name: Proceedings of the IEEE.
- S. M. Vieira, U. Kaymak, and J. M. C. Sousa. Cohen’s kappa coefficient as a performance measure for feature selection. In *International Conference on Fuzzy Systems*, pages 1–8, July 2010. doi: 10.1109/FUZZY.2010.5584447. ISSN: 1098-7584.
- G. Urbancic and V. Podgorelec. Automatic classification of motor impairment neural disorders from eeg signals using deep convolutional neural networks. *Electronics & Electrical Engineering*, 24(4):3 – 7, 2018. ISSN 13921215. URL <https://libcon.rec.uabc.mx:5471/login.aspx?direct=true&db=iih&AN=131379067&lang=es&site=ehost-live>.
- J. Walters-Williams and Y. Li. Comparative Study of Distance Functions for Nearest Neighbors. In K. Elleithy, editor, *Advanced Techniques in Computing Sciences and Software Engineering*, pages 79–84, Dordrecht, 2010. Springer Netherlands. ISBN 978-90-481-3660-5. doi: 10.1007/978-90-481-3660-5_14.
- H. Wang, Q. Song, T. Ma, H. Cao, and Y. Sun. Study on Brain-Computer Interface Based on Mental Tasks. *The 5th Annual IEEE International Conference on Cyber Technology in Automation, Control and Intelligent Systems*, pages 841–845, 2015. doi: 10.1109/CYBER.2015.7288053.
- L. Wei, Q. Hong, H. Yue, and C. Xi. The research in a plantar pressure measuring system connected with EEG. In *IEEE 10th INTERNATIONAL CONFERENCE ON SIGNAL PROCESSING PROCEEDINGS*, pages 434–437, Oct. 2010. doi: 10.1109/ICOSP.2010.5655374. ISSN: 2164-523X.
- Worldshapers Health. Routine EEG vs Longitudinal EEG with video, Aug. 2022. URL <https://worldshapers.org.uk/2022/08/15/routine-eeg-vs-longitudinal-eeg-with-video/>.
- B. Xu, W. Li, X. He, Z. Wei, D. Zhang, C. Wu, and A. Song. Motor Imagery Based Continuous Teleoperation Robot Control with Tactile Feedback. *Electronics*, 9(1):174, Jan. 2020. ISSN 2079-9292. doi: 10.3390/electronics9010174. URL <https://www.mdpi.com/2079-9292/9/1/174>. Number: 1 Publisher: Multidisciplinary Digital Publishing Institute.

- A. Yazdani, T. Ebrahimi, and U. Hoffmann. Classification of EEG signals using Dempster Shafer theory and a k-nearest neighbor classifier. In *2009 4th International IEEE/EMBS Conference on Neural Engineering*, pages 327–330, Apr. 2009. doi: 10.1109/NER.2009.5109299. ISSN: 1948-3554.
- Y. You, W. Chen, and T. Zhang. Motor imagery EEG classification based on flexible analytic wavelet transform. *Biomedical Signal Processing and Control*, 62:102069, Sept. 2020. ISSN 1746-8094. doi: 10.1016/j.bspc.2020.102069. URL <https://www.sciencedirect.com/science/article/pii/S1746809420302251>.
- T. O. Zander and C. Kothe. Towards passive brain–computer interfaces: applying brain–computer interface technology to human–machine systems in general. *Journal of Neural Engineering*, 8(2):025005, mar 2011. doi: 10.1088/1741-2560/8/2/025005.
- J. Zhang and M. Wang. A survey on robots controlled by motor imagery brain–computer interfaces. *Cognitive Robotics*, 1:12–24, Jan. 2021. ISSN 2667-2413. doi: 10.1016/j.cogr.2021.02.001. URL <https://www.sciencedirect.com/science/article/pii/S266724132100001X>.
- Y. Zhang and C. Ling. A strategy to apply machine learning to small datasets in materials science. *npj Computational Materials*, 4(1):25, 2018. doi: 10.1038/s41524-018-0081-z.
- D. Zwillinger and S. Kokoska. *CRC Standard Probability and Statistics Tables and Formulae*. CRC Press, Dec. 1999. ISBN 978-1-4200-5026-4. Google-Books-ID: tB3RVEZ0UIMC.